REMOVAL OF ARSENIC CONTAMINATED IN WATER BY CHITOSAN-MODIFIED NANOSCALE ZERO-VALENT IRON (CNZVI)

Miss Thanatorn Yoadsomsuay

A Dissertation Submitted in Partial Fulfillment of the Requirements
for the Degree of Doctor of Philosophy Program in Environmental Management
(Interdisciplinary Program)
Graduate School
Chulalongkorn University
Academic Year 2014

การกำจัดสารหนูปนเปื้อนในน้ำด้วยเหล็กศูนย์ขนาดนาโนปรับสภาพด้วยไคโตซาน

นางสาวธนธร ยอดสมสวย

วิทยานิพนธ์นี้เป็นส่วนหนึ่งของการศึกษาตามหลักสูตรปริญญาวิทยาศาสตรดุษฎีบัณฑิต
สาขาวิชาการจัดการสิ่งแวดล้อม (สหสาขาวิชา)
บัณฑิตวิทยาลัย จุฬาลงกรณ์มหาวิทยาลัย
ปีการศึกษา 2557

Thesis Title	REMOVAL OF ARSENIC CONTAMINATED IN WATER BY CHITOSAN-MODIFIED NANOSCALE ZERO-VALENT IRON (CNZVI)
By	Miss Thanatorn Yoadsomsuay
Field of Study	Environmental Management
Thesis Advisor	Associate Professor Nurak Grisdanurak, Ph.D.
Thesis Co-Advisor	Professor Chih-Hsiang Liao, Ph.D.

Accepted by the Graduate School, Chulalongkorn University in Partial Fulfillment of the Requirements for the Doctoral Degree

.....Dean of the Graduate School
(Associate Professor Sunait Chutintaranond, Ph.D.)

THESIS COMMITTEE

.....Chairman
(Assistant Professor Chantra Tongcumpou, Ph.D.)
.....Thesis Advisor
(Associate Professor Nurak Grisdanurak, Ph.D.)
.....Thesis Co-Advisor
(Professor Chih-Hsiang Liao, Ph.D.)
.....Examiner
(Associate Professor Jin Anotai, Ph.D.)
.....Examiner
(Assistant Professor Patiparn Punyapalakul, Ph.D.)
.....External Examiner
(Tanapon Phenrat, Ph.D.)

ธนธร ยอดสมสวย : การกำจัดสารหนูปนเปื้อนในน้ำด้วยเหล็กศูนย์ขนาดนาโนปรับสภาพด้วยไคโตซาน (REMOVAL OF ARSENIC CONTAMINATED IN WATER BY CHITOSAN-MODIFIED NANOSCALE ZERO-VALENT IRON (CNZVI)) อ.ที่ปรึกษาวิทยานิพนธ์หลัก: รศ. ดร. นุรักษ์ กฤษดานุรักษ์, อ.ที่ปรึกษาวิทยานิพนธ์ร่วม: ศ. ดร. จื้อเฉียง เลียว, 99 หน้า.

เหล็กศูนย์ขนาดนาโนปรับสภาพด้วยไคโตซาน (CNZVI) ถูกสังเคราะห์ขึ้นเพื่อใช้ในการกำจัดสารหนูในน้ำ โดยกรดอะซิติกเป็นกรดที่มีความเหมาะสมในการใช้เป็นตัวทำละลายไคโตซานเพื่อใช้ในการสังเคราะห์ CNZVI ลักษณะพื้นผิวและขนาดของอนุภาครวมทั้งค่าซึ่งประจุที่ผิวเป็นศูนย์ของเหล็กศูนย์ขนาดนาโน (NZVI) และ CNZVI ถูกนำไปวิเคราะห์ด้วยเครื่องมือ SEM/EDS TEM และวิธี salt addition ตามลำดับ จากภาพถ่ายลักษณะพื้นผิวพบว่าใน CNZVI มีการกระจายตัวของอนุภาคเหล็กมากกว่าใน NZVI และพบว่าอนุภาคของ NZVI ถูกปกคลุมด้วยไคโตซาน ซึ่งช่วยลดการรวมตัวเป็นกลุ่มก้อนของอนุภาค NZVI และอนุภาคของ CNZVI มีขนาดเล็กกว่า NZVI ค่าพีเอชที่ทำให้ประจุที่ผิวของ NZVI เป็นศูนย์ เท่ากับ 7.8 ในขณะที่ CNZVI มีค่าอยู่ในช่วงระหว่าง 7.83 ถึง 10.1 ซึ่งการทดลองแบบทีละเทได้ถูกจัดทำขึ้นเพื่อศึกษาผลของปริมาณไคโตซานที่ใส่ลงไปใน NZVI โดยอยู่ในช่วงระหว่างร้อยละ 2.5-30 โดยน้ำหนัก ศึกษาผลของค่าพีเอชเริ่มต้นในสภาวะที่เป็นกรด เป็นกลาง และเป็นด่าง และพบว่าอัตราการกำจัดอาร์ซีไนท์และอาร์ซีเนตจะเพิ่มขึ้นเมื่อร้อยละโดยน้ำหนักของไคโตซานเพิ่มขึ้นแต่จะลดลงเมื่อค่าพีเอชเริ่มต้นสูงขึ้น นอกจากนี้เมื่อมีการใช้ไคโตซานในปริมาณที่สูงขึ้นพบว่าประสิทธิภาพในการกำจัดสารหนูไม่มีความเปลี่ยนแปลงอย่างมีนัยสำคัญในสภาพความเป็นกรด-ด่างทั้งสามแบบ สำหรับการทดลองในเรื่องไอโซเทอมและจลนพลศาสตร์ของการดูดซับพบว่าข้อมูลสอดคล้องกับไอโซเทอมของแลงเมียร์และเป็นปฏิกิริยาอันดับสองเทียบเท่า โดยกลไกในการดูดซับสารหนูมีสามแบบประกอบด้วย การดูดซับระหว่างไคโตซานและสารหนู การดูดซับระหว่างผลิตภัณฑ์จากการกัดกร่อนของเหล็กและสารหนู และการตกตะกอนร่วมระหว่างอาร์ซีเนตและผลิตภัณฑ์จากการกัดกร่อนของเหล็กและไคโตซานสามารถยับยั้งการเกิดปฏิกิริยาออกซิเดชั่นของ NZVI ได้ ดังนั้น CNZVI จึงสามารถรักษาประสิทธิภาพในการกำจัดสารหนูไว้ได้มากกว่า NZVI เมื่อมีการศึกษาผลของการเก็บรักษาไว้เป็นเวลาสองถึงสามสิบวัน

สาขาวิชา การจัดการสิ่งแวดล้อม ลายมือชื่อนิสิต .....

ปีการศึกษา 2557 ลายมือชื่อ อ.ที่ปรึกษาหลัก .....

ลายมือชื่อ อ.ที่ปรึกษาร่วม .....

5287774020 : MAJOR ENVIRONMENTAL MANAGEMENT
KEYWORDS: ADSORPTION, ARSENIC REMOVAL, NZVI, CHITOSAN

THANATORN YOADSOMSUAY: REMOVAL OF ARSENIC CONTAMINATED IN WATER BY CHITOSAN-MODIFIED NANOSCALE ZERO-VALENT IRON (CNZVI). ADVISOR: ASSOC. PROF. NURAK GRISDANURAK, Ph.D., CO-ADVISOR: PROF. CHIH-HSIANG LIAO, Ph.D., 99 pp.

Chitosan-modified nanoscale zero-valent iron (CNZVI) was synthesized for arsenic removal from water. Acetic acid was suitable as a solvent to dissolve chitosan facilitate the CNZVI synthesis. Surface morphology, the particle size, and the point of zero charge of NZVI and CNZVI were characterized by SEM/EDS, TEM, and salt addition method, respectively. The surface images showed the more dispersion of iron particle in CNZVI than in bare NZVI and also the coverage of chitosan over iron particles were found. Chitosan can reduce the agglomeration of NZVI particles. The particle size of CNZVI was smaller than NZVI. The point of zero charge of NZVI was at pH 7.8, while that of CNZVI is in the range of 7.83-10.1. Batch experiments were carried out to examine the influence of weight percent of chitosan loading (2.5-30%wt) in the CNZVI, and the initial solution pH including acidic, neutral, and basic (4, 7, 9) conditions. Both arsenite and arsenate removal rate increased with higher weight percent of chitosan loading but decreased with higher initial pH. In addition, the efficiencies of CNZVI for arsenic removal did not change significantly for the three investigated pH conditions, when higher percentage of chitosan loading was applied. The isotherm and kinetic adsorption experimental data fit well into Langmuir isotherm and the pseudo second-order model. The mechanisms of arsenic removal by CNZVI are proposed. Three kinds of mechanism pathways consist of adsorption of chitosan and As species, adsorption of iron corrosion products and As species, and co-precipitation of As(V) and iron corrosion products. Chitosan could retard the oxidation reaction of NZVI. CNZVI, therefore, could retain its activity on arsenic removal higher than NZVI, in the shelf-life study between 2-30 days.

Field of Study: Environmental Management Student's Signature .....
Academic Year: 2014 Advisor's Signature .....
Co-Advisor's Signature .....

ACKNOWLEDGEMENTS

I would like to express my sincere and deepest gratitude to my advisor, Assoc. Prof. Dr. Nurak Grisdanurak, who gives me the good opportunities, great supports, generous encouragements, resounding helps, and all valuable suggestions. Without his persistent push forward this dissertation would not have been possible. And also would like to thanks Prof. Dr. Chih-Hsiang Liao for the opportunities to be his student and lots of guidance throughout the experiment. I was taken care like home in Taiwan. Besides, I would like to express my gratitude to my committee members, Assist. Prof. Dr. Chantra Tongcumpou, Assist. Prof. Dr. Patipan Punyapalakul, Assoc. Prof. Dr. Jin Anotai, and Dr. Tanapon Phenrat for your kind and valuable suggestions.

Catalyst laboratory at Thammasat University where is full of friendship, help, and sympathy. Everybody supported me in both academic and laboratory works including encourages me to pass through difficult time. Furthermore, my special thanks go to my Thai, Taiwanese and Filipino friends at Chia Nan University of Pharmacy and Science for your kindness and helpful assistances in everything about 2 years I spent my life there. I also would like to thank all my friends at International Program in Hazardous Substance and Environmental Management, Chulalongkorn University for their willingness to share and advise their knowledge and academic information. Moreover, thank you my colleagues at Department of Industrial Works, Ministry of Industry for your kind and always cheering me up.

Furthermore, I would like to express my sincere and deepest gratitude to my family for their supports which make me feel that they are always there for me through thick and thin. Without their encouragements, I would not even have a chance to get a doctoral degree. Special thanks to my lovely sister, Noy who took care our parents while I stayed in Taiwan and willing to supports me all the times and that allows me to step through all troubles. I feel very lucky that having Prakaii and your family who always encourages me in everything. Last but not least, I would like to thank my mom and dad who cheer me up all the time and I always hear their love loudly in my heart.

CONTENTS

Page

Page

Page

LIST OF TABLES

LIST OF FIGURES

NOMENCLATURE

CNZVI	chitosan modified nanoscale zero-valent iron
CNZVI-a	CNZVI synthesis by chitosan dissolved in acetic acid
CNZVI-n	CNZVI synthesis by conventional method using chitosan dissolved in nitric acid
CNZVI-n_{impreg}	CNZVI synthesis by impregnation method using chitosan dissolved in nitric acid
Eh	redox potential
NZVI	nanoscale zero-valent iron
PZC	Point of zero charge

Abbreviation

As(III)	arsenite
As(V)	arsenate
$AsNaO_2$	sodium arsenite
C	the concentration of arsenic in the solution
C_0	the initial arsenic concentration
Ca^{2+}	calcium
Fe	iron
Fe^0	zero-valent iron
Fe^{2+}	ferrous ion
Fe^{3+}	ferric ion
$FeC1_2$	ferrous chloride
$FeC1_3$	ferric chloride
FeOOH	goethite
Fe_2O_3	hematite
Fe_3O_4	magnetite
GFH	granular ferric hydroxide
H^+	hydrogen ions
HCl	hydrochloric acid
HCO_3^-	bicarbonate

HFO	hydrous ferric oxide or iron hydroxide
H_2SO_4	sulfuric acid
µg/L	microgram per liter
Na_2HAsO_4	sodium arsenate
$NaBH_4$	sodium borohydride
O_2	oxygen

CHAPTER 1
INTRODUCTION

1.1 Background for the study

Arsenic (As), which is a well-known carcinogen, has been strictly monitored in groundwater in many countries. In water resource, arsenic can be found in both forms of inorganic and organic compounds. Between those, inorganic species are higher toxic. Arsenic presents in several oxidation states (-3, 0, +1, +2, +3 and +5) but the predominant forms are arsenite (AsO_3^{3-}) and arsenate (AsO_4^{3-}) which are with the oxidation states, As(III) and As(V), respectively. In oxic condition and pH 5-12, the dominant arsenic species is arsenate (As(V)). Meanwhile, arsenite (As(III)) which is more mobile and more toxic is usually found in anoxic condition and neutral water like groundwater that is the major source of drinking water. According to its toxicity, The World Health Organization (WHO) therefore mandated the maximum contaminant level of arsenic in drinking water from 50 to 10 μg/l. The regulation has been effective since 1993 (Mondal et al., 2006; Iesan et al., 2008; Malik et al., 2009; Triszcz et al., 2009).

Several conventional methods have been used to remove arsenic such as precipitation, membrane filtration, ion exchange and adsorption. Adsorption is widely used because it is simple, efficient and low cost (Zhang et al., 2010). This process operates by using solid material to remove the contaminant by physical and chemical forces. For arsenic removal, many kinds of iron adsorbents have been developed such as granular ferric hydroxide (Daus et al. 2004), iron oxide coated sand (Gupta et al., 2005), and zero-valent iron (Fe^0 or ZVI) (Bang et al., 2005; Mohan and Pittman, 2007). Zero valent iron (ZVI) is found to be one of the effective adsorbents for removing both of As(V) and As(III) in water . However, laboratory studies have stated that ZVI in nanoscale seems to has more potential in arsenic adsorption due to its larger surface area and subsequently higher surface reactivity than microscale ZVI. Arsenic can be removed by nanoscale zero-valent iron (NZVI) through adsorption on iron oxides/hydroxides and/or chemical reduction after the NZVI react with dissolved

oxygen (DO) and/or water (Iesan et al., 2008; Triszcz et al., 2009; Zhu et al., 2009; Litter et al., 2010).

However, the problem of in situ NZVI application is that the NZVI tends to agglomerate because of van der Waals force and magnetic interaction. The agglomeration causes the decrease of reactive surface area. The larger particle sizes also show the limit of their mobility in subsurface area. Moreover, NZVI is promptly oxidized in the atmosphere before reaching to the contaminants; therefore, its chemical reactivity is decreased. In order to overcome these obstacles, several materials such as polymers, polyelectrolytes, and surfactants has been used as a modifier or a stabilizer to enhance NZVI stability but retain the reactivity (Phenrat and Lowry, 2009; Lin et al., 2010).

Chitosan is a kind of biopolymers that can be derived from exoskeleton of crustaceans such as shrimp and crab and cell wall of fungi. It consists of glucosamine units and acetylglucosamine units. The amine groups in the structure lead to having the positive charge in acid solutions and also chelating to metal ions (Guibal, 2005). Previous studies stated that chitosan can be used as a modifier for metallic nanoparticles preparation, for instance, silver, gold, platinum, and palladium to increase the dispersion of nanoparticles (Huang et al., 2004). In addition, chitosan is nontoxic and biodegradable.

However, a limited number of the studies on the modified NZVI by chitosan in order to reduce the agglomeration of the nanoparticles and enhance the resistance of its oxidation have been found. Therefore, this study will focus on the enhancement of the stability of NZVI by using chitosan as a modifier. The appropriate and applicable synthesis method of modified NZVI will be studied. The comparative performance between pristine NZVI and chitosan-modified nanoscale zero-valent iron (CNZVI) will be investigated. In addition, both kinds of stored nanoparticles will be examined for their efficiencies in arsenic removal in order to prove the ability of oxidation resistance of modified NZVI. The important factors that affect the arsenic removal by using NZVI and CNZVI will also be investigated.

1.2 Objectives

Main objectives:

To enhance the stability of nanoscale zero-valent iron (NZVI) for the removal of arsenic in water.

Sub-objectives:

1. To investigate the effect of chitosan on NZVI used in arsenic removal in term of activity performance.
2. To evaluate the significant factors on the arsenic removal efficiency over CNZVI, including arsenic species, initial pH, and percent chitosan loading.
3. To study the capability of oxidation resistance of NZVI under chitosan incubation.

1.3 Hypotheses

1. Chitosan can decrease the agglomeration of NZVI particles.
2. CNZVI has a higher efficiency in arsenic removal than bare NZVI.
3. CNZVI would be oxidized less than NZVI due to the covering of chitosan over NZVI.

1.4 Scope of the study

This study is focused on the arsenic removal efficiency of the synthesized nanoparticles which are NZVI and CNZVI. In order to simplify the synthesis process, both of them were synthesized in the laboratory under the normal atmosphere instead of under inert atmosphere of nitrogen that needs more complicated devices. Chitosan was ordered from Acros Organics. Types of arsenic solution were arsenate and arsenite. Field groundwater used in this study was pumped from a groundwater site at Chia Nan University of Pharmacy and Science, Taiwan. All batch experiments were done at room temperature.

Normally, the effective NZVI will be synthesized at the field and immediately applied for remediation. It should be better if there is a delivery time from a plant to a field. In this study, dried NZVI and CNZVI were kept in desiccator for 2, 7, and 30 days after they were synthesized, and then used in arsenic removal test in order to

examine whether chitosan can maintain the arsenic removal efficiency of stored NZVI. These durations are the estimate time of transportation from the factory to the field.

1.5 Benefits of the study

The results from this study can be used for the improvement of NZVI efficiency in arsenic and other toxic pollutants. Chitosan would be the appropriate modifier to improve the properties of NZVI in term of enhancing the stability and oxidation resistance. The factors that influence to the performance of CNZVI can be utilized in the upscale system and this CNZVI will be beneficial for in situ arsenic removal.

1.6 Organization of the content

The content of this dissertation consists of the introduction in Chapter 1, theoretical background and literature reviews in Chapter 2, and then methodology in Chapter 3, Results and discussion states in Chapter 4. The last chapter is the conclusion and recommendations.

CHAPTER 2
THEORETICAL BACKGROUND AND LITERATURE REVIEWS

2.1 Theoretical background

2.1.1 Arsenic (As)

Arsenic (As) is the element that is ubiquitous in the earth's crust. Natural processes such as volcanic emission and anthropogenic activities in agricultural and industrial sections, for instance, crop desiccation, mining, and burning of fossil fuel, cause the distribution of arsenic in environment. In groundwater, which is the main source of drinking water, the problem of arsenic contamination at significant level has been found in many countries such as Argentina (1-7500 µg/L), Chile (100-1000 µg/L), USA (1-2600 µg/L), China (40-750 µg/L), Bangladesh (0.5-3200 µg/L), Vietnam (1-3050 µg/L), and Taiwan (10-1820 µg/L). The contamination of arsenic in shallow groundwater in the southern region of Thailand because of the previous tin-mining at the concentration of 1-5000 µg/L has also been reported by the late 1990s (Smedley and Kinniburgh, 2002)

For the adverse effect of high levels of inorganic arsenic exposure through drinking water and food in long-term, the first symptoms are usually observed in the skin, pigmentation changes, skin lesion, and hard patches on the palms and the feet (hyperkeratosis). Besides, drinking water containing arsenic can be harmful to respiratory, digestive, renal circulatory, neutral systems and internal organs. The most significant effect of chronic arsenic intoxication is the induction of cancer in many organs such as liver, lung, kidney, or bladder. Therefore, arsenic has been classified as Class I human carcinogen by the International Agency for Research on Cancer (IARC). World Health Organization (WHO) revised the maximum contaminant level of arsenic in drinking water from 50 to 10 µg/l in 1993 (Mondal et al., 2006; Choong et al., 2007; Malik et al., 2009).

Arsenic in environment can be found in both organic and inorganic form and it is rarely encountered as a free element. Arsenic that combines with carbon and oxygen is kind of organic arsenic compounds. Inorganic arsenic is more concerned because it is generally more toxic than organic species. It can be found in water in several oxidation states (+5, +3, 0, -3). Redox potential (Eh) and pH are the most important factors controlling arsenic speciation.

The predominant forms of inorganic arsenic in water as oxyanions are trivalent arsenite (AsO_3^{3-}) and pentavalent arsenate (AsO_4^{3-}) which are with the oxidation states, As(III) and As(V), respectively. As^0 and As^{3-} are hardly found in aquatic environment (Mondal et al., 2006; Iesan et al., 2008; Malik et al., 2009; Triszcz et al., 2009). In oxidizing and oxic condition, the dominant arsenic species is arsenate (As(V) as H_3AsO_4, $H_2AsO_4^-$, $HAsO_4^{2-}$, and AsO_4^{3-}), while arsenite (As(III) as H_3AsO_3, $H_2AsO_3^-$, and $HAsO_3^{2-}$ which is more mobile and more toxic is usually found in reducing and anoxic environment. The stability of arsenic species under different pH and redox conditions are shown in Table 2.1 (Vu et al., 2003). In addition, the pH and Eh diagram of arsenic is shown in Figure 2.1 (Smedley and Kinniburgh, 2002).

Table 2.1 Stability of arsenic species.

Reducing Conditions		**Oxidizing Conditions**	
pH	As(III)	pH	As(V)
0-9	H_3AsO_3	0-2	H_3AsO_4
10-12	$H_2AsO_3^-$	3-6	$H_2AsO_4^-$
13	$HAsO_3^{2-}$	7-11	$HAsO_4^{2-}$
14	AsO_3^{3-}	12-14	AsO_4^{3-}

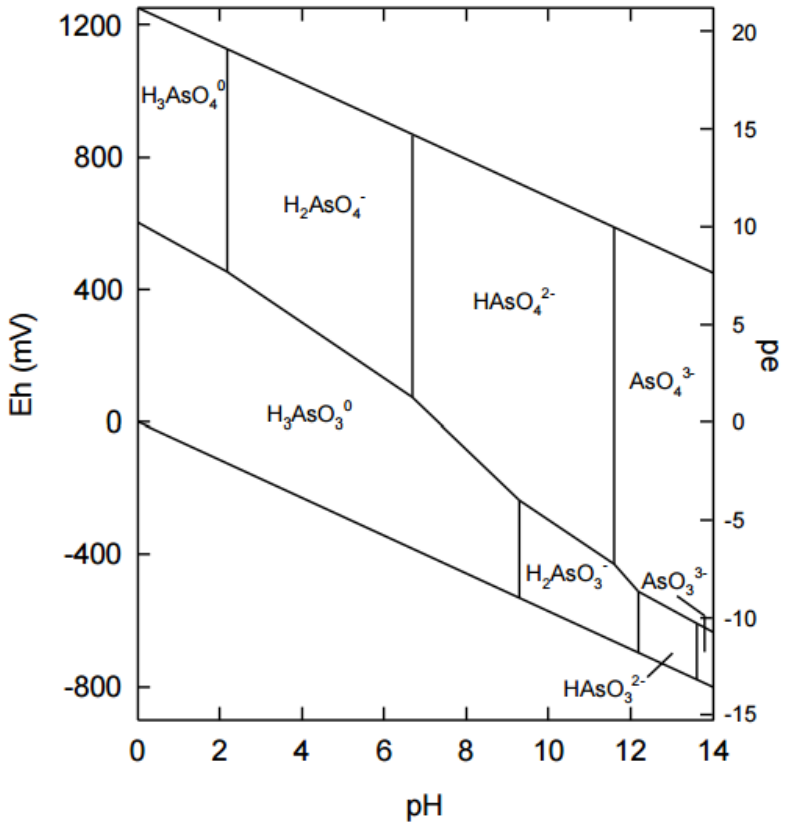

Figure 2.1 Eh-pH diagram of aqueus arsenic species in the system As-O_2-H_2O at 25 ºC, 1 atm.

From the Eh-pH diagram in Figure 2.1, it can be noticed that both forms of arsenic (III) and (V) exist under specific conditions. For example, under oxidizing conditions, $H_2AsO_4^-$ is dominant at low pH (less than about pH 6.9), whilst at higher pH, $HAsO_4^{2-}$ becomes dominant. $H_3AsO_4^0$ and AsO_4^{3-} may be present in extremely acidic and alkaline conditions respectively. Under reducing conditions at pH less than about pH 9.2, the uncharged arsenite species $H_3AsO_3^0$ will predominate.

2.1.2 Arsenic removal

Several conventional methods have been used to remove arsenic such as precipitation-coagulation, membrane filtration, ion exchange, reverse osmosis, and adsorption (Mondal et al., 2006). Membrane filtration is very effective but the cost is high. Ion exchange is very limited in ability due to exchange competition from other

anions found in groundwater. Meanwhile, precipitation-coagulation and adsorption processes are low cost and effective. Reverse osmosis are generally highly effective but the operating cost is high, so it is not recommend for very small system. Adsorption is a process using solid material to remove the contaminant by physical and chemical forces. It was found that iron adsorbents have been developed for applying in arsenic removal such as hydrous ferric oxide, granular ferric hydroxide, iron oxide coated sand, and zero valent iron (Fe^0 or ZVI). (Daus et al., 2004; Mondal et al., 2006; Choong et al., 2007; Mohan and Pittman, 2007; Malik et al., 2009)

Hydrous ferric oxide (HFO) has been examined as a promising adsorptive material for As(V) and As(III) removal from aqueous phase because of its high iso-electric point (8.1) (Dixit and Hering, 2003) and selectivity for arsenic species. Due to its low value of hydraulic conductivity, the hydrous ferric oxide was not suitable for column applications (Zeng, 2003). To overcome this disadvantage, granulation or coating techniques have been used for the modification.

First we started with granular ferric hydroxide (GFH). In this form, higher porosity of a poorly crystallized β-FeOOH was developed approximately 75%–80%. This would provide higher surface area of 250–300 m^2 /g. The synthesis method was quite simple. It requires a neutralization and precipitation of ferric chloride solution with sodium hydroxide, followed by centrifugation and granulation under high-pressure (Thirunavukkarasu et al., 2003; Gu et al., 2005). It was found that GFH showed high active sites for adsorption capacity. A column test packed with GFH operated at pH 7.6 could remove As from 50 ppb to 10 ppb MCL for 25,000 BVs when the EBCT is 2.5 min (Westerhoff et al., 2005). However, with a media particle size of 0.8–2.0 mm GFH, a significant amount of head loss pressure might be built up in the system (Selvin et al., 2000; Gu et al., 2005).

In order to reduce the pressure drop effect built up in the system, a coating technique has been developed. As known, iron (III) possesses high affinity toward inorganic arsenic species. Therefore, the modifications have been focused on the stable iron bearing adsorbents, as discussed;

1. Iron oxide coated sand

Sand usually is served as a support. Iron oxide coated sand was studied on arsenic removal and it was found that material could adsorb As (III) 0.03 mg/g at pH 7.5 (Gupta et al., 2005).

2. Iron oxide impregnated activated carbon.

Since activated carbon seems to be cheap compared to other supports, iron salts were precipitated onto activated carbons. It was expected that only external loading was studied. Under the 7% loading of iron on activated carbon, it was found the increase in capacities; 4.7 mg/g for As (III) adsorption and 4.5 mg/g for As (V) adsorption (Vaughan Jr and Reed, 2005), compared to iron oxide coated sand.

3. Fe (III)-loaded cellulose sponge.

Support containing ethyleneamine and iminodiacetate functional groups, interacted with Fe (III) using chelation and ion exchange techniques. With the loading of Fe (III) of 0.25 mmol Fe/g sponge, which corresponded to a 1.4% Fe content, the media could show As (V) adsorption capacity of 1.83 mmol As /g sponge; and an As (III) adsorption capacity of 0.24 mmol As/g sponge (Munoz et al., 2002).

4. Granular activated carbon (GAC) based iron containing adsorbents.

Refer to iron oxide impregnated activated carbon, it could be improved the capacity by the modification after the coating. First Fe (II) was adsorbed onto GAC which was synthesized by lignite, and then the Fe (II) was oxidized to Fe (III) by air oxidation, H_2O_2 or NaClO. Iron loading using impregnation method was reached 8%wt. The study was carried out in pack bed column to 50–60 ppb of As (V) or As (III). It was found that more than 7,000 bed volumes could be run to meet 10 ppb breakthrough (Gu et al., 2005). This seems to be 3–5 times longer bed life than original GAC support.

5. A combination supporter

Iron oxide has been loaded on several kinds, such as sand and melted slag (Zhang and Itoh, 2005) and macroporous cation exchange bead (DeMarco et al., 2003). The porous cation exchange resins with a loading of 50% in the form of FeOOH. This product could remove arsenic from 50 ppb down to 10 ppb for 45,000 BVs. DeMarco et al. (2003)showed the stability of HFO agglomerates in the beads. Even the turbulence and mechanical stirring did not affect to HFO, meaning that there was no loss of HFO in the process of removal. It was understood that there was chemical bondings between

iron oxide with the Si inside the slag, which prevented the crystallization of FeOOH. The material showed better arsenic removal (arsenate of 78.5 mg/g slag) capacity than FeOOH (Zhang and Itoh, 2005).

Zero-valent iron as iron (oxyhydr) oxide has shown the performance on its initial removal capacity that may come about after iron metal corrodes in water (Lackovic et al., 2000; Su and Puls, 2001). There are many phenomena through the arsenic removal. For examples; a possible arsenic removal processes in zero-valent iron was provided by surface adsorption onto corrosion products, e.g. iron (oxyhydr)oxides (Manning et al., 2002; Dixit and Hering, 2003), precipitation such as formation of symplesite ($Fe_3(AsO_4)_2 \cdot 8H_2O$) (Nikolaidis et al., 2003), co-precipiration which arsenic may co-precipitate with carbonate green rust (Lien and Wilkin, 2005) or redox reactions via As (III) oxidized to As(V) by corrosion products or impurities such as MnO_2 (Manning et al., 2002; Melitas et al., 2002). Melitas et al. (2002) mentioned that arsenate removal rates over ZVI were highly dependent on the continuous generation of iron oxide adsorption sites by comparing arsenate removal with freely corroding and cathodically protected iron. Municipal service representatives comment that zero-valent iron systems have considerable problems with plugging and hydraulic pressure build up.

2.1.3 Nanoscale zero-valent iron (NZVI)

Nanoscale zero-valent iron (NZVI) which is a very active nanomaterial is a promising and effective treatment technology for a wide variety of contaminants such as halogenated hydrocarbons, nitroaromatic compounds, and heavy metal ions including both of As(V) and As(III) in water. Laboratory studies have stated that NZVI in the size range of 1-100 nm has more potential in arsenic removal than microscale ZVI or larger iron filings due to its larger surface area and subsequently higher surface reactivity (Iesan et al., 2008; Triszcz et al., 2009; Zhu et al., 2009; Litter et al., 2010). The advantage of using NZVI is its capability to be directly injected into a contaminated aquifer instead of a trench digging for the PRB installation. The expectation of injection method is the more quickly and effective for groundwater treatment compare to pump and treat or PRB techniques (Keane, 2009).

Prior publication demonstrated the core-shell structure of NZVI that comprise of a metal iron core and a thin layer of iron oxide/hydroxide on the surface. The metallic core with highly reducing characteristic has an important role in redox reaction, while the oxide shell takes part in contaminants adsorption. It is generally accepted that the iron oxide shell of the nZVI material is highly reactive, particularly when exposed to both oxygen and water and may even oxidize in air (Ramos et al., 2009; Yan et al., 2010). Contaminants can be removed by NZVI through adsorption on iron hydroxides and/or chemical reduction after the NZVI react with dissolved oxygen (DO) and/or water. According to Triszcz et al., 2009, NZVI serving as a strong reductant which can react with water and oxygen, leading to formation of ferrous iron (Fe^{2+}), as shown in Reactions (2.1) and (2.2)

$$Fe^0 + H_2O + ½\ O_2 \rightarrow Fe^{2+} + 2OH^- \qquad (2.1)$$

$$Fe^0 + 2H_2O \rightarrow Fe^{2+} + H_2 + 2OH^- \qquad (2.2)$$

Due to the subsequent oxidation of Fe^{2+}into Fe^{3+} in the presence of oxygen, the precipitation of iron (hydr)oxides occurs and the removal of As is enhanced because of the adsorption of As on the iron precipitates. The reactions which may involve in the forming of iron species in aqueous solution are demonstrated in Reactions (2.3) to (2.5).

$$Fe^{2+} + 1/2H_2O + ¼\ O_2 \rightarrow Fe^{3+} + OH^- \qquad (2.3)$$

$$Fe^{3+} + 3H_2O \rightarrow Fe(OH)_3 + 3H^+ \qquad (2.4)$$

$$Fe^0 + 2Fe^{3+} \rightarrow 3Fe^{2+} \qquad (2.5)$$

Also, Fe^{3+} reacts with OH^- or H_2O and to yield an oxyhydroxide layer (Li et al., 2006).

$$Fe^{3+} + 3OH^- \rightarrow Fe(OH)_3 \qquad (2.6)$$

$$Fe^{3+} + 2H_2O \rightarrow FeOOH + 3H^+ \qquad (2.7)$$

$Fe(OH)_3$ can also dehydrate to form FeOOH:

$$Fe(OH)_3 + 3H^+ \rightarrow FeOOH + H_2O \qquad (2.8)$$

It was suggest that the oxide shell is composed of mainly iron hydroxides or iron oxyhydroxide. As a result of iron oxidation, Fe^{2+} is first formed on the surface. At low pH (less than pH_{pzc}), iron oxides are positively charged and attract anionic ligands. When the solution pH is above the isoelectric point, the oxide surface becomes negatively charged and can form surface complexes with cations (e.g., metal ions). As known, zero valent iron can serve as very effective electron donors. ZVI (Fe^{2+}/Fe) has a standard reduction potential (E^0) of −0.44 V, which is lower than many metals such as Pb, Cd, Ni, and Cr, as well as many organic compounds like chlorinated hydrocarbons. These compounds are thus susceptible to the reduction by NZVI. Reactions at the NZVI surface involve many steps, for example, mass transport of molecules to the surface and electron transfer (ET) from the ZVI to the surface adsorbed molecules. Kinetic analysis suggests that for many organic compounds such as PCE and TCE, the surface reaction or electron transfer is the dominant factor or the rate limiting step. There are several potential pathways for the electron transfer (ET) to occur:

(1) direct ET from Fe^0 through defects such as pits or pinholes, where the oxide layer acts as a physical barrier;

(2) indirect ET from Fe^0 through the oxide layer via the oxide conduction band, impurity bands, or localized bands; or

(3) ET from sorbed or lattice Fe(II) surface site. In this regard, the iron oxide shell can appropriately be considered as n-type semiconductor.

2.1.4 Chitosan

Chitosan is a kind of natural polymers that is the derivative of chitin (a polymer of N-acetylglucosamine). Chitin is an abundant polymer on earth because it can be found in exoskeleton of insects and crustaceans such as shrimps and crabs and also in cell wall of fungi. Chitosan composes of N-acetyl glucosamine units and glucosamine units that occur by the partial deacetylation of chitin under alkaline condition. The structures of chitin and chitosan are shown in Figure 2.2 (Guibal, 2005).

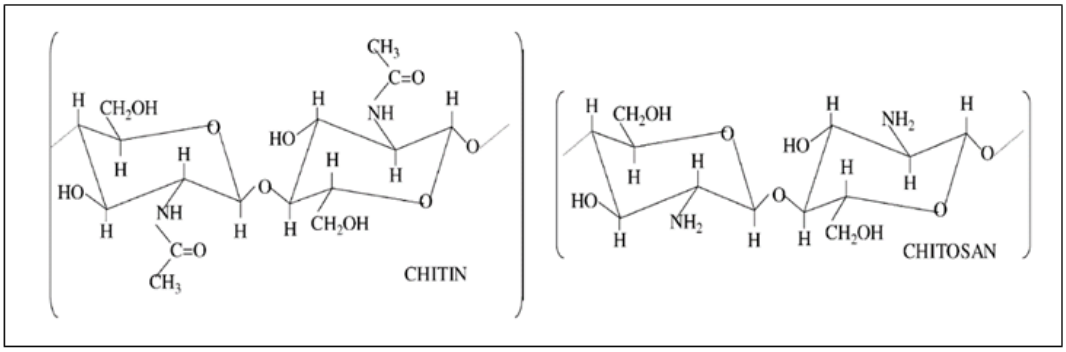

Figure 2.2 Structure of (a) chitin (poly (N-acetylglucosamine)) and (b) chitosan.

Important chemical properties of chitosan are linear polyamine, reactive amino groups, reactive hydroxyl groups available, and chelates many transitional metal ions (Dutta et al., 2004). Due to hydroxyl (-OH) and amino ($-NH_2$) groups in the structure, chitosan can dissolve in acidic solution and bind with metal ions. Guibal, 2005 reviewed that the main reactive units of chitosan for metal ions is at amine sites. Furthermore, the presence of positive charge because of the protonation of amine groups in acidic solution facilitates the attraction of metal anions.

The interaction of chitosan with metal ion can be described by three mechanisms as follow (Guibal, 2005).

(1) Metal chelation

(2) Electrostatic attraction (or ion exchange)

(3) Formation of ion pairs

In addition, chitosan is biodegradable, biocompatible, non-toxic, and polycationic biopolymer. With these properties, chitosan has been studied and applied in several fields such as in agriculture (e.g., seed coating and time release of fertilizer into the soil), food and beverages (e.g., lipid binding and preservative), cosmetics (e.g., hair and oral care, and skin moisturizing), biopharmaceutics (e.g., antitumoral and anticoagulant), and environmental remediation (e.g., flocculation, metal ion removal, and odors reducing) (Dutta et al., 2004; Rinaudo, 2006).

2.2 Literatures review

NZVI has been used to remove several kinds of contaminant including both volatile organic compounds and heavy metals.

2.2.1 VOC treatment

One of hazardous contaminated compounds in groundwater is VOCs (Volatile organic compounds), which is always found in industrial areas. Most of the VOCs contaminated in groundwater are chlorinated VOCs. For examples; tetrachloroethylene (PCE) and trichloroethylene (TCE), *cis*-dichloroethylene (*cis*-DCE) and vinyl chloride compounds. They are regulated and required the treatments.

The removal of chlorinated hydrocarbons is generally based on a reduction scheme. Arnold and Robert (2000) proposed the mechanism by starting with a hydrogenolysis (replacement of a halogen by hydrogen), following with reductive elimination (dihaloelimination), and hydrogenation (reduction of multiple bonds), as represented in Figure 2.3. For many compounds, more than one reaction may exist, and partially dehalogenated products may form by more than one route. Branching ratios between competing reactions will thus play an important role in product distributions. Table 2.2 summarized the treatment of VOCs by NZVI and related materials.

2.2.2 Heavy metal treatment

In-situ remediation of heavy metal contaminated groundwater by NZVI were studied in many researches. Several mechanisms to remove heavy metal were proposed including redox, precipitation, co-precipitation and adsorption. Copper is characterized by reduction and precipitation mechanisms and typical interactions for nickel are reduction, adsorption and co-precipitation (O'Carroll et al., 2013). The mechanism of Cr(VI) removal from aqueous solutions by NZVI particles consists of the reduction, complexation, adsorption, precipitation or co-precipitation (Yang et al., 2007). Many types of heavy metal that were treated by NZVI and related NZVI is shown in Table 2.3 ((Arnold and Roberts, 2000).

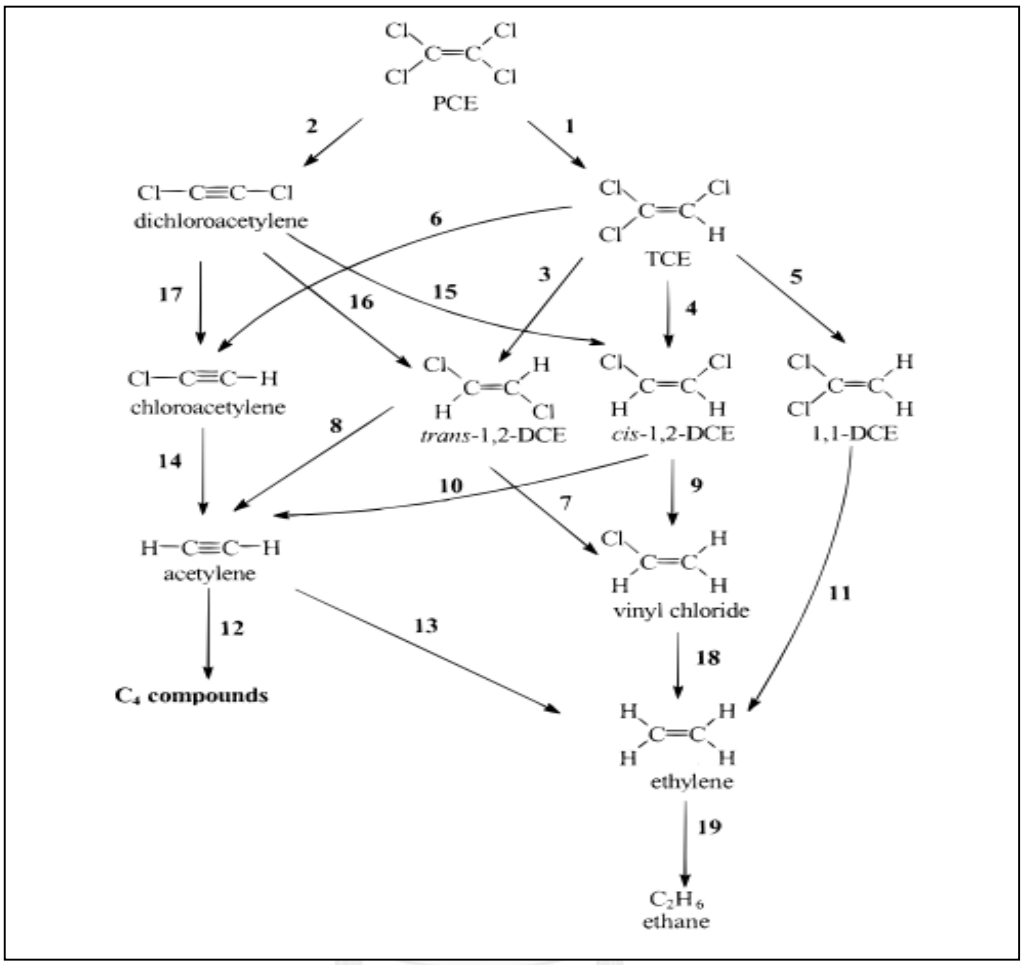

Figure 2.3 Proposed mechanism of PCE reduction by NZVI.

Table 2.2 VOC treatment by NZVI and related NZVI.

Pollutants	NZVI or Modified NZVI	Conditions	Capacity	Kinetic	Other	Ref.
1,1,1-Trichloroethane (TCA)	NZVI	[TCA] = 0.1 mM NZVI = 0.05 g Temp. = 25°C	-	1st order k_{obs} = 1.08 h^{-1}	Reactor = 24 mL of amber glass vials sealed with three-layered septum system	Bae and Lee (2010)
1,1,1-Trichloroethane (TCA)	NZVI + magnetite	[TCA] = 0.1 mM NZVI=0.05 g + 0.5 g magnetite Temp. = 25°C	-	1st order k_{obs} = 6.7 x 10^{-1} h^{-1}	Reactor = 24 mL of amber glass vials sealed with three-layered septum system	Bae and Lee (2010)
Trichloroethylene (TCE)	NZVI	[TCE] = 0.04 mM [NZVI] = 0.86 mM Temp. = 23°C	-	1st order k_{SA} = 1.0×10^{-3} L/hr·m^2	160 mL serum bottles capped by Teflon Mininert valves rotated on an end-over-end rotator at 30 rpm	Liu and Lowry (2006)

Pollutants	NZVI or Modified NZVI	Conditions	Capacity	Kinetic	Other	Ref.
Trichloro phenol (TCP)	Pd/NZVI	[TCP] = 0.05 mmol/L Pd/NZVI = 0.59 g/ 40mL pH = 5.6 Reaction = 25 min	3.39 x 10^{-5} mmol/g	-	-	Chang et al. (2015)
p-nitro phenol (PNP)	NZVI/Si	[PNP] = 200 mg/L NZVI/Si = 5g/L	40 mg/g	1st order k_{obs} = 0.8875 min^{-1}	--	(Tang et al., 2015)
Nitro benzene (NB)	NZVI/Si	[NB] = 20 mg/L NZVI/Si = 0.252 g/L pH = 5.5 Reaction = 15 min	2.38 mg/g	1st order k_{obs} = 0.215 min^{-1}	serum bottle sealed with a Teflon-coated septa	Sun et al., 2014
1,2-dichloroethane (DCA)	NZVI/ poly acrylic acid (PAA)	DCA = 2.0 µM NZVI/PAA = 17.8 g/L (as NZVI)	Removed 99% (at middle layer of site)		Site injection	(Wei et al., 2012)
Metro nidazole (MNZ)	Poly (vinyliden efluoride)-supported NZVI	MNZ = 67.44 mg/L PSN = 9.52 mg/50mL	268.59 mg/g	1st order k_{obs} = 0.1015 min^{-1}		(Yang et al., 2014)

Pollutants	NZVI or Modified NZVI	Conditions	Capacity	Kinetic	Other	Ref.
Bismer thiazol (BMT)	ZVI	[BMT] = 10 mg/L ZVI = 0.5 g/L pH = 6.0	99% removal	2nd order k_{obs} = 0.425 L/ mg· hr.	granular zerovalent iron (0.12–0.15 mm)	(Shen et al., 2015)
Reactive Blue 21 (RB21)	NZVI	[RB21] = 30 mg/L NZVI = 0.5 g pH = 6.5 Reaction = 90 s	99.5 % removal			(Sohrabi et al., 2014)

Table 2.3 Heavy metal treatment by NZVI and related NZVI

Pollutants	NZVI or Modified NZVI	Conditions	Capacity	Other	Ref.
Cd	NZVI	[Cd] = 40 g/L, [NZVI] = 500 mg/L Temp. = 25°C Ar atmosphere Reaction = 90 min	40 mg/g	-	(Su et al., 2014)
Cd	NZVI	[Cd] = 40 mg/L, [NO_3^-] = 15 mg/L [NZVI] = 500 mg/L Temp. = 25°C Ar atmosphere Reaction = 90 min	80 mg/g	-	(Su et al., 2014)
Cr(VI)	NZVI assembled on Fe_3O_4/ graphene	[Cr(VI)] = 40 mg/L NZVI-Fe_3O_4/graphene = 0.41 g pH = 3 Temp. = 30°C	49.5 mg/g	2nd order k_{obs} = 0.583 g/ mg· min	(Lv et al., 2014)
Zn	ZVI	[Zn] = 5-8 mg/L ZVI = 6 g/L Reaction = 7 days	0.83 mg/g	1st order k_{obs} = 66 d^{-1}	(Dries et al., 2005)

Pollutants	NZVI or Modified NZVI	Conditions	Capacity	Other	Ref.
Ni	ZVI	[Ni] = 5-8 mg/L ZVI = 6 g/L Reaction = 7 days	1.79 mg/g	1st order k_{obs} = 117 d^{-1}	Dries et al., 2005
As	NZVI/ starch	[As] = 2 mg/L, NZVI /starch = 0.045 g Temp= 25ºC Reaction = 120 min	As(III) = 12.21 mg/g As(V) = 14 mg/g	2nd order k_{obs} = 0.089 g/ mg· min	Mosaferi et al., 2014
Pb(II)	Biomaterial-supported NZVI	[Pb] = 5- 1000 mg/L, Adsorbent = 0.1 g Temp= 25ºC 24 h.	225 mg/g	2nd order k_{obs} = 0.0292 g/ mg· min	Arshadi et al, 2014
Pb(II)	Kaolin supported NZVI	[Pb] = 50- 1000 mg/L, Adsorbent = 0.1 g Temp= 30ºC Reaction = 30 h.	242 mg/g		Zhang et al. (2010)
Se(IV)	NZVI	Se(IV) = 13 mM/L NZVI = 1 g/L Temp= 22ºC	13 mM/g		Ling et al., 2015
Hg(II)	Pumice-supported NZVI	[Hg] = 60 mg/L	332.4 mg Hg/g Fe	Polytetra fluoroethylene bottles	Liu et al., 2014

2.2.3 Nanoscale zero-valent iron (NZVI) utilization in arsenic removal

Arsenic can be removed from water by several methods such as precipitation-coagulation, membrane filtration, ion exchange and adsorption (Mondal et al., 2006). Chen et al., 2009 summarized that the removal of arsenic in water can be applied with the charge-based process such as adsorption because of the oxyanionic forms of As. The dominant form of As(V) in the range of pH 2-7 is $H_2AsO_4^-$, while the form of $HAsO_4^{2-}$ will be found under alkaline condition. For arsenite, the predominant form of As(III) in the pH range of 4-7 is H_3AsO_3, whereas $H_2AsO_3^-$ and $HAsO_3^{2-}$ with negative charges can be found under the alkaline condition.

Using of nanoscale zero-valent iron (NZVI) in arsenic removal has been investigated by many researchers in the past decade. NZVI can remove contaminants via reduction or adsorption according to the core-shell structure. It has been found that the HR-TEM study of pristine NZVI showed clearly a core-shell structure that consists of zero-valent iron cover with iron oxide(s). In addition, the pristine NZVI can remove As(III) and As(V) by a rapid adsorption and then the co-precipitation with the iron corrosion product (Kanel et al. (2005); Kanel et al., 2006). Tanboonchuy et al. (2011) proposed the mechanism of arsenic removal in co-existence of both species, as shown in Figure 2.4. The proposed mechanism implied that the adsorption of As(III) can be increased through the creating of new adsorptive sites by the co-precipitation of As(V) with ferrous of ferric ion.

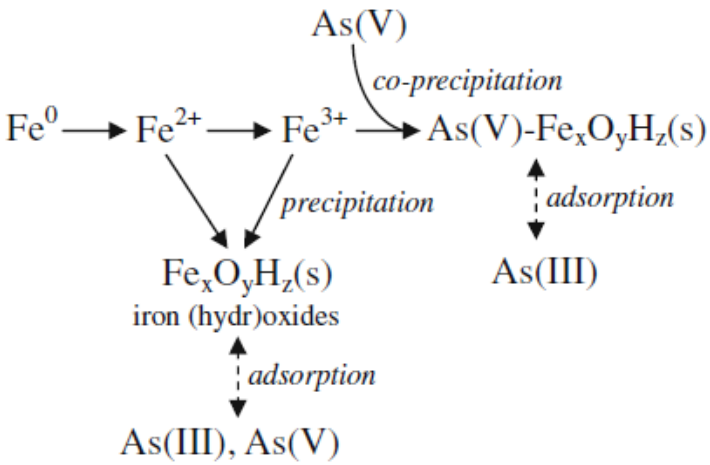

Figure 2.4 Proposed mechanism of arsenic adsorption in the co-existence of As(III) and As(V).

The performance of NZVI on arsenic removal depends on many factors. It can be summarized that As(V) can be better removed under acidic conditions than under base conditions (Bang et al., 2005; Kanel et al., 2006; Sun et al., 2006). Furthermore, there has been reported that a high amount of NZVI is needed for As(V) removal in field groundwater. The causes are the lacking of dissolved oxygen and the competition between arsenic and coexisting species. Besides of the aqueous solution pH, the amount of dissolved oxygen is also important to arsenic removal by NZVI because it is essential for the iron oxidation reaction.

The effect of species containing in groundwater has become the main issue on arsenic removal performance. Tanboonchuy et al. (2012) described the removal of arsenic removal by nano zero-valent iron process under different ions. The ions including phosphate (PO_4^{3-}), bicarbonate (HCO_3^-), sulfate (SO_4^{2-}), calcium (Ca^{2+}), chloride (Cl^-), and humic acid (HA) were studied. The work was done by 2^{6-2} fractional factorial design (FFD). It identified for major or interacting factors. As a result of FFD evaluation, $PO_4^{3-}$and HA played negatively inhibition on arsenic removal. On the other hand, Ca^{2+} was observed to play positively promoting one. As for HCO_3^- and Cl^-, the former one inhibits As(III) removal, whereas the later one enhances its removal; on the other hand, As(V) removal was affected only slightly in the presence of HCO_3^- or Cl^-. Hence, it was suggested that the arsenic removal by the nanoiron process can be improved through pretreatment of PO_4^{3-} and HA. In addition, for the groundwater with high hardness, the nanoiron process can be an advantageous option because of enhancing characteristics of Ca^{2+}.

2.2.4 Nanoscale zero-valent iron (NZVI) modification

Although NZVI is the effective material for remediation of contaminated groundwater, there are some obstacles of the in situ application. Due to NZVI tends to aggregate because of van der Waals force and magnetic interaction, this can limit its mobility in the subsurface. Moreover, the reactive surface will be deteriorated because the decreasing of surface area. In order to overcome these limitations, the using of stabilizer is one of interesting alternatives.

Phenrat and Lowry (2009) stated that the modification of the nanoparticle is typically achieved by: (1) grafting polyelectrolytes from the surface of pre-synthesized

nanoparticles; (2) physisorption of polyelectrolytes onto the surface of pre-synthesized nanoparticles; or (3) incorporating polyelectrolytes into the nanoparticles during the particle synthesis.

The last approach is a single-step synthesis procedure where a polymeric modifier interacts with the particle surface during nanoparticle synthesis. He et al. (2007) demonstrated that Fe-Pd nanoparticle synthesized in the presence of sodium carboxymethyl cellulose (CMC) are reported to be colloidally stable and are more reactive than bare Fe-Pd nanoparticles. In contrast, NZVI particles modified by physisorption of CMC become less reactive, have moderate colloidal stability, but poor transportability through porous media (Phenrat et al., 2008).

Other studies on the stabilization of NZVI have been developed. In this case, two kinds of coating materials, including poly acrylic acid (PAA) and carboxymethyl cellulose (CMC) were used to understand their mechanism. The modified NZVI was tested through the fundamental of transport in porous media. The modified NZVI with PAA (PNZVI) provided a uniform particle size of 12 nm. Both the PNZVI and the modified NZVI with CMC (CNZVI) exhibited amorphous structures, and the stabilizer was bound to particle surfaces in the form of bidentate bridging via the carboxylic group, which could provide both electrostatic and steric repulsion to prevent particle aggregation. On the basis of the breakthrough curves and mass recovery, this study observed that the mobility of PNZVI in classic Ca^{2+} concentration of groundwater was superior to CNZVI. Nonetheless, the mobility of CNZVI would be decreased less significantly than PNZVI when encountering high Ca^{2+} concentrations (40 mM). Overall, the results of this study indicate that PNZVI has the potential to become an effective reactive material for in situ groundwater remediation (Lin et al., 2010).

Moreover, modifications on NZVI by starch (S) and carboxymethyl cellulose (CMC) were examined and compared for their ability in removing As(III) and As(V) from aqueous solutions (Mosaferi et al., 2014). The batch operations were studied under following parameters such as contact time, nanoparticles concentration, initial arsenic concentration and pH. It was interesting that starch stabilized particles (S-nZVI) presented an outstanding ability to remove both arsenate and arsenite over CIt showed about ~ 36.5% greater removal for As(V) and 30% for As(III). The study also showed

removal efficiency was enhanced with increasing the contact time and iron loading but reduced with increasing initial As (III, V) concentrations and pH. Starched nanoparticles was effective in slightly acidic and natural pH values. It could be concluded that starch stabilized Fe^0 nanoparticles showed remarkable potential for As (III, V) removal from aqueous solution e.g. contaminated water.

A proper stabilizer must be cheap, widely available, and can well disperse the metals to form right particle size. Moreover, it should stimulate the reaction on the surface (Geng et al., 2009). Inoue et al. (1999) stated that chitosan is a good natural adsorbent for metal ions due to (i) high hydrophilicity of chitosan owing to a large number of hydroxyl groups, (ii) large number of primary amino groups as adsorption sites and (iii) flexible structure of the polymer chain which provides suitable configuration for complexation of metal ions. In addition, previous researches have been reviewed that chitosan nanoparticles of silver (Ag), gold (Au), platinum (Pt), and palladium (Pd) are stable in aqueous solution (Geng et al., 2009).

Chitosan was also used to stabilize bimetallic Fe/Ni nanoparticles (CS–Fe/Ni). It was confirmed that chitosan served as a stabilizer to enhance the stability of Fe/Ni and to reduce aggregation of nanoparticles. When it was tested on Cd removal, it showed a chemically controlled reaction and adsorption (Weng et al., 2013).

It was found that chitosan-carboxymethyl b-cyclodextrin complex has been successfully carried out for arsenic removal. The stabilizer by chitosan improved Fe^0 particle stabilization, when carboxymethyl b-cyclodextrin gave the composite more active sites to interact with the target ions. Removal of As (III) and As (V) was studied through batch adsorption at pH 6.0. The rate of reduction can be expressed by pseudo-second-order reaction kinetics plus the equilibrium data were well fitted to Langmuir adsorption models. The adsorbent can be separated magnetically and thus reused successfully for the removal of total inorganic arsenic from water (Sikder et al., 2014).

CHAPTER 3
RESEARCH METHODOLOGY

3.1 Experimental framework

To achieve the objectives on arsenic removal, the experiments in this study were divided to preliminary work, effect of chitosan modifying onto NZVI, and characterization. The experimental framework is illustrated in Figure 3.1.

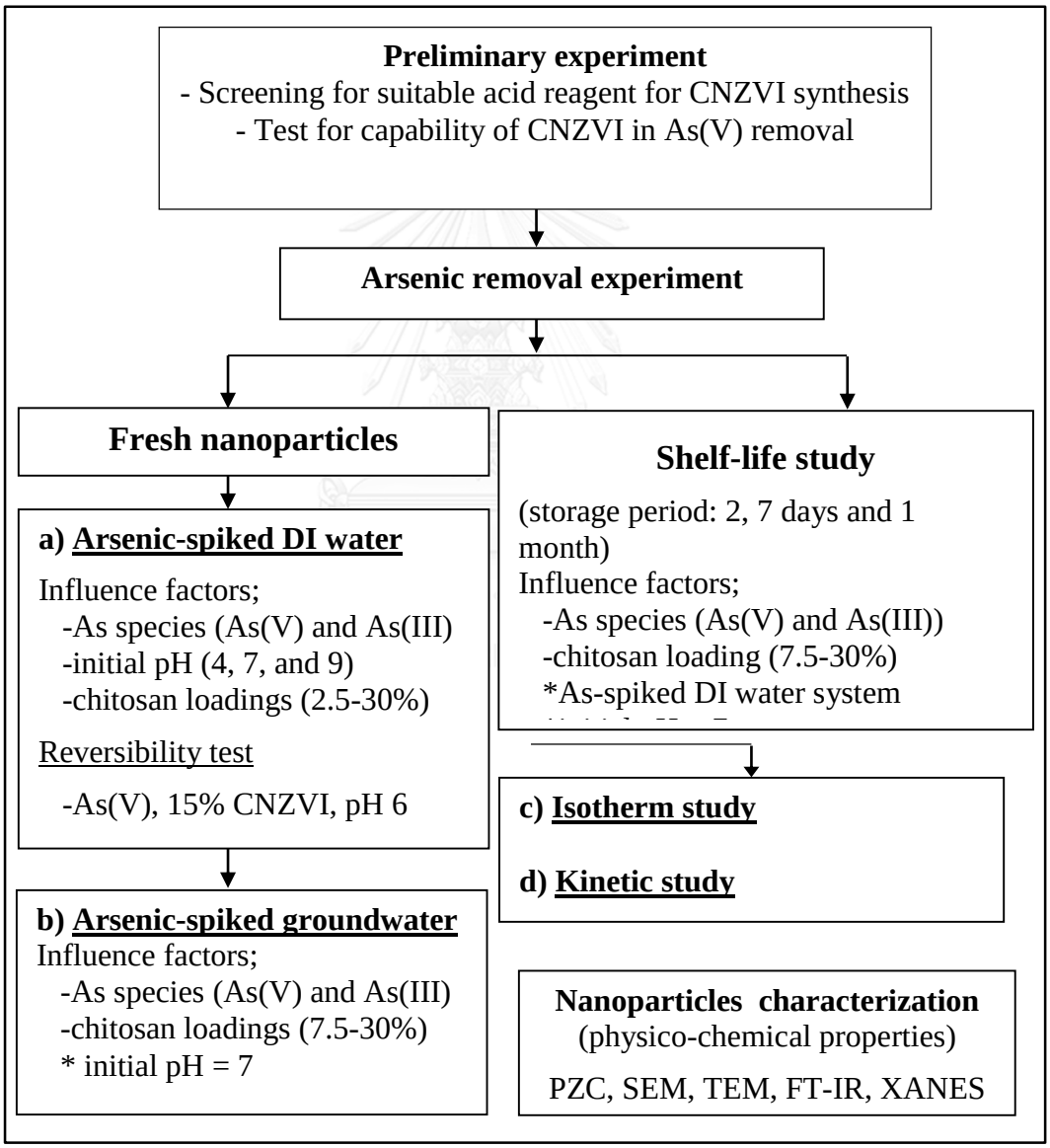

Figure 3.1 Experimental framework.

The detail of each experiment is explained as follows;

3.1.1 Preliminary experiments

The preliminary experiments were carried to determine the appropriate method for CNZVI synthesis and to evaluate whether an opportunity of using CNZVI on the arsenate removal compare to NZVI and chitosan flake. 30% by weight of chitosan loading on 0.1 g of NZVI was applied in this trial experiment.

3.1.2 Arsenic removal experiment

1) Fresh nanoparticles

Fresh nanoparticles represent as-synthesized NZVI modified with chitosan. They were used right after the synthesis. The experiment was divided into 2 parts. Firstly, the particles were tested in arsenic-spiked deionized water system. The studied factors were arsenic speciation, initial pH, and chitosan loading concentration. The performance of CNZVI and NZVI on arsenic removal in spiked groundwater was also studied as the second part. The optimal initial pH getting from the first part would be applied.

2) Shelf-life study

The study was to prove whether chitosan could prevent the oxidation of air onto NZVI. NZVI and CNZVI were kept in different time periods (2, 7, and 30 days). The comparisons were tested against arsenic removal efficiencies. The kinetic study of storage particles was also studied.

3) Reversibility study

This objective in this part of experiment was to confirm whether arsenic could be leached from the adsorptive material. Therefore, only As(V) was used as a probe chemical. One spent material was selected to investigate its reversibility by soaking it in $MgCl_2$ solution at pH 6. As concentration in filtered supernatant was examined after 16 hours of soaking.

3.1.3 Nanoparticles characterizations

Physical and chemical properties of CNZVI particles were characterized to explain the roles of chitosan on arsenic removal by NZVI.

3.2 Materials and reagents

All chemicals used in this research were analytical reagent grade. All solutions were prepared using deionized water produced by a Millipore-Q system (18.2 MΩ Mull-Q) except the experiments in As-spiked field groundwater system.

1. Ferric Chloride, $FeCl_3.6H_2O$ (99%, Merck)
2. Sodium Borohydride, $NaBH_4$ (>96%, Merck)
3. Chitosan (Acros Organics, molecular weight of 100,000-300,000)
4. Acetic acid, CH_3COOH (65%, Merck)
5. Nitric acid, HNO_3 (70%, Merck)
6. Di-Sodium hydrogen arsenate, $Na_2HAsO_4 \cdot 7H_2O$ (99-102%, Panreac Quimica SA)
7. Sodium meta-arsenite, $NaAsO_2$ (98%, Panreac Quimica SA)
8. Sulfuric acid, H_2SO_4 (96%, Carlo Erba)
9. Sodium hydroxide, NaOH (99%, Merck)
10. Magnesium chloride, $MgCl_2$ (98%, Merck)

3.3 Experimental procedures

The main procedures in this study can be categorized into 5 parts that consist of the preliminary experiments, the preparation of nanoparticles which include the pristine and dried nanoparticles, batch experiments of As removal, the study of the storage period of CNZVI, and particles characterization. The description in each procedure is explained as the following.

3.3.1 Preliminary experiments

Two kinds of acid reagent for chitosan dissolution including acetic acid and nitric acid were compared in order to select the suitable reagent for CNZVI synthesis. In view of the best condition for nanomaterial synthesis, it usually bases on the characterization such as particle size, surface area, and/or solution pH of zero point charge. However, all these are time and cost consuming. In this study, three kinds of synthesized CNZVI were tested for their removal efficiency by using As(V) as a chemical probe, compared with bare NZVI and chitosan flake. The amount of chitosan that was modified to NZVI would be expressed as percent by weight of chitosan on 0.1 g of NZVI denoted as %CNZVI. The chitosan loadings at 30%CNZVI was tested for arsenate (As(V)) removal in this step. Three kinds of CNZVI are stated as the following.

1. CNZVI-a:

   Chitosan was dissolved in acetic acid, and used in CNZI synthesis using a conventional method.

2. CNZVI-n:

   Chitosan was dissolved in 0.05M nitric acid, and used in CNZI synthesis using a conventional method.

3. CNZVI-n_{impreg}:

   Chitosan dissolved in nitric acid-impregnation method, bare NZVI was firstly synthesized and separated from solution by magnet. Then, chitosan in HNO_3 solution was added in order to mix with NZVI for five minutes.)

3.3.2 Preparation of the nanoparticles

Two types of nanoparticles which were NZVI and CNZVI were synthesized. This should be noted that the chemical reaction of the synthesis process was done under normal atmosphere, not under the inert atmosphere of nitrogen like the studies of others (Geng et al., 2009; Liu et al., 2010). The synthesis method was adapted from Wang and Zhang, 1997. The generation of NZVI by the reduction of ferric (Fe(III)) salts with sodium borohydride has been used by many research groups.

1) NZVI synthesis

According to Wang and Zhang, 1997, NZVI will be synthesized by adding 40 mL of 0.25 M $NaBH_4$ at the 4 mL/min feeding rate into 40 mL of 0.045M $FeCl_3 \cdot 6H_2O$ aqueous solution. According to the procedure, 0.1 g of NZVI will be obtained. During dropwise added, the mixture was agitated by a revolving propeller. Schematic diagram of NZVI synthesis is shown in Figure 3.2. After ten minutes, the ferric iron (Fe^{3+}) is reduced to nanoscale zero-valent iron (Fe^0) by borohydride (BH_4^-), as shown in Reaction (3.1);

$$Fe(H_2O)_6^{3+} + 3BH_4^- + 3H_2O \longrightarrow \mathbf{Fe^0} + 3B(OH)_3 + 10.5H_2 \qquad (3.1)$$

2) CNZVI synthesis

CNZVI was prepared in a single step synthesis procedure which involved the use of a modifier to react with the forming nanoparticles during the synthesis. The method of CNZVI preparation was similar to NZVI synthesis, except that a solution of chitosan (0.5% w/v) in 1% acetic acid was mixed with $FeCl_3 \cdot 6H_2O$ solution about five minutes before the $NaBH_4$ was added dropwisely. The resulted CNZVI particles were separated from the liquid by a magnet.

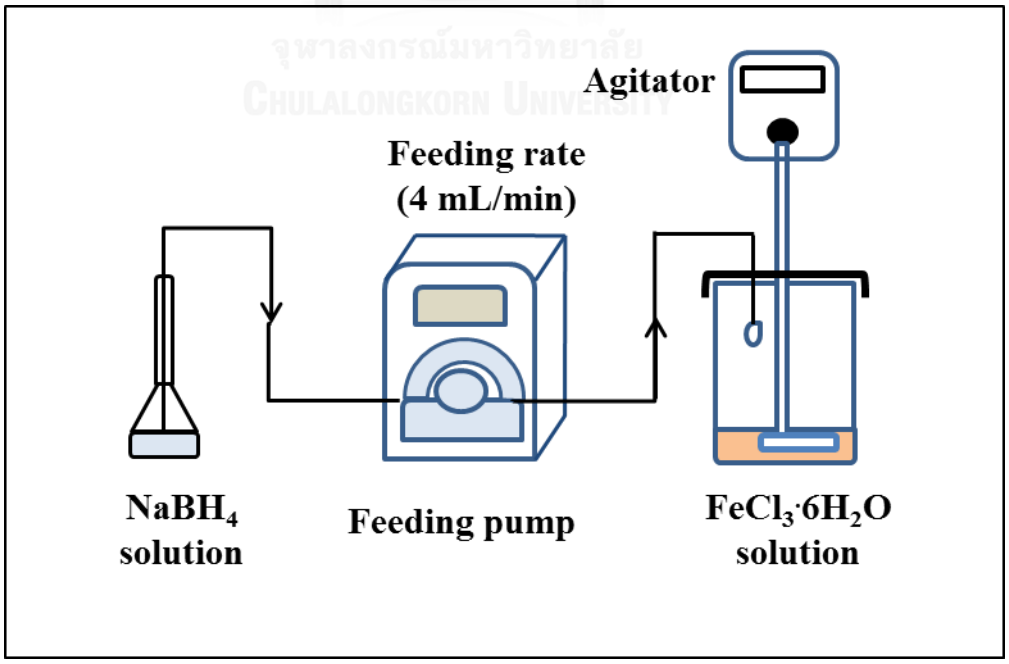

Figure 3.2 Schematic diagram for NZVI synthesis.

In case of shelf-life study and particles characterization, all fresh NZVI and CNZVI were kept in the freezer overnight. After that, the frozen nanoparticles were vacuum-dried in freeze drier for 24 hours and then kept in a desiccator until it was used and/or characterizations. The devices and the preparation steps for dried nanoparticles is shown in Figure 3.3.

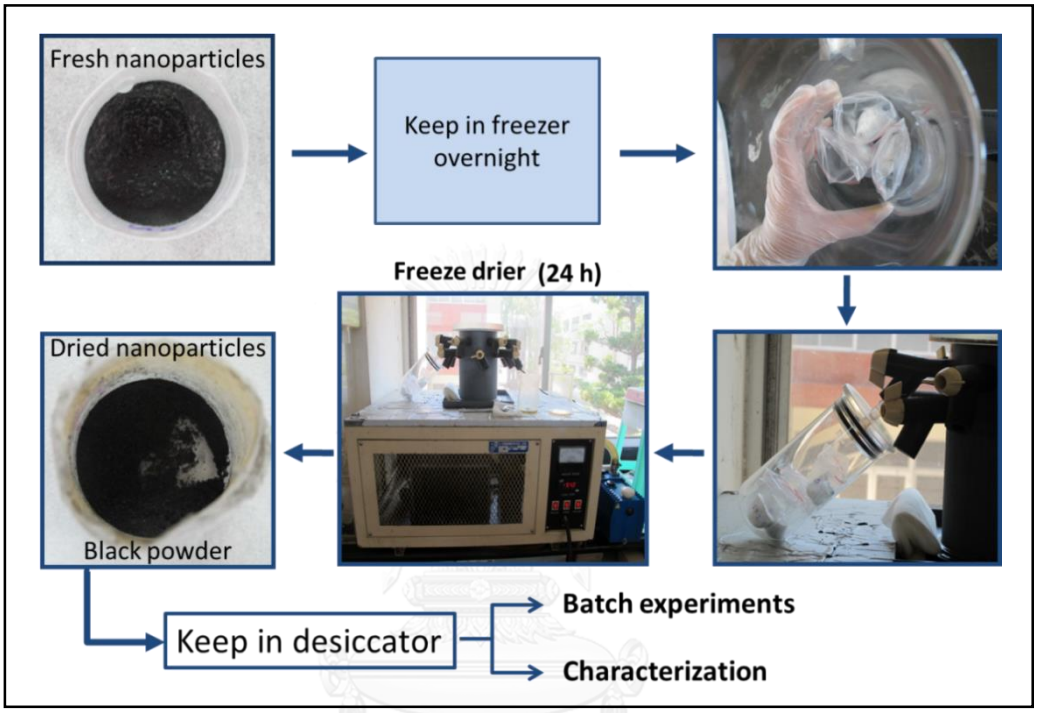

Figure 3.3 Devices and preparation steps for dried nanoparticles.

3.3.3 Arsenic removal

The experiments were carried out to examine the relative removal performances between NZVI and CNZVI. Three types of arsenic solution including arsenate (As(V)) and arsenite (As(III)) were used in the study. Each type of arsenic solution was prepared in a beaker at the concentration of 3000 µg/L with a volume of 1.5 L. An initial pH of the solution was adjusted by H_2SO_4 or NaOH solution. In case of groundwater experiment, the initial concentration of As will also be adjusted to approximately 3000 µg/L. NZVI or CNZVI was applied immediately right after the synthesis. NZVI dosage in all batches is 0.067 g/L.

The mixture was stirred under 300 rpm for 60 minutes. During the adsorption study, 10 mL sample was taken at different time intervals. It was filtrated through 0.45 µm membrane to remove the solid particles. Nitric acid was added into the sample before the ICP analysis as shown in Figure 3.4. All batch experiments were done in duplicate.

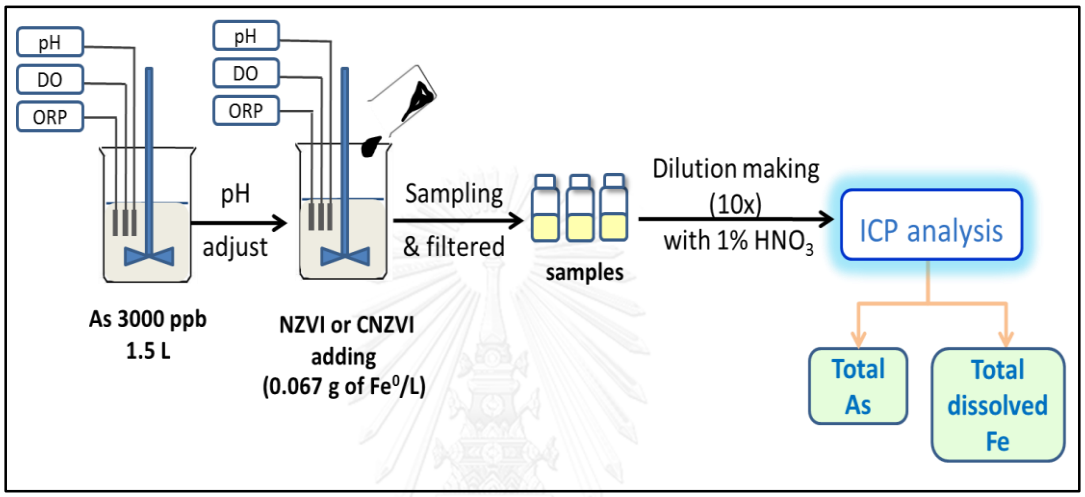

Figure 3.4 Schematic diagram for As removal experiment.

This experiment was divided into 2 parts as follows;

1) As-spiked DI water

Arsenic solution was prepared in deionized water (DI water). To study the efficiency of CNZVI in arsenic removal, the parameters were varied as the following.

(a) Initial As species; As(V) and As(III)

(b) Chitosan loadings; 2.5%, 7.5%, 15%, and 30% CNZVI

(c) Initial pH; 4, 7, and 9

All results were compared with those over NZVI.

2) As-spiked field groundwater

As(V) and As(III) were spiked into field groundwater of Chia Nan University of Pharmacy and Science to prove the removal reactivity of CNZVI and NZVI. The average concentration of total arsenic in this field groundwater has found to be approximately 40 µg/L. Then, the field groundwater would be spiked with As to obtain an initial concentration of 3000 µg/L. The initial pH of the solution was adjusted to the optimal value that can be concluded from the experiment in DI water. The effect of chitosan loadings was studied. The background ions in groundwater, such as phosphate, bicarbonate, and calcium, were examined in order to use as baseline data.

3) Shelf-life study

Stored nanoparticles of NZVI and CNZVI were tested for their arsenic removal efficiency to prove whether chitosan can protect NZVI from air oxidation. NZVI and CNZVI were vacuum-dried in freeze drier for 24 hours and then kept in desiccator. The storage periods were 2, 7 days, and 1 month since the nanoparticles were synthesized. The batch experiments of As removal were done at the initial pH 7. The studied factors were as follow;

: storage period; 2, 7 days, and 1 month

: chitosan loading; 7.5%, 15% and 30% CNZVI

: initial arsenic species; As(V) at the concentration of 1000 µg/L

3.3.4 Reversibility test

One spent material (in this case 15%CNZVI) was selected to investigate its reversibility. The As(V)-treated CNZVI was separated and washed with water to remove aqueous As. Then, it was soaked into 50 mL of 0.05 M $MgCl_2$ solution overnight. During the soaking, a mild stirring was applied. The pH condition was set at 6, adjusted by HCl and/or NaOH. Aliquots of supernatant solution were filtered through 0.45 µm membrane to remove the solid particles. Nitric acid was added into the sample before the ICP analysis for the amount of As(V) desorbed. This objective in this part of experiment was to confirm whether arsenic could be leached from the adsorptive material. Therefore, only As(V) was used as a probe chemical.

3.4 Particle characterization

Five main characterizations were used to evaluate material properties as the following.

1. Surface charge was measured by salt addition method (Mustafa et al. 2002).
2. Surface morphology and elements composition was analyzed by scanning electron microscopes with energy-dispersive X-ray spectroscopy (SEM-EDS: JSM-5800LV).
3. Morphology of the particles (particle image and dispersion) was observed by transmission electron microscopy (TEM: TECNAI G^2 20 (FEI)).
4. Interaction between NZVI and chitosan molecule has identified by Fourier transform infrared spectroscopy (FTIR: JASCO 460 PLUS) spectrometer.
5. Iron (Fe) speciations was analysed by X-ray absorption near edge structure (XANES) technique. The analysis was supported by Synchrotron Light Research Institute (Public Organization), Thailand.

3.5 Analytical methods

The total dissolved iron and total arsenic concentration were measured by inductively coupled argon plasma (ICP) using Thermo Scientific, Model iCAP 6000 series (Thermo Scientific, USA) and Optima 7300DV (PerkinElmer, USA). For the DO measurement, the DO meter (Oxi 330i) was used, while the pH and ORP meters (Suntex TS-1) were used for pH and ORP measurements, respectively.

CHAPTER 4
RESULTS AND DISCUSSION

4.1 Preliminary experiment

Acetic acid and nitric acid that can be used for dissolving of chitosan was studied to compare their effects on a complex of nanoscale zero-valent iron with chitosan (CNZVI) synthesis and CNZVI performance. The efficiency of synthesized CNZVI was proved by using As(V) as a chemical probe, compared with bare nanoscale zero-valent irons (NZVI) and chitosan flake.

4.1.1 Effect of acid reagents

Due to chitosan flakes can dissolve in several kinds of acid solution, the acid reagents which were nitric acid (HNO_3) and acetic acid (CH_3COOH) were tested for the CNZVI synthesis. Chitosan solution with a concentration of 0.5% (w/v) was prepared in each kind of acid. Chitosan when dissolved in acidic solution gives viscous solutions. CNZVI-n and CNZVI-a stand for the CNZVI synthesized by using nitric acid and acetic acid as reagents for chitosan dissolution, respectively. The amount of chitosan loading to 0.1 g of NZVI was 30% by weight, and donated as 30%CNZVI. The agglomeration characteristic and also magnetic property of CNZVI particles were compared with NZVI by an observation. Then, As(V) removal performances on each kind of synthesized nanoparticles were tested.

Figure 4.1 presents the images of four kinds of synthesized nanoparticles. Black particles of NZVI (Figure 4.1(a)) were quickly agglomerate and easy to separate from solutions by a magnet after the synthesis was finished. On the other hand, dark reddish-brown particles of CNZVI-n was dispersed in solution but their magnetic property were disappeared because they were unable to separate from solution by a magnet as shown in Figure 4.1(b). Nitrate ion was claimed about its potential negative effects on NZVI reactivity. Nitrate reduction to nitrite and ammonia by NZVI was previously reported (Yang and Lee, 2005; Hwang et al., 2011; Kim et al., 2015), but these products were not measured here. Mishra and Farrell (2005) suggested that nitrite, which is an intermediate of nitrate reduction by NZVI, may be responsible for the

formation of the protective ferric oxide outer layer. In addition, Liu et al. (2007) also reported that the passivating iron oxide layer is formed by the promoting of nitric acid.

For the reason that CNZVI-n particles cannot separate from the solution by magnet, therefore, the other synthesis method which was impregnation method was attempted. This means bare NZVI was firstly synthesized and separated from solution by magnet. Then, chitosan in HNO_3 solution was added in order to mix with NZVI for five minutes. The image of CNZVI-n that was obtained by impregnation method is shown in Figure 4.1(c). The particle agglomeration was observed similar to bare NZVI. This kind of particles (CNZVI-n_{impreg}) was tested for the capability of As(V) removal in the next experiment.

In case of CNZVI-a, it was observed that black particles of NZVI were covered by a viscous film as shown in Figure 4.1(d). It was observed that CNZVI-a particles were much more difficult to separate from solution by magnet compare with bare NZVI. However, it was applicable. It could be expected that NZVI particles were covered with chitosan.

4.1.2 Discussion of acid influence

The synthesized materials obtained from section 4.1.1, NZVI and chitosan flakes were tested for the removal capacity by using As(V) as a chemical probe. As(V) solution of an initial concentration 3000 µg/L with initial pH solution at 7 were used. The profiles of As(V) removal are shown in Figure 4.2(a).

Insignificant As(V) removal was observed by using chitosan flakes, while reduction of As(V) was obviously found by using NZVI and CNZVIs. Interestingly, CNZVI-a could improve the As(V) removal performance over using bare NZVI and CNZVI-n.

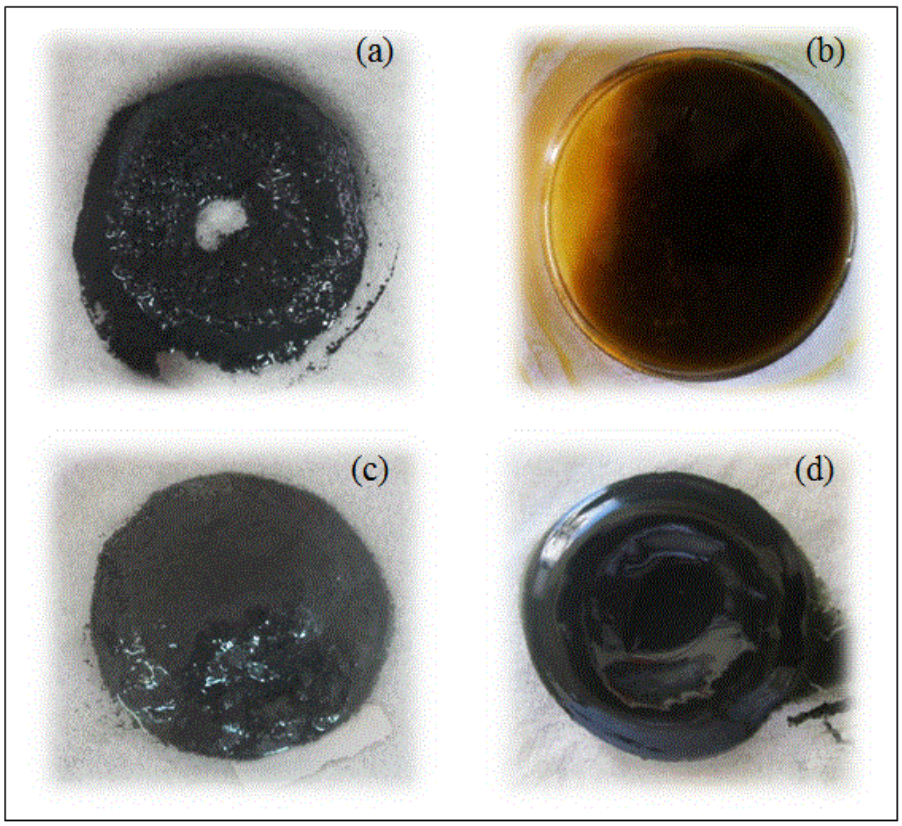

Figure 4.1 Images of synthesized nanoparticles (a) NZVI, (b) CNZVI-n (chitosan in nitric acid-conventional method), (c) CNZVI-n_{impreg} (chitosan in nitric acid-impregnation method), and (d) CNZVI-a (chitosan in acetic acid).

NZVI or Fe^0 in the solution can be readily oxidized into a primary product which is ferrous iron or Fe^{2+}. Then, Fe^{2+} can be further oxidized into ferric iron or Fe^{3+}, as shown in reaction (4.1) - (4.3) (Triszcz et al., 2009).

$$Fe^0 + 2H_2O \rightarrow Fe^{2+} + H_2 + 2OH^- \quad (4.1)$$

$$2Fe^0 + 2H_2O + O_2 \rightarrow 2Fe^{2+} + 4OH^- \quad (4.2)$$

$$4Fe^{2+} + 2H_2O + O_2 \rightarrow 4Fe^{3+} + 4OH^- \quad (4.3)$$

Figure 4.2(b) shows total dissolved iron profiles using those materials. The profiles of total dissolved iron of material combined with chitosan, especially by using acetic acid as a solvent were found compared to using NZVI.

Considering nitric acid as a solvent for chitosan preparation, the total dissolved iron on CNZVI-n could be referred to the passivation phenomena. As known, nitric acid could readily react with iron and form oxide film layer on iron surface (Thanos, 1986; Mishra and Farrell, 2005). That oxide film on CNZVI-n_{impreg} surface may protect Fe^0 from further oxidation reaction resulted in less total dissolved iron detected in the sample solution.

In case of CNZVI-a usage, it could be observed that lowest concentration of total dissolved iron was detected. After ferric iron (Fe^{3+}) was reduced to Fe^0 by borohydride (BH_4^-), some of Fe^0 may react with acetate ion to form iron acetate [$Fe(CH3COO)_2$], as presented in Equation (4.4) (Weber et al., 2011). Besides, Das et al. (2013) reported that iron acetate could be utilized as an adsorbent for arsenic removal.

$$Fe + 2CH_3COOH \rightarrow Fe(CH_3COO)_2 + H_2 \qquad (4.4)$$

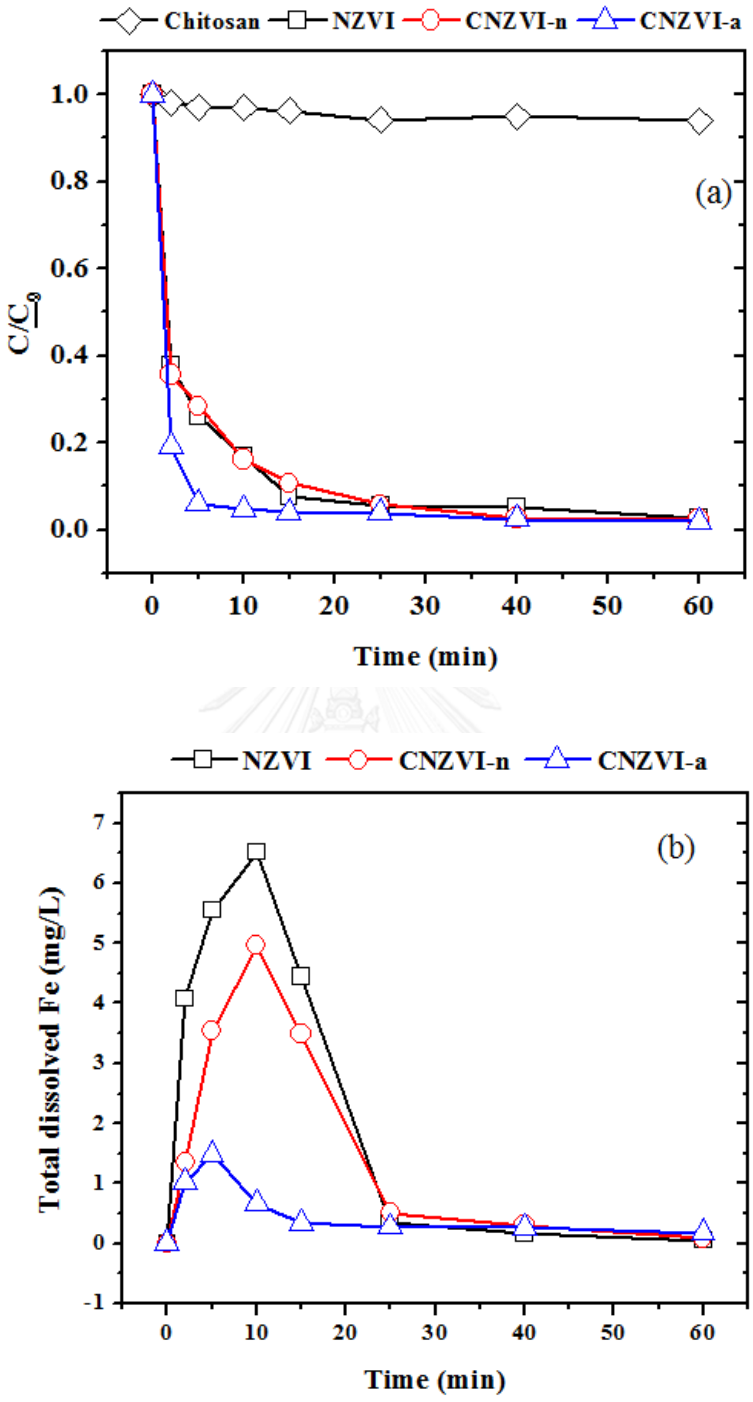

Figure 4.2 Profiles of (a) As(V) reduction and (b) Total dissolved iron concentration in the presence of different materials. Condition: $[As(V)]_i$ = 3000 µg/L, NZVI dosage = 0.067 g/L, and chitosan loading on NZVI = 30% (w/w).

4.1.3 Conceptual behavior of synthesized CNZVI

Based on above results, possible reaction pathways of CNZVI synthesized was illustrated in Figure 4.3. The amine groups of chitosan polymer are weak bases that will deprotonate water. As shown in Figure 4.3, chitosan first complexes with ferric ion at the amine sites in their deprotonated form. The Fe^{3+} may be then reduced to Fe^{0} after the addition of sodium borohydride.

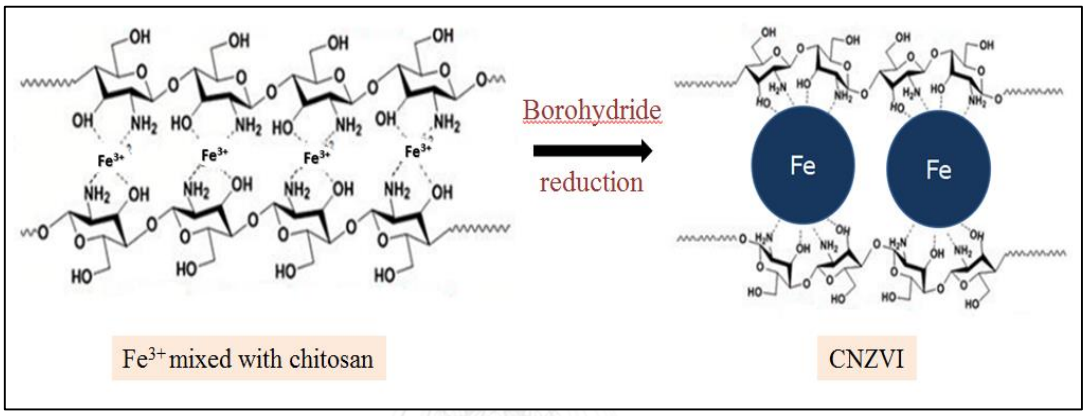

Figure 4.3 Conceptual behavior of CNZVI synthesized.

As mentioned earlier, when NZVI was presented in the solution, it can be oxidized by dissolved oxygen to the primary product Fe^{2+} rapidly, according to Equations (4.1) and (4.2). The Fe^{2+} will be further oxidized into Fe^{3+}, as shown in Equation (4.3) Then, with the oxygen dissolving in the solution, both Fe^{2+} and Fe^{3+} resulted in several forms of iron (hydr)oxides, Equations (4.5)-(4.9).

$$Fe^{2+} + 2OH^{-} \rightarrow Fe(OH)_2\downarrow \quad (4.5)$$

$$Fe^{3+} + 3H_2O \rightarrow Fe(OH)_3\downarrow + 3H^{+} \quad (4.6)$$

$$6Fe(OH)_2\downarrow + O_2 \rightarrow 2Fe_3O_4\downarrow + 6H_2O \quad (4.7)$$

$$Fe(OH)_3\downarrow + 3H^{+} \rightarrow FeOOH\downarrow + H_2O \quad (4.8)$$

$$FeOOH\downarrow + Fe^{2+} \rightarrow Fe_3O_4\downarrow + 2H^{+} \quad (4.9)$$

From this initial step, acetic acid (CH_3COOH) was selected as a solvent for chitosan by preparing 0.5% by weight of chitosan in 1% (v/v) of acetic acid in order to synthesis modified NZVI in further studies.

4.2 Characterizations

4.2.1 Point of zero charge (PZC)

NZVI and all levels of chitosan loading of CNZVI were measured for the PZC by the salt addition method (Mustafa et al., 2002). The PZC values of 2.5, 7.5, 15, and 30% w/w chitosan loading on NZVI are shown in Table 4.1. It was found that the higher chitosan loading, the higher value of pH_{PZC} was observed. This may be caused by the hydrogen of amino group ($-NH_2$) in chitosan. As known, the surface charge of particles will be predominantly positive when the solution pH is lower than pH_{PZC}, whereas a negative charge will be observed at the pH value higher than pH_{PZC} (Hiemenzm and Rajagopalan, 1997). This implies that the charge of 30% CNZVI still remaining positive in the solution until the pH value is higher than 10.1, while the NZVI turns to be negatively charged when the pH is higher than 7.75. The result agrees with previous studies which presented that the PZC of pristine NZVI were 7.0 – 8.0 (Li et al., 2006; Tanboonchuy et al., 2011). Such results indicated that chitosan could improve NZVI adsorption performance, due to increasing range of positive charge of particles surface.

Table 4.1 pH_{PZC} of synthesized nanoparticles.

Sample	pH_{PZC}
NZVI	7.75
2.5% CNZVI	7.83
7.5% CNZVI	8.3
15% CNZVI	9.2
30% CNZVI	10.1

4.2.2 Nanoparticles image and dispersion

TEM images of dried unmodified and modified samples were taken as shown in Figure 4.4. The thin shell of iron oxides was clearly seen around NZVI particles in Figure 4.4(a) similar to others studies (Martin et al., 2008; Ramos et al., 2009; Liu et al., 2015). Due to the magnetic properties, there was the chain-like aggregation among the NZVI particles which the diameter was in the range of 30-50 nm. Although the area of each CNZVI particle was difficult to separate, it can be observed that the smaller size of NZVI were formed and cover by chitosan as shown in Figure 4.4 (b-d). The diameter of 7.5% CNZVI, 15% CNZVI and 30% CNZVI particle were found in the range of 20-40 nm, 20-30 nm, and 10-20 nm, respectively. The coverage of chitosan around NZVI may help to against the oxidation of NZVI and extend the shelf life of NZVI. This expectation will be confirmed by XANES result.

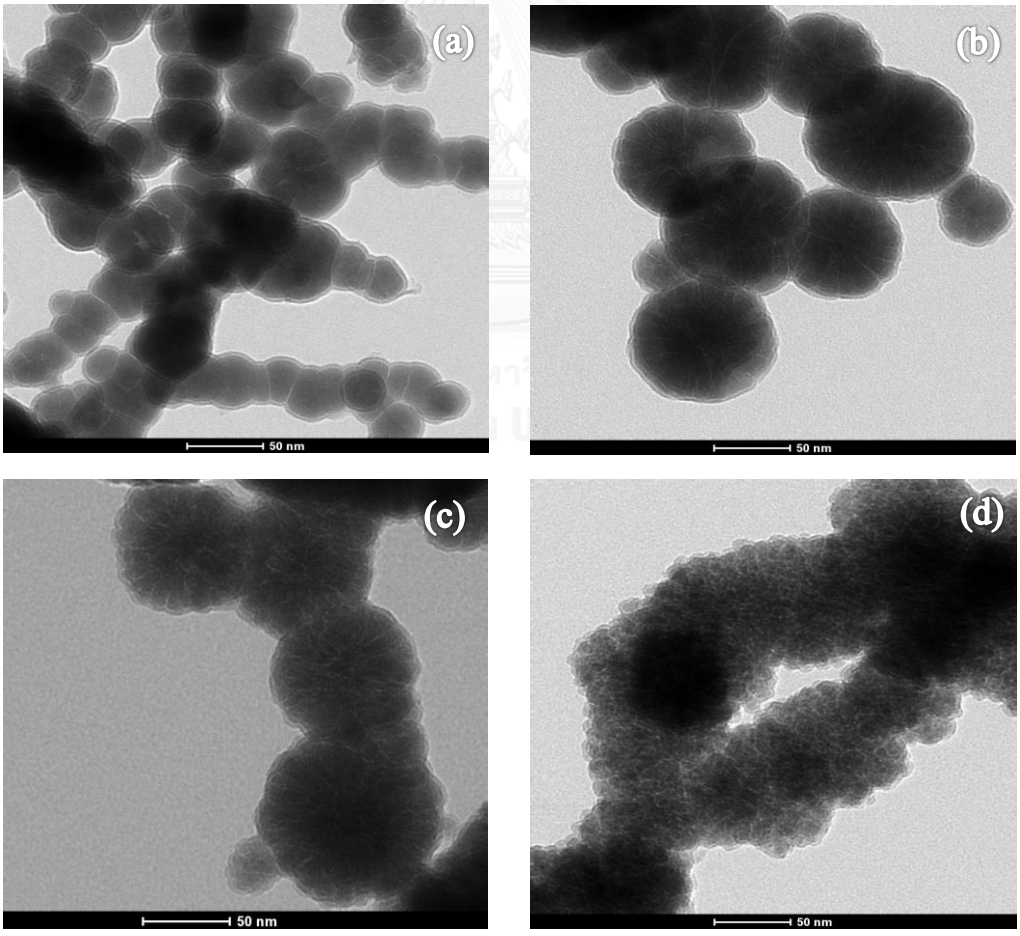

Figure 4.4 TEM Images of (a) NZVI, (b) 7.5% CNZVI, (c) 15% CNZVI, and (d) 30% CNZVI.

4.2.3 Surface morphology and element composition

SEM images of dried NZVI and CNZVI are depicted in Figure 4.5. More agglomeration seemed to be found in NZVI than in CNZVI.The roughly spherical shape of nanoparticles can be obviously seen in CNZVI images. Moreover, it looked like that the globular particles of NZVI distribute among chitosan. This result was similar to the study of chitosan stabilized bimetallic Fe/Ni nanoparticles (Weng et al., 2013). The primarily element composition at the surface of NZVI and CNZVI comprised of iron (Fe) and oxygen (O) as shown in Figure 4.6 by EDS analysis. The detected oxygen content may be the composition of iron oxides from oxidation reaction.

As presented in Figure 4.7, the X-ray element mapping demonstrates homogeneous distribution of iron (Fe). This could be concluded that the preparation technique provides well dispersion of NZVI within the modified of chitosan.

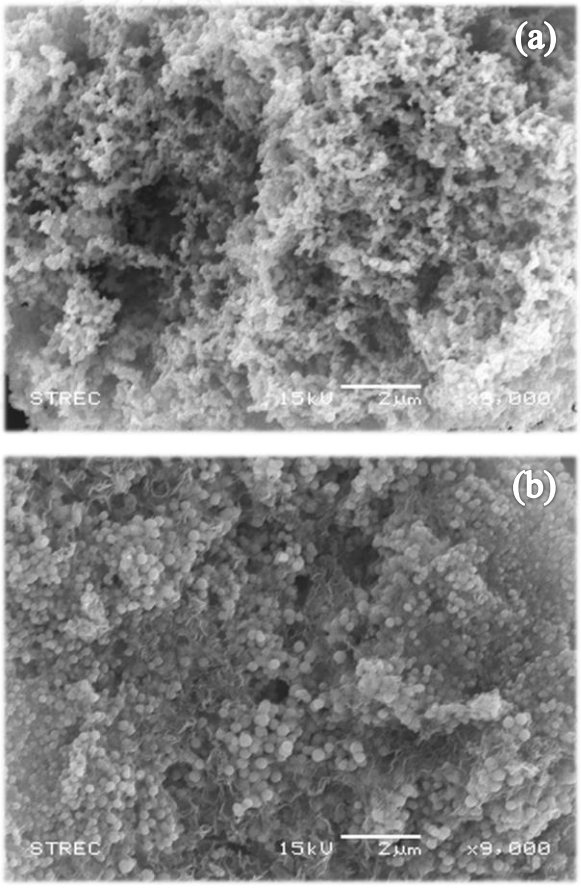

Figure 4.5 SEM Images of (a) NZVI and (b) 15% CNZVI.

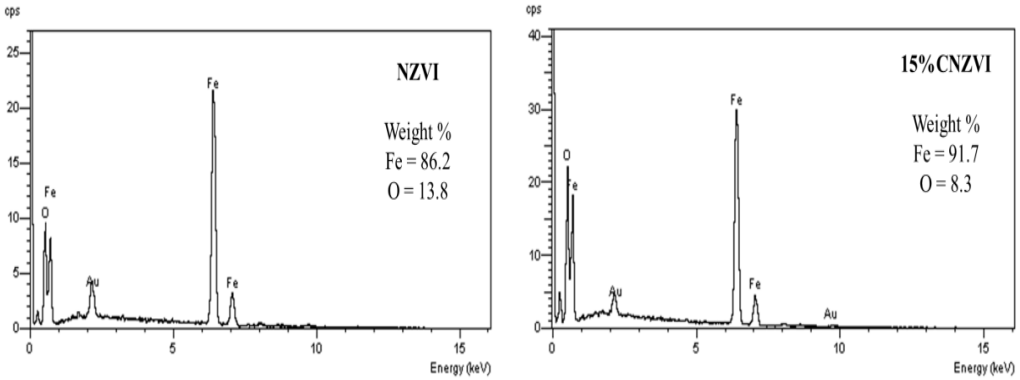

Figure 4.6 EDX spectrums of (a) NZVI and (b) 15% CNZVI.

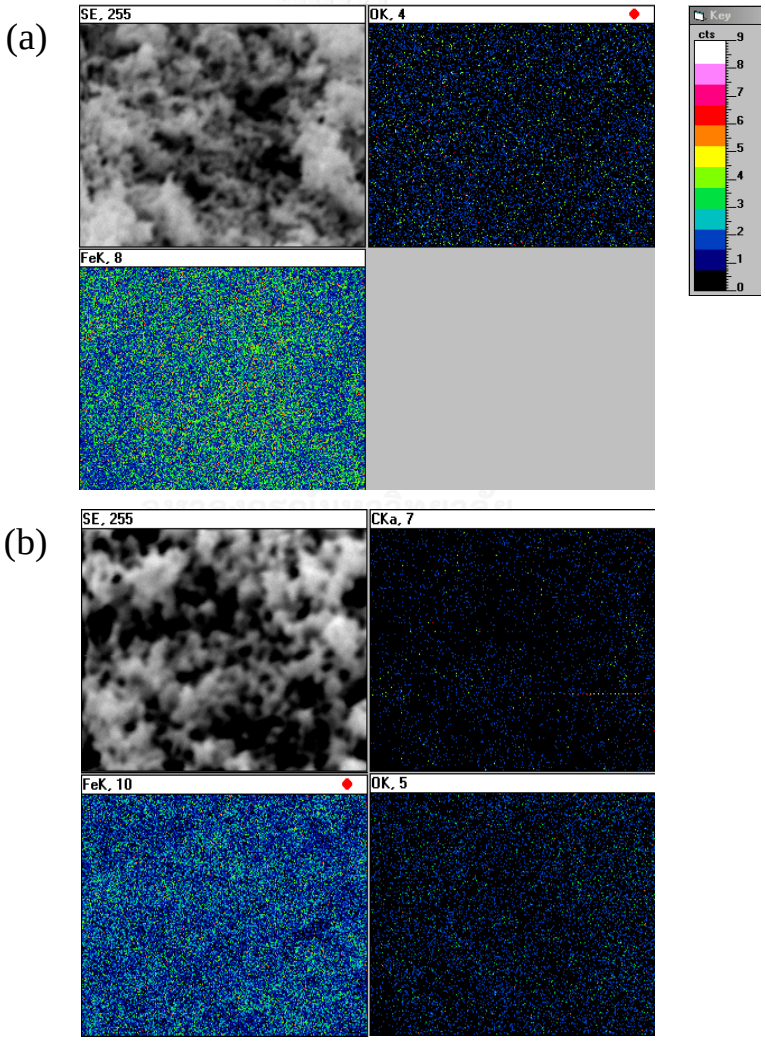

Figure 4.7 Element mappings for nanoparticles of (a) NZVI and (b) 15% CNZVI.

4.2.4 Interaction between NZVI and chitosan by FT-IR measurement

FT-IR absorption spectra of the NZVI and CNZVI samples are presented in Figure 4.8 in order to determine possible interactions of NZVI and chitosan. The characteristic peak at 3445 cm^{-1} is contributed to the N-H and O-H stretching vibration, 2918 cm^{-1} and 2877 cm^{-1} for C-H stretching, 1603 cm^{-1} may be from C-N stretching, and 1379 cm^{-1} for C-O stretching, indicating the existing of amide (II) and hydroxyl groups in chitosan (Liu et al., 2012; Horzum et al., 2013). In case of NZVI spectrum, it shows only vibration of water (3,399 and 1,630 cm^{-1}) and Fe-O stretching (596 cm^{-1}) (Bumajdad et al., 2011). After the synthesis reaction, the spectrum of modified NZVI (Figure 4.8 b-d) showed additional strong peak at 3433 to 3428 cm^{-1} that similar to that of chitosan. However, there are shifts in the bands corresponding to N-H and O-H stretching (approx.3440 cm^{-1}) that probably due to the reaction between NZVI and chitosan through the amine and hydroxide groups.

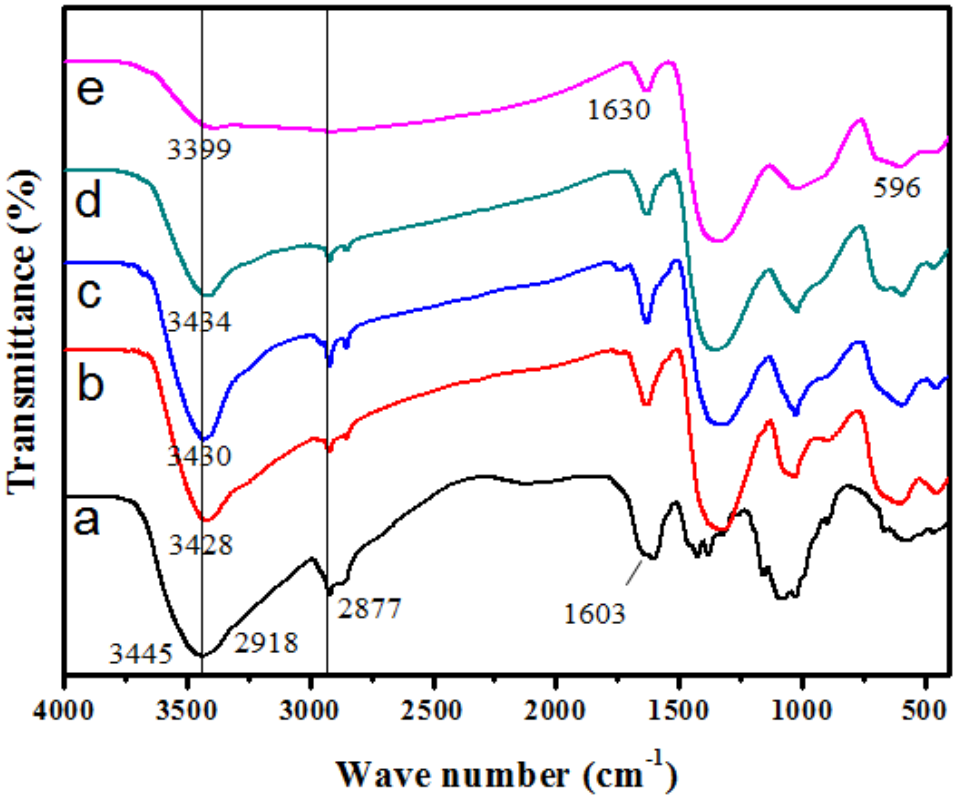

Figure 4.8 FTIR spectral. (a) Chitosan, (b) 30% CNZVI, (c) 15% CNZVI, (d) 7.5% CNZVI, and (e) NZVI.

4.2.5 Characterization by X-ray absorption near edge structure (XANES) technique

Fresh and spent materials of NZVI and CNZVI were investigated by the XANES in order to identify forms of Fe species. In addition, the amount of each Fe form was quantified. The linear combination fit of the XANES spectra was performed using XANES data of standard materials (Fe foil, Fe_3O_4, Fe_2O_3, FeO, and $FeCl_3$) as possible compositions. The composition and weight percentage of Fe species in materials are states in Table 4.2.

Approximately 60% by weight in both fresh NZVI and CNZVI samples was Fe^0 but the differences were found in others Fe speciation. Both ferrous iron (Fe^{2+}) and ferric iron (Fe^{3+}) were found in fresh NZVI meanwhile only Fe^{2+} was found in fresh CNZVI. This can be implied that the oxidation of Fe^0 to Fe^{3+} in CNZVI was retard or CNZVI was more reactive than NZVI. In addition, the existence of magnetite (Fe_3O_4) which had high magnetic property was found in NZVI only (Cornell and Schwertmann, 2004). This resulted in more agglomeration occurred in NZVI. Few amount of Iron(III) chloride ($FeCl_3$) in fresh CNZVI must be due to the remaining of chemical reagent in the synthesis.

For spent materials composition, much lower percentage of Fe^0 was found in CNZVI than that of NZVI. Since fresh CNZVI contained more Fe^0 and Fe^{2+}, it was more reactive for the further oxidation than NZVI. As many literatures claimed that higher efficiency because of higher surface area (Mayo et al., 2007; Ibrahem et al., 2012; O'Carroll et al., 2013). Therefore, more dispersion of fresh CNZVI due to less Fe_3O_4 may promote arsenic removal because of reactive surface area increasing. XANES spectra of fresh and spent materials are illustrated in Figures 4.9 and 4.10, respectively.

Table 4.2 Composition of Fe species in materials from linear combination fitting of XANES spectra

Samples	Weight (%)	R-factor	Chi-square	Reduced chi-square
Fresh NZVI		0.00004	0.004	0.00002
1. Fe foil	60.3			
2. Fe_3O_4	24.7			
3. Fe_2O_3	15.0			
Fresh CNZVI		0.0005	0.069	0.0002
1. Fe foil	62.8			
2. FeO	34.9			
3. $FeCl_3$	2.3			
Spent NZVI		0.021	0.012	0.00005
1. Fe foil	31.2			
2. FeO	24.5			
3. Fe_3O_4	19.0			
4. Fe_2O_3	25.3			
Spent CNZVI		0.0003	0.036	0.00014
1. Fe foil	15			
2. FeO	40.8			
3. Fe_3O_4	44.2			

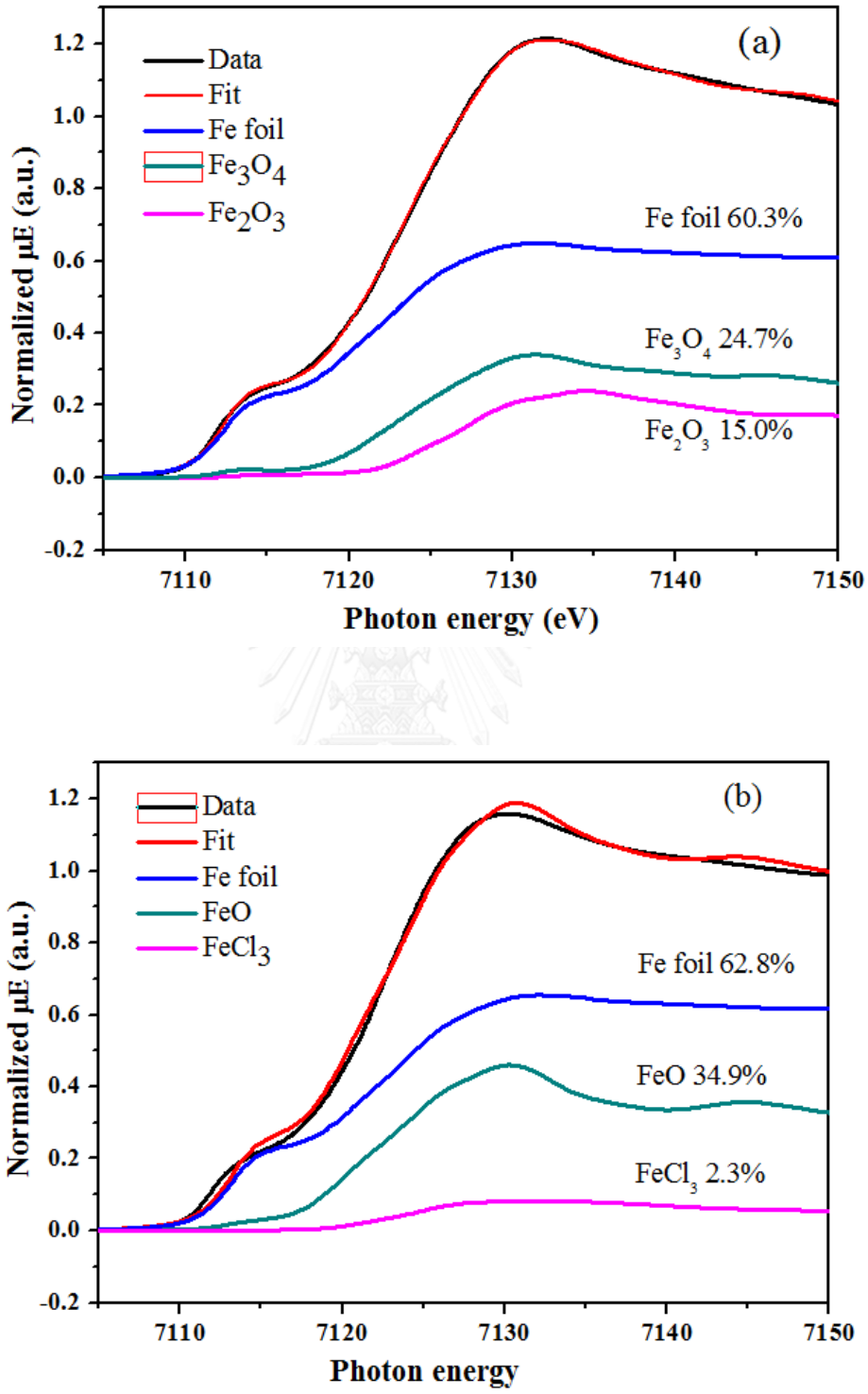

Figure 4.9 XANES spectra of fresh materials (a) NZVI and (b) CNZVI.

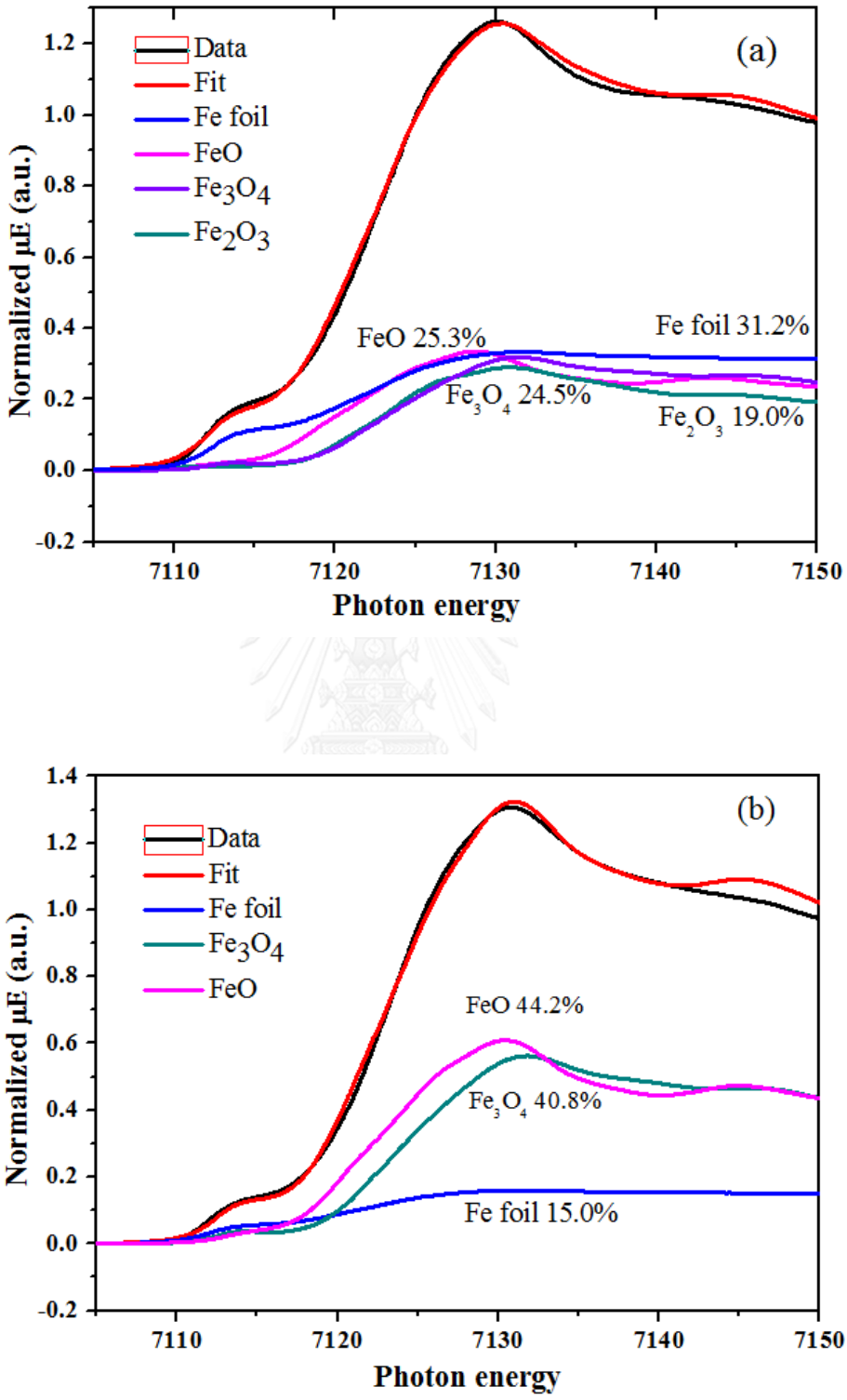

Figure 4.10 XANES spectra of spent materials (a) NZVI and (b) CNZVI.

4.3 Effect of chitosan modifying on NZVI by arsenic removal experiment

The batch experiments were carried out to examine the relative arsenic removal performance between NZVI and CNZVI. As a result of preliminary experiment, CNZVI which was synthesized by one step reaction method and using acetic acid as a reagent for chitosan dissolution were applied in all experiments.

4.3.1 Effect of chitosan loadings

With an initial As(III) and As(V) concentration of 3,000 µg/L, an influence of chitosan loading on As removal was studied under the initial pH at 7. In the preliminary experiment, 30% CNZVI was proven to accelerate As(V) removal significantly. As a result, fresh CNZVI with various percent loadings of 2.5, 7.5, 15, and 30% by weight on 0.1 g of NZVI was prepared in order to compare with bare NZVI. Arsenic removal efficiency of nanomaterials and arsenic removal profiles are shown in Table 4.3 and Figures 4.11, respectively.

As shown in Table 4.3, over 90% of both As(III) and As(V) were removed by NZVI and CNZVI but it can be observed that CNZVI seem to have more removal efficiency than bare NZVI. The highest performance was found in 30% CNZVI in both As(III) and As(V) removal. In Figure 4.11, a higher removal rate on CNZVI is found when compared to that on NZVI and both As(III) and As(V) were removed faster when the higher loading of chitosan was applied.

Table 4.3 Removal efficiency (%) of arsenic by NZVI and CNZVI.

	As(III)	As(V)
NZVI	94.9	95.7
2.5% CNZVI	96	97.1
7.5% CNZVI	97.0	98.2
15% CNZVI	97.5	98.5
30% CNZVI	99.1	98.7

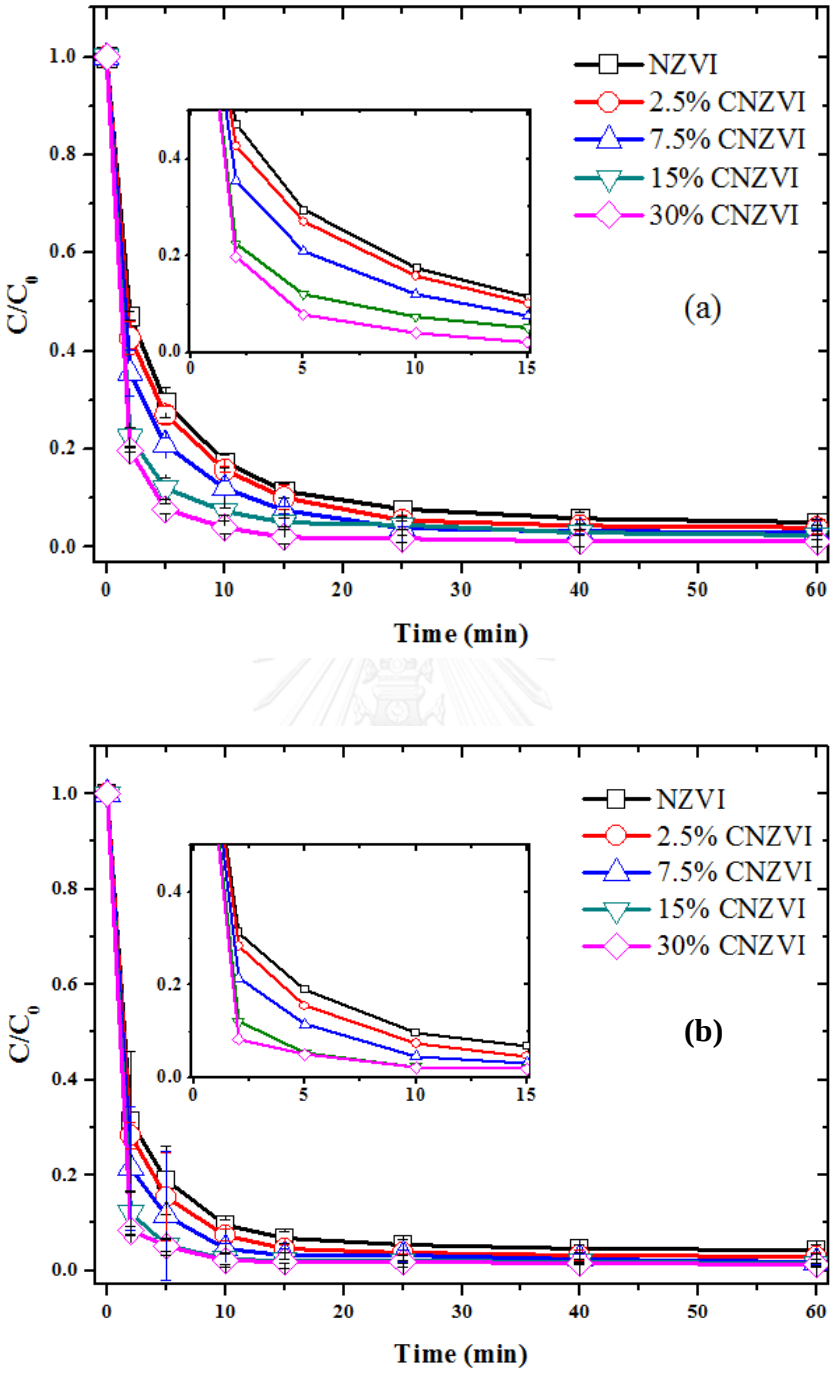

Figure 4.11 Effect of Chitosan loading on total remaining fraction of (a) As(III) and (b) As(V). Condition; As concentration 3000 µg/L, initial pH=7.

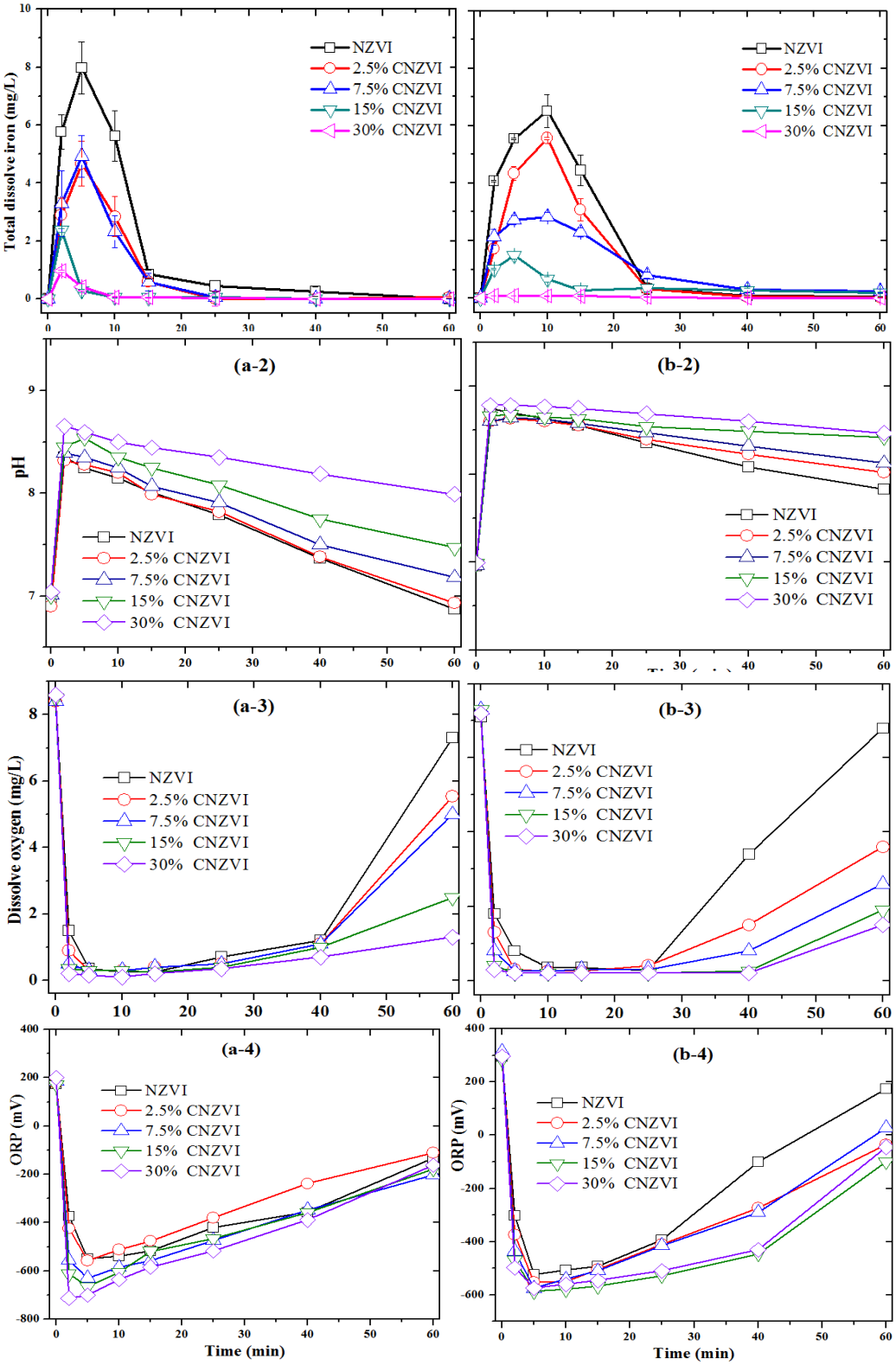

Figure 4.12 Effect of Chitosan loading on total dissolved iron, pH, DO, and ORP in the removal of (a) As(III) and (b) As(V).

Condition; As concentration 3000 µg/L, initial pH=7.

Figure 4.12 illustrates the total dissolved iron, pH, ORP, and dissolved oxygen (DO) profiles in As(III) and As(V) removal experiment. Focusing on pH variation in the system, the solution pH increased from 7 to approximately 8.4 and 8.7 within 2 minutes in case of As(III) and As(V) removal as shown in Figure 4.12 (a-2) and (b-2), rescpectively. After that, the profiles of pH gradually decreased but lower pH was found in NZVI using than that of using CNZVI. The increasing of pH value can be described by OH^- producing after NZVI/CNZVI reacted with water and oxygen to as referred in Equations (4.1) – (4.3) (Triszcz et al., 2009).

$$Fe^0 + 2H_2O \rightarrow Fe^{2+} + H_2 + 2OH^- \quad (4.1)$$

$$2Fe^0 + 2H_2O + O_2 \rightarrow 2Fe^{2+} + 4OH^- \quad (4.2)$$

$$4Fe^{2+} + 2H_2O + O_2 \rightarrow 4Fe^{3+} + 4OH^- \quad (4.3)$$

In addition, the reaction of amine groups on chitosan and water molecules leading to the release of hydroxide ions (OH^-) as shown in Equation (4.10) (Kwok et al., 2014). Therefore, the solution pH of CNZVI system was found to be slightly higher than in NZVI system. Besides, increasing amount of chitosan loading resulted in higher solution pH.

$$R\text{-}NH_2 + H_2O \leftrightarrow R\text{-}NH_3^+ + OH^- \quad (4.10)$$

The DO profiles along the experiments are shown in Figure 4.12 (a-3) and (b-3), respectively. More decreasing of DO in solution by CNZVI in two minutes indicated that the reactivity of NZVI was more accelerated because of more oxygen consumption. This may be due to the smaller particles of CNZVI provides more surface reactivity. After 25 minutes, DO in CNZVI system gradually increased meanwhile the rapidly increase was found in that of NZVI system. In both cases, the increasing of DO during this period came from the stirring effect, but the difference may be due to the reactivity of NZVI and CNZVI particles. Almost of NZVI may be already corroded, while CNZVI still reactive. This implied the coverage of chitosan can preserve Fe^0 reactivity for a longer time.

As illustrated in Figure 4.12 (a-3) and (b-3), the highest concentration of total dissolved iron was found in NZVI meanwhile the decreasing was found when percentage of chitosan loading increased during 15 minutes of reaction. After 25 minutes, very low concentration of dissolved iron was found in both NZVI and CNZVI. Moreover, almost As was removed from the solution at the same time. This may be described that almost As was removed by being adsorbed onto the iron corrosion products. The presence of iron in solution could related to the formation of iron (hydr)oxides from Fe^{2+} and Fe^{3+} according to Equation (4.5) - (4.9).

$$Fe^{2+} + 2OH^- \rightarrow Fe(OH)_2\downarrow \quad (4.5)$$

$$Fe^{3+} + 3H_2O \rightarrow Fe(OH)_3\downarrow + 3H^+ \quad (4.6)$$

$$6Fe(OH)_2\downarrow + O_2 \rightarrow 2Fe_3O_4\downarrow + 6H_2O \quad (4.7)$$

$$Fe(OH)_3\downarrow + 3H^+ \rightarrow FeOOH\downarrow + H_2O \quad (4.8)$$

$$FeOOH\downarrow + Fe^{2+} \rightarrow Fe_3O_4\downarrow + 2H^+ \quad (4.9)$$

The less amount of total dissolved iron in CNZVI system can be explained by the coverage of chitosan. Chitosan which covered Fe^0 particles can retard the oxidation of iron core structure. EDS and XANES analysis results also support this assumption. Less oxygen content was found in CNZVI surface than that of NZVI. In addition, Fe^{2+} and Fe^{3+} were found in fresh NZVI meanwhile only Fe^{2+} was found in fresh CNZVI. Although iron corrosion products have an important role in As removal due to being an adsorption sites for As, the protonated amine group on chitosan molecule as stated in Equation (4.10) can be served as adsorption site for As adsorption also. However, it can be observed that dissolved oxygen in the CNZVI system was faster consumed than that of NZVI in two minutes of reaction. This may be assumed that more Fe^0 in CNZVI reacted with dissolved oxygen than bare NZVI. Even Fe^0 was covered by chitosan, but the smaller particles can increase the reactive surface of nanoparticles. Therefore, fresh and smaller CNZVI particles may have more opportunities to be oxidized compare to the agglomerated particles of NZVI. The possibility for adsorption and co-precipitation between As and Fe^0 may be increased.

Considering at pH condition, As(III) and As(V) ions at the initial solution pH 7 are dominantly in forms of H_3AsO_3 and $HAsO_4^{2-}$, respectively. In case of neutral As(III) species, Van der Waals attraction can be occurred as reported by Kwok et al. (2014). On the other hand, the different charges of the As(V) ion and CNZVI surface is proposed to be via electrostatic attraction force. As(V) anions can be adsorbed onto the protonated amine group on chitosan as express by:

$$R\text{-}NH_3^+ + HAsO_4^{2-} \leftrightarrow R\text{-}NH_3 \cdot HAsO_4 \cdot H_3N\text{-}R \qquad (4.11)$$

The positive charge of iron (hydr)oxides resulted in being the adsorptive sites for arsenic adsorption, which enhance arsenic removal efficiency.

In addition, Manindy-Pajany et al., (2011) reported that higher As(V) adsorption capacity was found in Fe_3O_4 than in Fe_2O_3 due to the higher iron content. Regarding XANES analysis in this study, more amount of Fe_3O_4 which was 44.2% were detected in spent CNVI, meanwhile 19% of Fe_3O_4 were detected in spent NZVI. It can be concluded that CNZVI can adsorbed more arsenic than NZVI.

4.3.2 Effect of initial pH

The removal of As(V) and As(III) by using fresh NZVI and three kinds of CNZVI which were 7.5, 15 and 30% chitosan loading were carried out under the initial pH of 4, 7, and 9. As shown in Figures 4.13(a) and 4.13(b), the results demonstrate that the arsenic adsorption performance by NZVI at the inititial state is apparently influenced by initial solution pH, as also evidenced by other similar researches (Borah et al., 2009). This study found that the acidic condition favored the removal of As(V) and As(III) when the NZVI was applied as many literatures (Bang et al., 2005; Kanel et al., 2006; Sun et al., 2006; Choong et al., 2007). This may be reasoned due to electrostatic forces.

As presented in Table 4.1, the solution pH_{PZC}'s for the synthesized NZVI is 7.75. Therefore, the surface of particles would dominated by positive charges in the acidic and neutral solution. As well known, arsenic can exist in different forms, depending on the pH condition. The pK_a values of arsenic are summarized as follows: pK_1 = 9.22, pK_2 = 12.13, and pK_3 = 12.7 for As(III); and pK_1 = 2.2, pK_2 = 6.97, and pK_3

= 11.53 for As(V) (Raven et al., 1998), respectively. In the range of low pH, the dominant form of As(V) and As(III) are $H_2AsO_4^-$ and H_3AsO_3, respectively, whereas the NZVI surface shows positive charge. The different charges of the ion and the adsorbent surface will lead to the enhancement of the arsenic removal through electrostatic attraction force. In case of neutral As(III) species, Van der Waals attraction can be occurred as reported by Kwok et al. (2014).

For the alkaline pH condition, the dominant form of As(V) and As(III) are $HAsO_4^{2-}$ and $H_2AsO_3^-$ whereas the NZVI surface becomes negatively charged as the solution pH is higher than its pHPZC value (7.75), thus the electrostatic repulsion force resulted in decreased adsorption of arsenic. As a result, the removal efficiency will decrease due to electrostatic repulsion between As and NZVI at a higher solution pH.

The interesting results occured in the higher chitosan loading. The As(III) and As(V) removal seemed to have no significant difference in performance with respect to initial pH of the solution when 15% and 30%CNZVI were applied with pH_{PZC} values being 9.2 and 10.1, respectively. This implies that both cases still show the positive charges under alkaline condition. Therefore, the enhancement of the As(V) removal can be explained by electrostatic attraction between the negative charge of As(III)/As(V) and the positive charge of CNZVI. The higher amount of chitosan loading can reduce the sensitivity of initial pH effect on the As(III)/As(V) removal. When the contact time increased, pH changed to basic condition due to the formation of OH^- from the corrosion process

In arsenic removal process, the factor affected in the partition of arsenic and iron is ORP or Eh values. Besides a function of pH changes, ORP profiles were shown in Figure 4.12 for As(III) and As(V), respectively. Considering Eh profile with pH profiles as shown in Appendix D could be confirmed that dissolved iron (Fe^{2+}) tend to precipitates to Fe_3O_4, and ready to co-precipitate with arsenic.

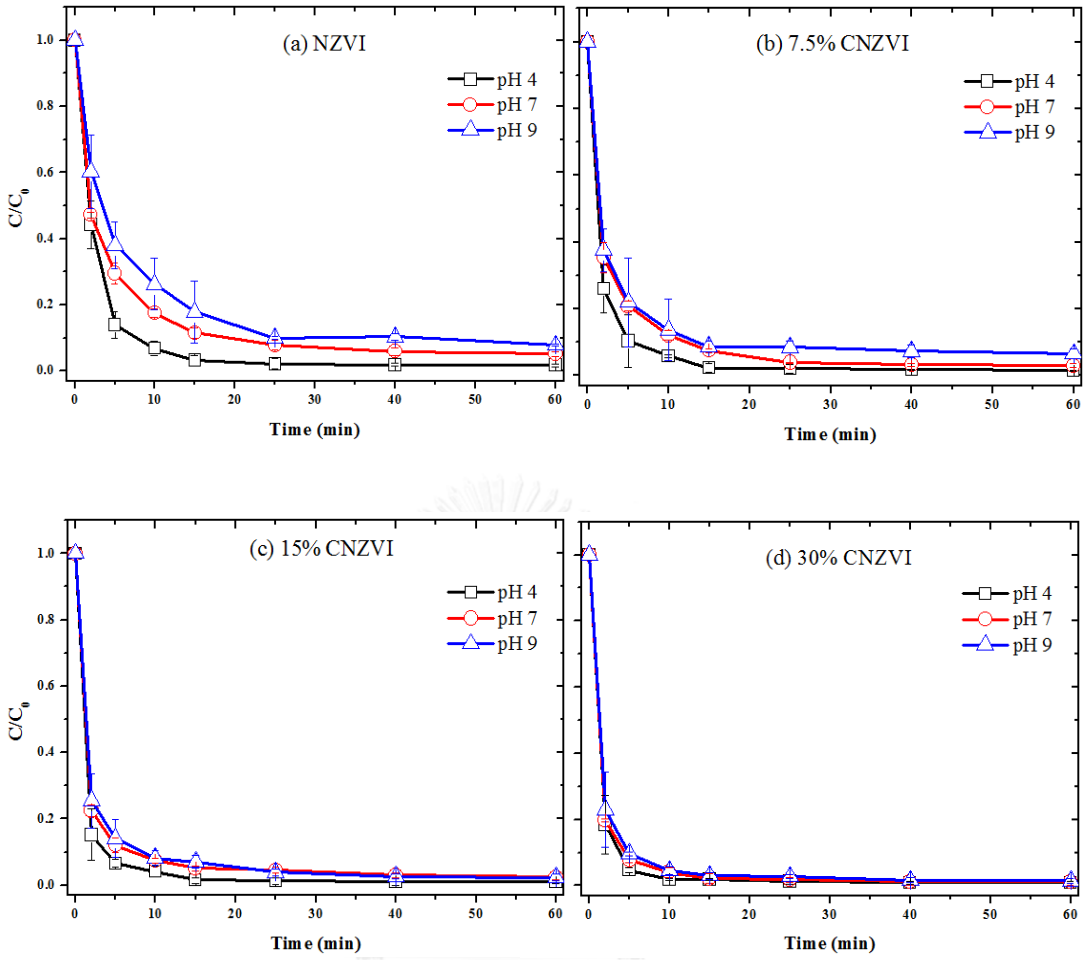

Figure 4.13 Effect of initial pH on As(III) removal by using (a) NZVI, (b) 7.5% CNZVI, (c) 15% CNZVI, and (d) 30% CNZVI.
Condition; As(III) concentration = 3000 µg/L.

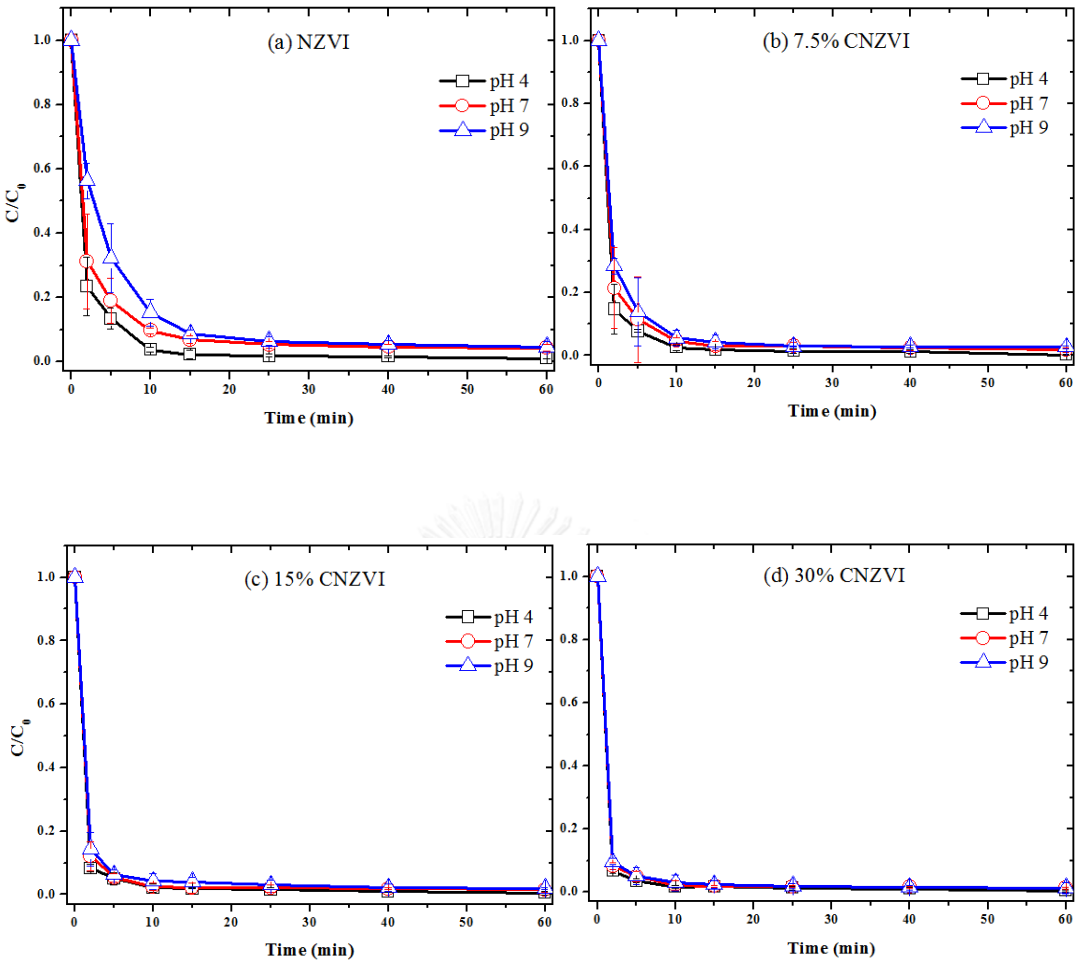

Figure 4.14 Effect of initial pH on As(V) removal by using (a) NZVI, (b) 7.5% CNZVI, (c) 15% CNZVI, and (d) 30% CNZVI. Conditions: Initial As(V) concentration = 3000 µg/L.

4.4 Field groundwater test

To determine the performance of CNZVI in As-spiked field groundwater, As(V) and As(III) were added into field groundwater collected from Chia Nan University to be approximately 3,000 µg/L of As solution. It was conducted by using 15% loading of chitosan, which was compared with the bare NZVI.

According to Figure 4.15, the higher arsenic removal in field groundwater test can be achieved by using CNZVI which it faster removal rate than NZVI. If compared with the DI water system, the removal efficiency for the groundwater test was lower due to the presence of background species present in groundwater (see Table 4.4). As reported, the sulfate can replace iron (hydr)oxides, which were adsorbed on the iron surface, leading to the decrease of adsorption sites available to arsenic (Bi et al., 2009) . The humic acid was reported to result in significant reduction in arsenic removal, due to its high tendency of being adsorbed onto the surface of iron (hydr)oxides (Rao et al., 2009). In addition, the phosphate was reported to reduce the performance of arsenic removal because of their competition for active sites on the adsorbent surface (Jegadeesan et al., 2005).

Table 4.4 Chemical characteristics of the field groundwater

Parameter	Value
pH	8-8.2
Conductivity (µS/cm)	2465-2480
Eh (mV)	28-33
Dissolved oxygen (mg/L)	4.0-5.5
Alkalinity (ppm as $CaCO_3$)	680-700
Ion species:	
Total organic carbon (ppm)	5.30
Sodium (ppm)	620.5
Calcium (ppm)	26.5
Chloride (ppm)	237
Sulfate (ppm)	33.5
Phosphate (ppm)	2.46
Heavy metals:	
Iron (ppm)	0.1-0.3
Manganese (ppm)	0.12

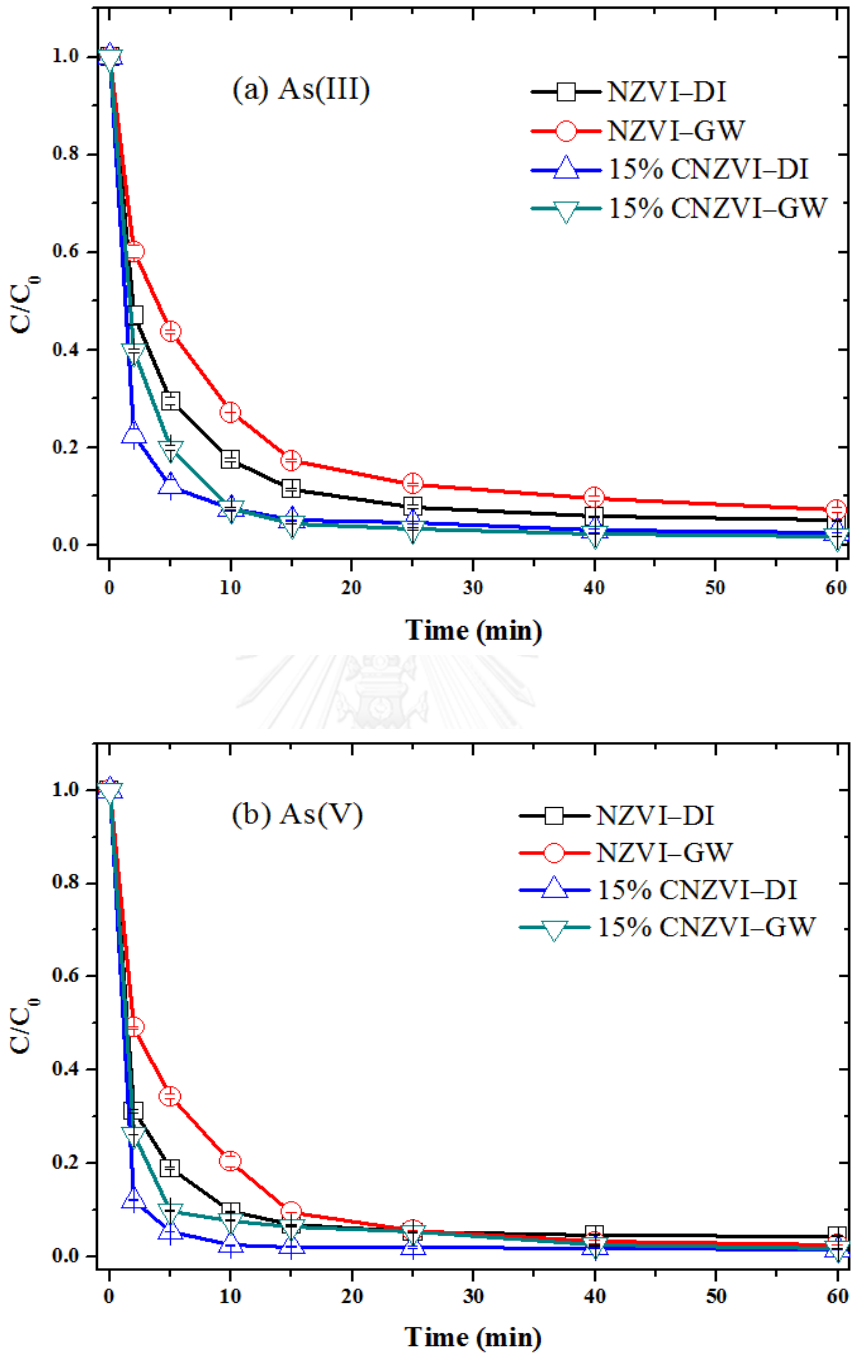

Figure 4.15 Comparison of (a) As(III) and (b) As(V) removals by NZVI and 15% CNZVI using field groundwater.

Condition; Initial As concentration = 3000 µg/L; Initial pH =7.

4.5 Reversibility test

The study of desorption of arsenic ion was carried out for spent adsorbents. In general, $MgCl_2$, Na_2HPO_4, KH_2PO_4, and NaOH have been used as desorptive solutions (Yean et al., 2005; Mamindy-Pajany et al., 2011; Tajuddin Sikder et al., 2014). In our study, $MgCl_2$ was selected for the study because it is a typical extraction solution used for trace metals, and was adopted to extract the ionic arsenic through anion exchange of Cl for arsenate (Ruttenberg, 1992; Shan et al., 2010). To scope the desorption study, 50 mL of 0.05 M $MgCl_2$ was used. The extraction time is 16 hours for extraction of the exchangeable arsenic phase.

The desorbed arsenic in this stage, representing the exchangeable arsenic phase, was found 27.2 mg/g adsorbent. Compare to its removal uptake (44.1 mg/g adsorbent), 38.3% of As(V) was desorbed from the filtrate. It indicated that arsenic in the solids was mildly sorbed on the surface of iron precipitates. The result was corresponded to the results by Mamindy-Pajany et al. (2011) involving the reversibility of As(V) adsorption onto several kinds of iron compounds such as hematite, magnetite and zero-valent iron (ZVI). It was reported that the maximum As(V) desorption which was 24% was found in magnetite, meanwhile 10% and 8% desorption were found in hematite and ZVI, respectively. Regarding to the analysis of iron species composition by XANES in this study, magnetite (Fe_3O_4) was detected as the major constituent in spent CNZVI. Even it has reported that arsenic removal process consists of many mechanisms including precipitation, co-precipitation, and adsorption. It can be concluded in this step that 40 % of arsenic removal was taken place by adsorption mechanism.

4.6 Adsorption isotherms

Arsenic removal in NZVI systems may involve many complicated processes such as surface adsorption, precipitation, co-precipitation, and redox reaction. However, the main mechanism is surface adsorption, as prove basically from its reversibility.

The adsorption isotherm is the equilibrium relationship between the concentration in the liquid phase and the concentration in the adsorbent particles at

constant temperature. The surface area and pore size are important factors. The equilibrium concentrations of the adsorbate in the liquid and solid phases are modeled using the well-known Langmuir and Freundlich isotherms.

Langmuir isotherm: The Langmuir adsorption isotherm is used to describe the equilibrium between surface and solution as a reversible chemical equilibrium between species (Crittenden et al., 2005). The adsorbent surface is made up of fixed individual sites where molecules of adsorbate may be chemically bond. Langmuir isotherm is assumed that the reaction has constant free-energy change for all sites. Moreover, each site is assumed to be capable of binding at most one molecule of adsorbate as a monolayer. The relevant formula in general form and linearized form of Langmuir isotherm are shown in Equation 4.12-4.13.

$$q_e = \frac{q_m C_e K}{C_e K + 1} \qquad (4.12)$$

$$\frac{C_e}{q_e} = \frac{1}{q_m K_L} + \frac{C_e}{q_m} \qquad (4.13)$$

where, q_e (mg/g) is the amount of arsenic ion adsorbed at equilibrium, C_e (mg/L) is the equilibrium concentration of arsenic, q_m is the maximum amount of arsenic adsorbed per unit mass of adsorbent for the formation of complete monolayer on the surface adsorbent (mg/g), and K (L/mg) is the Langmuir equilibrium constant related to energy of adsorption. The plot of C_e/q_e versus C_e as shown in Figure 4.16 (a) was used to determine q_m and K_L.

Freundlich isotherm: The Freundlich isotherm can be used for both physical and chemical sorption. It is used to describe the data for heterogeneous such as activated carbon. The Freundlich isotherm equation can be derived using the Langmuir equation to describe the adsorption onto sites of a given free energy and considering the assumption of the site energies changes logarithmically (Wittayakun and Grisdanurak, 2004). The general and linearized forms of Freundlich isotherm are presented in Equation 4.14-4.15.

$$q_e = kC_e^{1/n} \quad (4.14)$$

$$\ln q_e = \ln K + \frac{1}{n}\ln C_e \quad (4.15)$$

where, k and n are Freundlich constants, k is a measure of amount of adsorption, while n represents the degree of linearity. Both values are evaluated from the slope and interception of the plot of $\ln(q_e)$ versus $\ln(C_e)$, as shown in Figure 4.16 (b).

The investigations, to describe the interactive behavior between arsenic species and CNZVI, were conducted at initial pH 7 for As(III) and As(V) species at initial concentrations of 3000-10000 µg/L. The dosage of Fe^0 was maintained at 0.067 mg/L whereas the percentage of chitosan loading was fixed at 30% by weight.

The fitted parameters of Langmuir and Freundlich models are listed in Table 4.5. As a result of data fitting, the correlation coefficients, R^2, of the Langmuir isotherm model for As(III) and As(V) are of 0.934 and 0.979, respectively, slightly higher than those of the Freundlich isotherm model (0.849, and 0.985, accordingly). Thus, it appears that the Langmuir model can better describe arsenic adsorption in the studied system. Note that the Langmuir isotherm assumes the site energy for adsorption being equal for all surface sites and each site binding only one molecule, i.e., mono layer. As for adsorption capacity, both isotherm models show higher capacity for arsenate than for arsenite.

Table 4.5 Isotherm parameters for As(III) and As(V) adsorption

Model	Langmuir model			Freundlich model		
Parameters	q_m ($mg/g_{adsorbent}$)	K_L (L/mg)	R^2	k	1/n	R^2
As(III)	39.84	0.0250	0.934	0.0023	2.045	0.849
As(V)	46.30	0.0206	0.979	0.0106	1.528	0.985

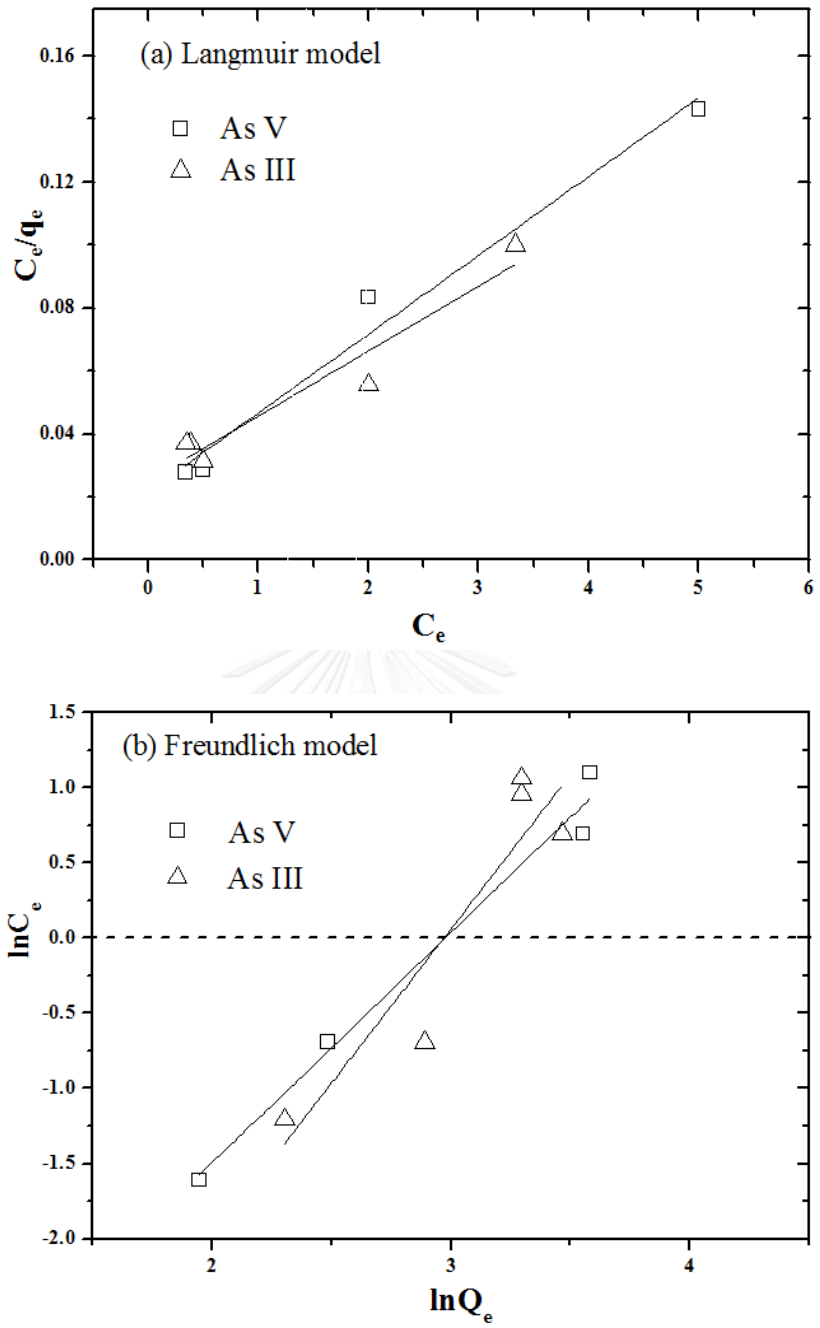

Figure 4.16 Linear plots of (a) Langmuir model and (b) Freundlich model, on As(III) and As(V) removal by 30%CNZVI.

The adsorption capacities by related chitosan modifiers were obtained from the adsorption isotherm, which was carried out in a wide range of concentration (up to 10^6 µg/L). In our study, the arsenic adsorption capacity of chitosan-composited NZVI was investigated with a lower arsenic concentration of 3000 µg/L, and it's noticed here that its capacity was calculated at the end of reaction time. As shown in Table 4.6, the as-obtained chitosan seems unfavorable to arsenate capture when compared to other reports.

Table 4.6 Literature data on arsenic adsorption capacity under different conditions

Arsenic adsorption, mg/g	Conditions	Ref.
As(V): 5.05 $_{isotherm}$ As(V): 20.9 $_{isotherm}$	Chitosan flakes; pH 7 Chitosan flakes; pH 5.5	Benavente (2008)
93.46$_{isotherm}$	Chitosan-coated Al_2O_3, pH 4 and $C_0 = 10^4–10^6$ µg /L	Boddu et al. (2008)
As(V): 1.33 $_{isotherm}$ As(V): 14.16 $_{isotherm}$	Chitosan, pH 5.5 Chitosan, pH 3.5 and C_0 = 100–10,000 µg/L	Kwok et al. (2009)
0.56 $_{isotherm}$ 200 $_{isotherm}$	Chitosan/PVA Chitosan/PVA/NZVI pH 4 and C_0 = 100–10,000 µg/L	Chauhan et al. (2014)
As(V): 2.92 $_{eq}$* As(III): 39.8 $_{isotherm}$ As(V): 46.3 $_{isotherm}$	- Chitosan flakes - 30 % CNZVI - 30 % CNZVI pH 7 and C_0 = 3,000 µg/L	This study

* Calculated at the end of the test.

4.7 Adsorption kinetics

It seems that all removals by adsorption are finished in a short period of time. In this study, the kinetics via an adsorption and overall are considered. First, the experimental data was analyzed by three general types of kinetic adsorption models. These include pseudo-first order, pseudo-second order, and intraparticle diffusion models, which are expressed as Equation (4.16)–(4.18) below.

Pseudo first-order model;

$$\frac{dq_t}{dt} = k_1(q_e - q_t) \qquad (4.16)$$

Pseudo second-order model;

$$\frac{dq_t}{dt} = k_2(q_e - q_t)^2 \qquad (4.17)$$

Intraparticle diffusion model;

$$q_t = k_i t^{0.5} + A \qquad (4.18)$$

where, q_t (mg/g) is the amount of arsenic adsorbed on the adsorbent surface at any time (min), q_e (mg/g) is the adsorption capacity of adsorbent at equilibrium, k_1 (min^{-1}) is the rate constant of pseudo first-order, k_2 (g/(mg·min)) is the rate constant of pseudo second-order, k_i (g/(mg·$min^{1/2}$)) is the rate constant of intraparticle diffusion model, t is the time (min) and A is the intraparticle diffusion constant.

The kinetic parameters of each model were evaluated by the linearization of model as described in Table 4.7. The plots of linearized equations are shown in Figure 4.17 (a-c). The calculated values were further taken from the slopes and intercepts and given in the same table. The results showed that the correlation coefficients (R^2) for the pseudo first-order model were 0.78 and 0.60 for As(III) and As(V), respectively. On the other hand, the correlation coefficients for the pseudo second-order model were 0.97 and 0.99 for As(III) and As(V), respectively, which are higher than those for the pseudo first-order model. The pseudo second-order model was, therefore, more appropriate to describe the kinetics for this adsorption.

Besides, the mechanism rate might be dominated and limited by chemical adsorption process between arsenic molecules and the active sites of NZVI surface. Since the structure of studied adsorbents contained pores, mass transport of adsorbate molecules (arsenic) within the pores of studied adsorbents, called “intraparticle diffusion”, was also tested for studying the limiting step of the adsorption. It was noted that the plot of linearized form, which passes through the origin, could refer to intraparticle diffusion as a limiting step of the adsorption (Vasiliu et al., 2011). However, shown in Figure 4.17 (c), the experimental data could not related to linear lines passing through the origin. This might be possible that the adsorption could be simultaneously controlled by multi-diffusion steps which were film diffusion and intraparticle diffusion.

Table 4.7 Kinetic parameters for arsenic adsorption onto adsorbents.

Model	As(III)		As(V)	
	k	R^2	k	R^2
Pseudo-first order: $\ln(\frac{q_e - q_t}{q_e}) = -k_1 t$	$-k_1 = 0.174$	0.78	$-k_1 = 0.333$	0.60
Pseudo-second order: $\frac{t}{q_t} = \frac{t}{q_e} + \frac{1}{k_2 q_e^2}$	$-k_2 = 0.037$	0.97	$-k_2 = 0.027$	0.99

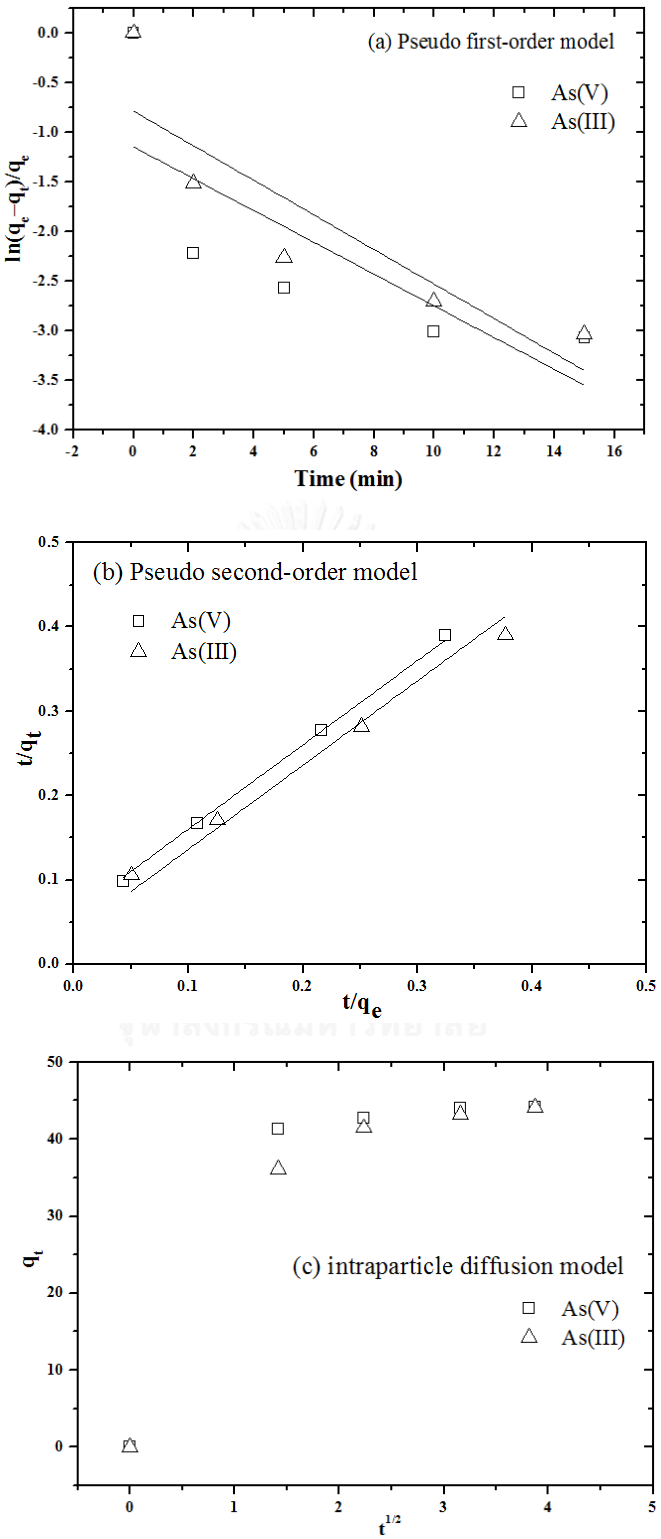

Figure 4.17 Linear plots of As(III) and As(V) adsorption on 30% CNZVI, evaluated for (a) pseudo first-order, (b) pseudo second-order, and (c) intraparticle diffusion models.

4.8 Overall removal kinetics

To understand the removal kinetics, on freshly used of NZVI and CNZVI, two kinetic models including pseudo first-order and pseudo second-order models were selected. The integration of pseudo first-order kinetic is given by Equation (4.19), where C_0 is the initial concentration of arsenate solution, C is concentration of arsenate as a function of time. k_1 (min^{-1}) is the pseudo-first order rate constant. Value of k_{10} can be calculated from the slope and intercept of the linear plotting of $\ln(C_0/C)$ versus t.

$$\ln\frac{C}{C_0} = -k_{10}t \qquad (4.19)$$

The integration of pseudo second-order model is expressed in Equation (4.20), where k_{20} ($L\cdot(\mu g\cdot min)^{-1}$) is the pseudo-second order rate constant. k_{20} can be calculated from the slope and intercept of *1/C* versus *t*, respectively.

$$\frac{1}{C} - \frac{1}{C_0} = k_{20}t \qquad (4.20)$$

The data on the removals of As(III) and As(V) by NZVI and CNZVI under different loadings of chitosan were further used to analyze their possible kinetic adsorption models, including pseudo first-order and second-order models. The kinetic parameters of each model for As(III) and As(V) are evaluated by linearization of model, as plotted in Figures 4.18 and 4.19 respectively. The results are tabulated in Tables 4.8 and 4.9. According to the correlation coefficient (R^2) of As(III) and As(V) removal, the small values (R^2 = 0.38–0.77 and 0.58-0.85) indicate poor fit on pseudo first-order kinetic model. On the other hand, the pseudo second-order model is satisfactorily fitted by the experimental data (R^2 = 0.94–0.99 and 0.994-0.996). The rate constant (k) was found to increase when the percentage of chitosan loading increased.

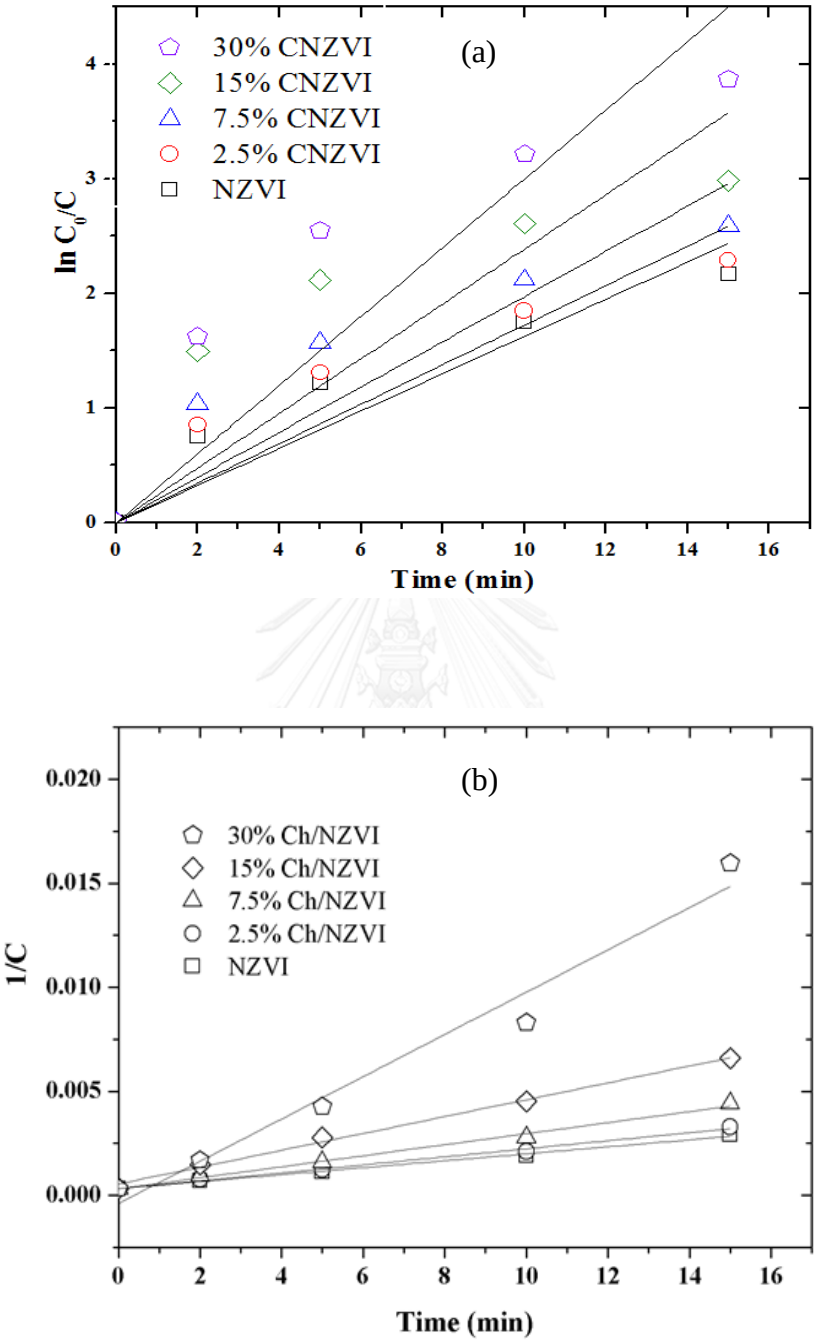

Figure 4.18 Linearization of kinetic model under different percentages of chitosan loading in As(III) removal: (a) pseudo first-order kinetic model, and (b) pseudo second-order kinetic model.

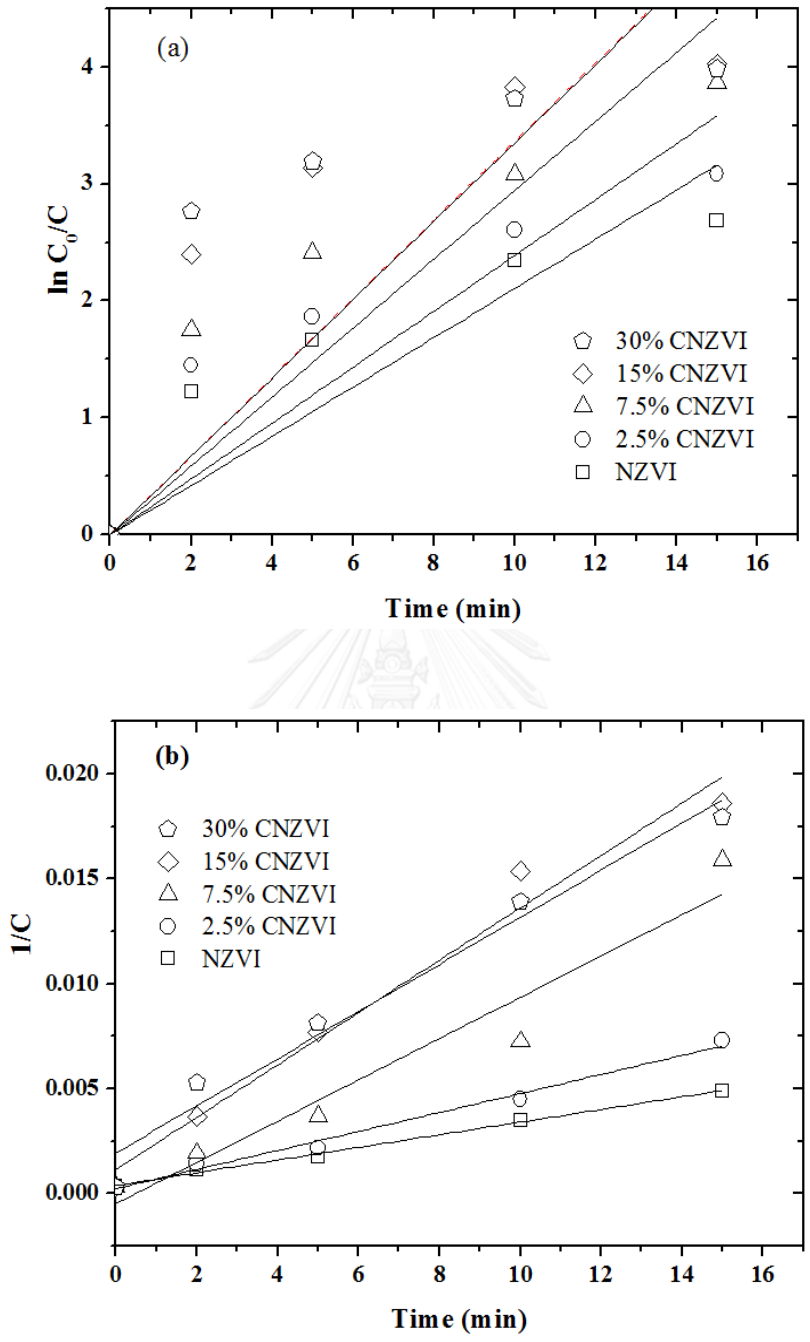

Figure 4.19 Linearization of kinetic model under different percentages of chitosan loading in As(V) removal: (a) pseudo first-order kinetic model, and (b) pseudo second-order kinetic model.

Table 4.8 Kinetic parameters for As(III) removal by fresh NZVI and CNZVI

samples	Model parameters			
	Pseudo first-order		Pseudo second-order	
	k_1 (min^{-1})	R^2	k_2 ($L\cdot(\mu g\cdot min)^{-1}$)	R^2
NZVI	0.1625	0.85	1.68×10^{-4}	0.996
2.5%CNZVI	0.1724	0.82	1.91×10^{-4}	0.994
7.5%CNZVI	0.1974	0.77	2.65×10^{-4}	0.994
15%CNZVI	0.2385	0.58	4.05×10^{-4}	0.996
30%CNZVI	0.2999	0.71	4.05×10^{-4}	0.996

Table 4.9 Kinetic parameters for As(V) removal by fresh NZVI and CNZVI

samples	Model parameters			
	Pseudo-first order		Pseudo-second order	
	k_1 (min^{-1})	R^2	k_2 ($L\cdot(\mu g\cdot min)^{-1}$)	R^2
NZVI	0.210	0.73	3.04×10^{-4}	0.99
2.5%CNZVI	0.238	0.77	4.6×10^{-4}	0.99
7.5%CNZVI	0.273	0.72	7.07×10^{-4}	0.94
15%CNZVI	0.322	0.49	10.97×10^{-4}	0.98
30%CNZVI	0.333	0.38	10.97×10^{-4}	0.98

4.9 Proposed removal mechanism of arsenic using CZNVI

Based on the results from batch experiments, CNZVI showed better arsenic removal than NZVI itself. In the removal process, arsenic was expected to adhere mainly onto CNZVI, as demonstrated by the reversibility experiment and XANES results. Besides, an incomplete reversibility of CNZVI has been observed. As the results, the mechanism of arsenic removal by CNZVI could be proposed, as shown in Figure 4.20. Three kinds of mechanism pathways, including adsorption of chitosan-As species, adsorption of iron (hydr)oxides- As species, and co-precipitation of As(V) and iron (hydr)oxides, are as follows;

1) Adsorption mechanism between chitosan and As(III)/As(V)

Chitosan is a polymer of N-acetylglucosamine which is partially deacetylated and contains reactive amine groups in their structure (Guibal, 2005). The amine groups can be protonated and becomes water soluble as stated in Equation 4.21 (Wang et al., 2006).

$$R\text{-}NH_2 + H_2O \leftrightarrow R\text{-}NH_3^+ + OH^- \qquad (4.21)$$

Therefore, arsenic ions which are in the form of oxyanions can be attached onto the available protonated amine groups ($R\text{-}NH_3^+$). The speciation of arsenic ions in aqueous solution mainly depends on the values of solution pH. Considering at pH condition of 7, As(III) and As(V) ions are dominantly in forms of H_3AsO_3 and $HAsO_4^{2-}$, respectively. Therefore, the different charges of the As(V) ion and the chitosan surface is proposed to be via electrostatic attraction force. In case of neutral As(III) species, Van der Waals attraction can be occurred as reported by Kwok et al. (2014). It is believed that As(V) anions can be adsorbed onto the protonated amine group on chitosan as express by:

$$R\text{-}NH_3^+ + HAsO_4^{2-} \leftrightarrow R\text{-}NH_3 \cdot HAsO_4 \cdot H_3N\text{-}R \qquad (4.22)$$

2) Adsorption mechanism between iron (hydr)oxides and As(III)/As(V)

Arsenic adsorption onto iron (hydr)oxides is explained by the formation of ferrous iron (Fe^{2+}) and ferric iron (Fe^{3+}) after NZVI react with water and oxygen. In the presence of oxygen, Fe^{2+} and Fe^{3+} can further oxidize and then the corrosion products of different iron (hydr)oxides such as Fe_3O_4, Fe_2O_3, FeOOH, FeO, $Fe(OH)_2$, and $Fe(OH)_3$ were formed and precipitated (Kanel et al., 2005; Triszcz et al., 2009). In the removal process, it was taken placed in vigorous stirring. Chitosan could therefore not completely coated NZVI and leave partial NZVI species exposing to water contaminated arsenic. As known, arsenic in aqueous system is usually found in negatively charged species. The positive charge of iron (hydr)oxides resulted in being the adsorptive sites for arsenic adsorption, which enhance arsenic removal efficiency. Noubactep (2008) indicated that arsenic was trapped on the iron corrosion products.

In addition, Manindy-Pajany et al (2011) reported that higher As(V) adsorption capacity was found in Fe_3O_4 than in Fe_2O_3 due to the higher iron content. Regarding XANES analysis in this study, more amount of Fe_3O_4 which was 44.2% were detected in spent CNVI, meanwhile 19% of Fe_3O_4 were detected in spent NZVI. It can be concluded that CNZVI can adsorbed more arsenic than NZVI.

3) Co-precipitation mechanism between As(V) and iron (hydr)oxides

In addition to the adsorption of As(V) at the outer surface of the oxide film around the reactive core of Fe, As(V) may adsorb to the surface inside the oxide-film and eventually co-precipitate with newly formed iron oxide (Noubactep, 2008). Tanboonchuy et al. (2011) also proposed that the co-precipitation with iron (hydr)oxides may facilitate the adsorption of As(III) by creating news adsorption sites.

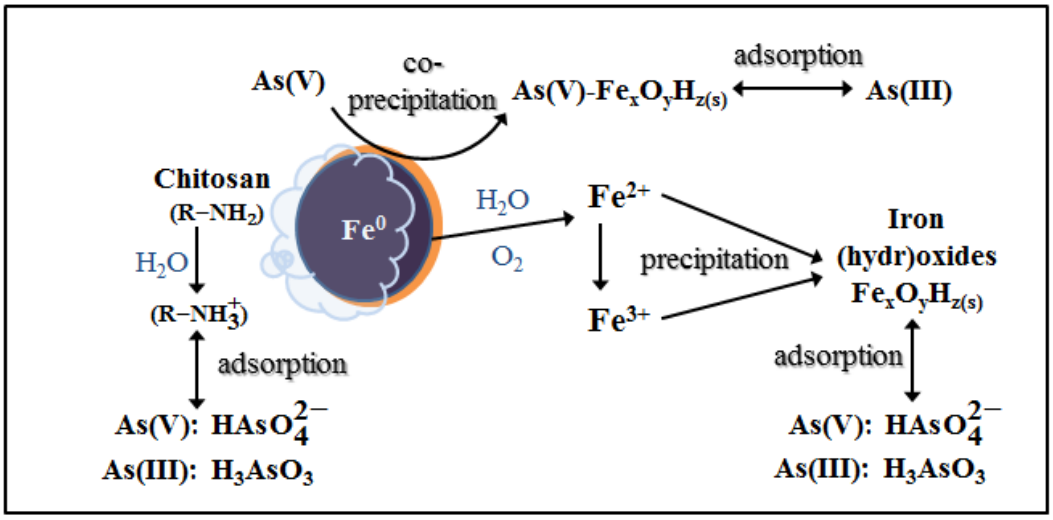

Figure 4.20 Proposed removal mechanism of arsenic using CNZVI.

4.10 Shelf-life study

4.10.1 Arsenate removal test

The performance of dried nanoparticles in As(V) removal has been investigated. The experiments were done in neutral solution (initial pH=7) at initial As(V) concentration 1,000 µg/L. The synthesized NZVI, 15% and 30% CNZVI were tested for their shelf-lives. Dried samples were kept in desiccator at ambient temperature for two days to one month. As shown in Figure 4.21, the removal efficiency of dried nanoparticles obviously decreased when compared with that of pristine nanoparticles. In addition, the As(V) removal efficiencies for all kinds of stored nanoparticles dropped along with the storage period. It was also found that NZVI lost their activity faster than CNZVI. Considering NZVI, the decreases of removal efficiency by ca. 30% and 45% were observed after 2 and 7 day storage, respectively. For 15% CNZVI, removal efficiency decreasing by ca. 20% and 30% were observed after 2 and 7 day storage, respectively. As a result, the oxidation over active iron might be retarded by a layer of chitosan (Geng et al., 2009). However, the tremendous loss was found for all adsorbents after one month storage.

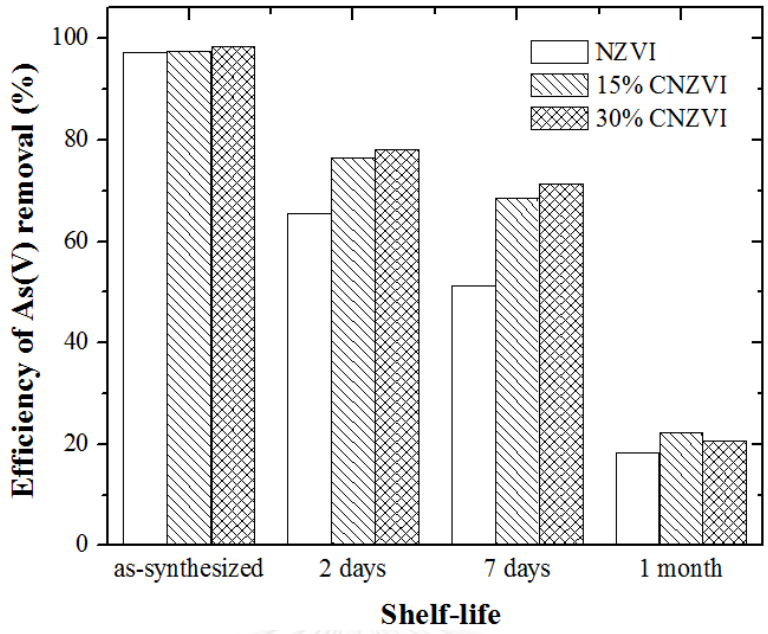

Figure 4.21 Effect of shelf-life on As(V) removal efficiency by NZVI, 15% CNZVI, and 30% CNZVI. Conditions: Initial As(V) concentration = 1000 µg/L, NZVI dosage = 0.067 mg/L, initial pH of 7.

4.10.2 Kinetic study in storage nanoparticles

In view of reaction kinetics under different storage period, the data showed in Figure 4.22 were further analyzed by using the linear form of pseudo-first order and pseudo-second order, according to Eqs (4.23) and (4.24) (Banerjee et al., 2008), respectively.

$$\ln\frac{C}{C_0} = -k_{10}t \qquad (4.23)$$

$$\frac{1}{C} - \frac{1}{C_0} = k_{20}t \qquad (4.24)$$

where $[C]_o$ and $[C]$ are the concentrations of arsenic at initial condition and time of reaction, t; k_1 and k_2 are the specific sorption rate constants for first-order and second-order reactions, respectively.

Based on Equations (4.23) through (4.24), the reaction rate constants (k_1 and k_2) of both As(III) and As(V) removal under different storage period were calculated and revealed in Table 4.10.

Among these models, the criterion for their applicability is based on the respective correlation coefficient (R^2). The results reveal that in both As(III) and As(V) removal system followed closely a pseudo-second order kinetic model. According to the rate constant (k), it was found that k1 and k2 tended to decreased in the longer storage period.

Table 4.10 Kinetic model parameter

Storage period	Arsenic species	% loading chitosan on NZVI (%)	Model parameters			
			Pseudo first-order		Pseudo second-order	
			k_1 (min^{-1})	R^2	k_2 ($L\cdot(\mu g\cdot min)^{-1}$)	R^2
Pristine NZVI	As(V)	0	0.219	0.63	0.0003	0.95
		15	0.280	0.24	0.0008	0.86
		30	0.425	0.34	0.0049	0.89
2 days storage	As(V)	0	0.025	0.94	2×10^{-5}	0.99
		15	0.034	0.97	5×10^{-5}	0.98
		30	0.031	0.96	4×10^{-5}	0.97
7 days storage	As(V)	0	0.018	0.92	1×10^{-5}	0.99
		15	0.029	0.92	3×10^{-5}	0.99
		30	0.023	0.87	2×10^{-5}	0.99

CHAPTER 5
CONCLUSIONS AND RECCOMENDATIONS

5.1 Conclusions

This study focus on the enhancement of the stability of NZVI by using chitosan as a modifier. Under several factors in the study, it could be concluded as follows;

1. Based on the characterization results by TEM and SEM analyses, the smaller particle size and more dispersion were observed in CNZVI particles compare to bare NZVI. These may be due to the coverage of chitosan over NZVI particles which resulted in the decreasing of magnetic property of NZVI. XANES analysis results also indicated that magnetite (Fe_3O_4) which has high magnetism was detected in freshly prepared NZVI meanwhile CNZVI was not. The reaction between NZVI and chitosan may be occurred at amine site of chitosan that was proved by FT-IR technique. Therefore, it can be concluded that chitosan can decrease the agglomeration of NZVI particles.

2. Batch experiments show that higher amount of chitosan accelerates the removal of arsenic from water. The higher chitosan ratio may result in the higher available protonated amine groups which contain positive charges, being as the binding sites for arsenic oxyanions. The acidic condition favors the removal of As when the NZVI was applied. On the other hand, the efficiencies of CNZVI for As removal did not change significantly for the three investigated pH conditions, when higher percentage of chitosan loading was applied. The effect of initial pH on As(V) removal may be overlooked when higher amount of chitosan was loaded onto NZVI. This outcome may be beneficial to *in situ* arsenic removal from groundwater which may show higher degree of pH variation.

3. The adsorption isotherm and the adsorption kinetics were reported. The results revealed that Langmuir isotherm provided a better fit to the experimental data. The adsorption capacity of As(III) and As(V) from Langmuir adsorption isotherms

were 39.84 mg/g and 46.30 mg/g, respectively. Pseudo second-order was applicable to describe adsorption kinetics.

4. Three mechanisms of arsenic removal by CNZVI are proposed. The first pathway is the adsorption between oxyanions of arsenic and the protonated amine group in chitosan molecules. The adsorption between iron corrosion products and As species be occurred. Moreover, the co-precipitation among iron corrosion products and As(V) may facilitate the adsorption of As(III) onto their precipitates.

5. The capability of oxidation resistance of NZVI under chitosan incubation is proved. CNZVI was found to be oxidized less than NZVI due to the covering of chitosan over NZVI. In the longer storage period (2-7 days) under dessicator atmosphere of the samples, the efficiency of CNZVI in As removal decreased but less than that of bare NZVI.

From a practical point of view, stability and reactivity are both important requirements for materials to treat environmental problems. Therefore, the CNZVI particles have the potential to be applied for in situ remediation of arsenic contaminated soil and groundwater.

5.2 Recommendations

1. As the result in the reversibility test, only 40 % of arsenic removal was taken place in the adsorption, sludge after the filtration should be characterized by XRD for any complex formation.
2. When nanoscale zero-valent iron modified by chitosan (CNZVI) is injected into an in-situ groundwater application, the good mobility of material is required. The column study of the dispersion of nanoparticles should be studied in a column packed with porous media.
3. Since the mobility can be affected by chemicals in aquifers, a more detailed study on the effect of dissolved anions and cations containing in groundwater on the removal mechanism of CNZVI in the presence of arsenic should be investigated.

4. The study of storage life, in this study, was carried out in the atmospheric in desiccator. It might be useful if we can keep it longer under other kind of solvents which do not react with CNZVI.

5. Approximately 0.1 g of NZVI nanoparticles could be generally produced for each batch. The scale-up synthesis condition for NZVI should be investigated

REFERENCES

Arnold, W. A. and A. L. Roberts (2000). "Pathways and Kinetics of Chlorinated Ethylene and Chlorinated Acetylene Reaction with Fe(0) Particles." Environmental Science and Technology **34**: 1794-1805.

Bae, S. and W. Lee (2010). "Inhibition of nZVI reactivity by magnetite during the reductive degradation of 1,1,1-TCA in nZVI/magnetite suspension." Applied Catalysis B: Environmental **96**: 10-17.

Banerjee, K., G. L. Amy, M. Prevost, S. Nour, M. Jekel, P. M. Gallagher and C. D. Blumenschein (2008). "Kinetic and thermodynamic aspects of adsorption of arsenic onto granular ferric hydroxide (GFH)." Water Res **42**(13): 3371-3378.

Bang, S., M. D. Johnson, G. P. Korfiatis and X. Meng (2005). "Chemical reactions between arsenic and zero-valent iron in water." Water Research **39**(5): 763-770.

Bang, S., G. P. Korfiatis and X. Meng (2005). "Removal of arsenic from water by zero-valent iron." Journal of Hazardous Materials **121**(1-3): 61-67.

Benavente, M. (2008). Adsorption of Metallic Ions onto Chitosan: Equilibrium and Kinetic Studies Licentiate Thesis Royal Institute of Technology (KTH).

Bi, E., I. Bowen and J. F. Devlin (2009). "Effect of mixed anions ($HCO3^-$ -SO_4^{2-})-ClO_4 on granular iron (Fe(0)) reactivity." Environmental Science & Technology **43**(15): 5975-5981.

Boddu, V. M., K. Abburi, J. L. Talbott, E. D. Smith and R. Haasch (2008). "Removal of arsenic (III) and arsenic (V) from aqueous medium using chitosan-coated biosorbent." Water Research **42**(3): 633-642.

Borah, D., S. Satokawa, S. Kato and T. Kojima (2009). "Sorption of As(V) from aqueous solution using acid modified carbon black." J Hazard Mater **162**(2-3): 1269-1277.

Bumajdad, A., S. Ali and A. Mathew (2011). "Characterization of iron hydroxide/oxide nanoparticles prepared in microemulsions stabilized with cationic/non-ionic surfactant mixtures." Journal of Colloid and Interface Science **355**(2): 282-292.

Chang, J., H. Woo, Ko, M.-S., , J. Lee, S. Lee, S.-T. Yun and S. Lee (2015). "Targeted removal of trichlorophenol in water by oleic acid-coated nanoscale palladium/zero-valent iron alginate beads1." Journal of Hazardous Materials **293**: 30-36.

Chauhan, D., J. Dwivedi and N. Sankararamakrishnan (2014). "Novel chitosan/PVA/zerovalent iron biopolymeric nanofibers with enhanced arsenic removal applications." Environmental Science and Pollution Research **21**: 9430-9442.

Choong, T. S. Y., T. G. Chuah, Y. Robiah, F. L. Gregory Koay and I. Azni (2007). "Arsenic toxicity, health hazards and removal techniques from water: an overview." Desalination **217**(1-3): 139-166.

Cornell, R. M. and U. Schwertmann (2004). Crystal Structure. The Iron Oxides, Wiley-VCH Verlag GmbH & Co. KGaA**:** 9-38.

Crittenden, J., R. Trussell, D. Hand, K. Howe and G. Tchobanoglous (2005). Water treatment: Principles and design. New York, John Wiley and Sons.

Das, B., R. R. Devi, I. M. Umlong, K. Borah, S. Banerjee and A. K. Talukdar (2013). "Arsenic (III) adsorption on iron acetate coated activated alumina: thermodynamic,

kinetics and equilibrium approach." Journal of Environmental Health Science and Engineering **11**(1): 42.
Daus, B., R. Wennrich and H. Weiss (2004). "Sorption materials for arsenic removal from water:: a comparative study." Water Research **38**(12): 2948-2954.
DeMarco, M. J., A. K. SenGupta and J. E. Greenleaf (2003). "Arsenic removal using a polymeric/inorganic hybrid sorbent." Water Research **37**(1): 164-176.
Dixit, S. and J. G. Hering (2003). "Comparison of arsenic(V) and arsenic(III) sorption onto iron oxide minerals: Implications for arsenic mobility." Environmental Science & Technology **37**(18).
Dries, J., L. Bastiaens, D. Springael, S. Kuypers, S. N. Agathos and L. Diels (2005). "Effect of humic acids on heavy metal removal by zero-valent iron in batch and continuous flow column systems." Water Research **39**: 3531-3540.
Dutta, P. K., J. Dutta and V. S. Tripathi (2004). "Chitin and Chitosan: Chemistry, Properties and Applications." Journal of Scientific & Industrial Research **63**: 20-31.
Geng, B., Z. Jin, T. Li and X. Qi (2009). "Kinetics of hexavalent chromium removal from water by chitosan-Fe0 nanoparticles." Chemosphere **75**(6): 825-830.
Geng, B., Z. Jin, T. Li and X. Qi (2009). "Preparation of chitosan-stabilized Fe0 nanoparticles for removal of hexavalent chromium in water." Science of The Total Environment **407**(18): 4994-5000.
Gu, Z. M., J. Fang and B. L. Deng (2005). "Preparation and evaluation of GAC-based ironcontaining adsorbents for arsenic removal." Environmental Science & Technology **39**(10).
Guibal, E. (2005). "Heterogeneous catalysis on chitosan-based materials: a review." Progress in Polymer Science **30**(1): 71-109.
Gupta, V. K., V. K. Saini and N. Jain (2005). "Adsorption of As(III) from aqueous solutions by iron oxide-coated sand." Journal of Colloid and Interface Science **288**(1): 55-60.
He, F., D. Zhao, J. Liu and C. B. Roberts (2007). "Stabilization of Fe-Pd nanoparticles with sodium carboxymethyl cellulose for enhanced transport and dechlorination of trichloroethylene in soil and groundwater." Industrial & Engineering Chemistry Research **46(1)**: 29-34.
Hiemenzm, P. C. and R. Rajagopalan (1997). Principles of colloid and surface chemistry. New York, Marcel Dekker, Inc.
Horzum, N., M. M. Demir, M. Nairat and T. Shahwan (2013). "Chitosan fiber-supported zero-valent iron nanoparticles as a novel sorbent for sequestration of inorganic arsenic." RSC Advances **3**(21): 7828-7837.
Huang, H., Q. Yuan and X. Yang (2004). "Preparation and characterization of metal-chitosan nanocomposites." Colloids and Surfaces B: Biointerfaces **39**(1-2): 31-37.
Hwang, Y.-H., D.-G. Kim and H.-S. Shin (2011). "Mechanism study of nitrate reduction by nano zero valent iron." Journal of Hazardous Materials **185**(2–3): 1513-1521.
Ibrahem, A. K., T. Abdel Moghny, Y. M. Mustafa, N. E. Maysour, F. Mohamed Saad El Din El Dars and R. Farouk Hassan (2012). "Degradation of Trichloroethylene Contaminated Soil by Zero-Valent Iron Nanoparticles." ISRN Soil Science **2012**: 9.
Iesan, C. M., C. Capat, F. Ruta and I. Udrea (2008). "Evaluation of a novel hybrid inorganic/organic polymer type material in the Arsenic removal process from drinking water." Water Research **42**(16): 4327-4333.

Inoue, K., K. Yoshizuka and K. Ohto (1999). "Adsorptive separation of some metal ions by complexing agent types of chemically modified chitosan." Analytica Chimica Acta **388**(1–2): 209-218.
Jegadeesan, G., K. Mondal and S. B. Lalvani (2005). "Arsenate remediation using nanosized modified zerovalent iron particles." Environmental Progress **24**(3): 289-296.
Kanel, S. R., J.-M. Greneche and H. Choi (2006). "Arsenic(V) Removal from Groundwater Using Nano Scale Zero-Valent Iron as a Colloidal Reactive Barrier Material." Environmental Science & Technology **40**: 2045-2050.
Kanel, S. R., B. Manning, L. Charlet and H. Choi (2005). "Removal of Arsenic(III) from Groundwater by Nanoscale Zero-Valent Iron." Environ. Sci. Technol **39**: 1291-1298.
Keane, E. (2009). Fate, Transport, and Toxicity of Nanoscale Zero-Valent Iron (nZVI) Used During Superfund Remediation , National Network for Environmental Management Studies Fellow, Duke University.
Kim, D.-G., Y.-H. Hwang, H.-S. Shin and S.-O. Ko (2015). "Kinetics of nitrate adsorption and reduction by nano-scale zero valent iron (NZVI): Effect of ionic strength and initial pH." KSCE Journal of Civil Engineering: 1-13.
Kwok, K. C. M., L. F. Koong, G. Chen and G. McKay (2014). "Mechanism of arsenic removal using chitosan and nanochitosan." Journal of Colloid and Interface Science **416**: 1-10.
Kwok, K. C. M., V. K. C. Lee, C. Gerente and G. McKay (2009). "Novel model development for sorption of arsenate on chitosan." Chemical Engineering Journal **151**.
Lackovic, J. A., N. P. Nikolaidis and G. M. Dobbs (2000). "Inorganic arsenic removal by zero-valent iron." Environmental Engineering Science **17**(1).
Li, X.-q., D. W. Elliott and W.-x. Zhang (2006). "Zero-Valent Iron Nanoparticles for Abatement of Environmental Pollutants: Materials and Engineering Aspects." Critical Reviews in Solid State and Materials Sciences **31**(4): 111-122.
Li, X. Q., D. W. Elliott and W. X. Zhang (2006). "Zero-Valent Iron Nanoparticles for Abatement of Environmental Pollutants: Materials and Engineering Aspects." Critical Reviews in Solid State and Materials Sciences **31**: 111-122.
Lien, H. L. and R. T. Wilkin (2005). "High-level arsenite removal from groundwater by zero-valent iron." Chemosphere **59**(3): 377-386.
Lin, Y.-H., H.-H. Tseng, M.-Y. Wey and M.-D. Lin (2010). "Characteristics of two types of stabilized nano zero-valent iron and transport in porous media." Science of The Total Environment **408**(10): 2260-2267.
Litter, M. I., M. E. Morgada and J. Bundschuh (2010). "Possible treatments for arsenic removal in Latin American waters for human consumption." Environmental Pollution **158**(5): 1105-1118.
Liu, A., J. Liu and W.-x. Zhang (2015). "Transformation and composition evolution of nanoscale zero valent iron (nZVI) synthesized by borohydride reduction in static water." Chemosphere **119**: 1068-1074.
Liu, T., Z. L. Wang, L. Zhao and X. Yang (2012). "Enhanced chitosan/Fe0-nanoparticles beads for hexavalent chromium removal from wastewater." Chemical Engineering Journal **189–190**: 196-202.

Liu, T., L. Zhao, D. Sun and X. Tan (2010). "Entrapment of nanoscale zero-valent iron in chitosan beads for hexavalent chromium removal from wastewater." Journal of Hazardous Materials **184**(1-3): 724-730.
Liu, Y. and G. V. Lowry (2006). "Effect of Particle Age (Fe0 Content) and Solution pH On NZVI Reactivity: H2 Evolution and TCE Dechlorination." Environmental Science & Technology **40**: 6085-6090.
Liu, Y., T. Phenrat and G. V. Lowry (2007). "Effect of TCE concentration and dissolved groundwater solutes on NZVI-promoted TCE dechlorination and H2 evolution." Environmental science & technology **41**(22): 7881-7887.
Lv, X., X. Xue, G. Jiang, D. Wu, T. Sheng, H. Zhou and X. Xu (2014). "Nanoscale Zero-Valent Iron (nZVI) assembled on magnetic Fe3O4/graphene for Chromium (VI) removal from aqueous solution." Journal of Colloid and Interface Science **417**: 51-59.
Malik, A. H., Z. M. Khan, Q. Mahmood, S. Nasreen and Z. A. Bhatti (2009). "Perspectives of low cost arsenic remediation of drinking water in Pakistan and other countries." Journal of Hazardous Materials **168**(1): 1-12.
Mamindy-Pajany, Y., C. Hurel, N. Marmier and M. Roméo (2011). "Arsenic (V) adsorption from aqueous solution onto goethite, hematite, magnetite and zero-valent iron: Effects of pH, concentration and reversibility." Desalination **281**: 93-99.
Manning, B. A., S. E. Fendorf, B. Bostick and D. L. Suarez (2002). "Arsenic(III) oxidation and arsenic(V) adsorption reactions on synthetic birnessite." Environmental Science & Technology **36**(5).
Martin, J. E., A. A. Herzing, W. Yan, X.-Q. Li, B. E. Koel, C. J. Kiely and W.-X. Zhang (2008). "Determination of the Oxide Layer Thickness in Core-Shell Zerovalent Iron Nanoparticles." Langmuir **24**: 4329-4334.
Mayo, J. T., C. Yavuz, S. Yean, L. Cong, H. Shipley, W. Yu, J. Falkner, A. Kan, M. Tomson and V. L. Colvin (2007). "The effect of nanocrystalline magnetite size on arsenic removal." Science and Technology of Advanced Materials **8**: 71-75.
Melitas, N., M. Conklin and J. Farrell (2002). "Electrochemical study of arsenate and water reduction on iron media used for arsenic removal from potable water." Environmental Science & Technology **36**(14).
Mishra, D. and J. Farrell (2005). "Evaluation of Mixed Valent Iron Oxides as Reactive Adsorbents for Arsenic Removal." Environmental Science & Technology **39**(24): 9689-9694.
Mohan, D. and J. C. U. Pittman (2007). "Arsenic removal from water/wastewater using adsorbents--A critical review." Journal of Hazardous Materials **142**(1-2): 1-53.
Mondal, P., C. B. Majumder and B. Mohanty (2006). "Laboratory based approaches for arsenic remediation from contaminated water: Recent developments." Journal of Hazardous Materials **137**(1): 464-479.
Mosaferi, M., S. Nemati, A. Khataee, S. Nasseri and A. A. Hashemi (2014). "Removal of Arsenic (III, V) from aqueous solution by nanoscale zero-valent iron stabilized with starch and carboxymethyl cellulose." Journal of Environmental Health Science and Engineering **12**: 74-74.
Munoz, J. A., A. Gonzalo and M. Valiente (2002). "Arsenic adsorption by Fe(III)-loaded opencelled cellulose sponge. Thermodynamic and selectivity aspects." Environmental Science & Technology **36**(15).

Mustafa, S., B. Dilara, K. Nargis, A. Naeem and P. Shahida (2002). "Surface properties of the mixed oxides of iron and silica." Colloids and Surfaces A: Physicochemical and Engineering Aspects **205**(3): 273-282.
Nikolaidis, N. P., G. M. Dobbs and J. A. Lackovic (2003). "Arsenic removal by zero-valent iron: field, laboratory and modeling studies." Water Research **37**(6): 1417-1425.
Noubactep, C. (2008). "A critical review on the process of contaminant removal in Fe^0-H_2O systems." Environmental Technology **29**(8): 909-920.
Noubactep, C. (2008). "A CRITICAL REVIEW ON THE PROCESS OF CONTAMINANT REMOVAL IN FE0–H2O SYSTEMS." Environmental Technology **29**(8): 909-920.
O'Carroll, D., B. Sleep, M. Krol, H. Boparai and C. Kocur (2013). "Nanoscale zero valent iron and bimetallic particles for contaminated site remediation." Advances in Water Resources **51**: 104-122.
Phenrat, T. and G. V. Lowry (2009). Physicochemistry of Polyelectrolyte Coatings that Increase Stability, Mobility, and Contaminant Specificity of Reactive Nanoparticles Used for Groundwater Remediation. Nanotechnology Applications for Clean Water. S. Nora, D. Mamadou, D. Jeremiah, S. Anita and S. Richard. Boston, William Andrew Publishing**:** 249-267.
Phenrat, T., N. Saleh, K. Sirk, H. J. Kim, R. D. Tilton and G. V. Lowry (2008). "Stabilisation of Aqueous Nanoscale Zero Valent Iron Dispersion by Anionic Polyelectrolytes: Adsorbate Anionic Polyelectrolyte Layer Properties and Their Effect on Aggregation and Sedimentation." Journal of Nanoparticle Research **10**: 795-814.
Ramos, M. A. V., W. Yan, X.-Q. Li, B. E. Koel and W.-X. Zhang (2009). "Simultaneous Oxidation and Reduction of Arsenic by Zero-Valent Iron Nanoparticles: Understanding the Significance of the Core-Shell Structure." The Journal of Physical Chemistry C **133**: 14591-14594.
Rao, P., M. S. Mak, T. Liu, K. C. Lai and I. M. Lo (2009). "Effects of humic acid on arsenic(V) removal by zero-valent iron from groundwater with special references to corrosion products analyses." Chemosphere **75**(2): 156-162.
Raven, K. P., A. Jain and R. H. Loeppert (1998). "Arsenite and Arsenate Adsorption on Ferrihydrite: Kinetics, Equilibrium, and Adsorption Envelopes." Environmental Science & Technology **32**(3): 344-349.
Rinaudo, M. (2006). "Chitin and chitosan: Properties and applications." Progress in Polymer Science **31**(7): 603-632.
Ruttenberg, K. C. (1992). "Development of a sequential extraction method for different forms of phosphorus in marine sediments." Limnology and Oceanography **37**(7): 1460-1482.
Selvin, N., G. Messham, J. Simms, I. Pearson and J. Hall (2000). The development of granular ferric media – arsenic removal and additional uses in water treatment. Water Quality Technology Conference, Salt Lake City , UT.
Shan, J., A. Sáez and W. Ela (2010). "Evaluating the Mobility of Arsenic in Synthetic Iron-Containing Solids Using a Modified Sequential Extraction Method." Journal of Environmental Engineering **136**(2): 238-245.
Shen, C., W. Lu, Y. Huang, J. Wu and H. Zhang (2015). "Removal of bismerthiazol from water using zerovalent iron: Batch studies and mechanism interpretation." Chemical Engineering Journal **260**: 411-418.

Sikder, M. T., S. Tanaka, T. Saito and M. Kurasaki (2014). "Application of zerovalent iron impregnated chitosan-caboxymethyl-β-cyclodextrin composite beads as a arsenic sorbent." Journal of Environmental Chemical Engineering **236**: 378-387.
Smedley, P. L. and D. G. Kinniburgh (2002). "A review of the source, behaviour and distribution of arsenic in natural waters." Applied Geochemistry **17**(5): 517-568.
Sohrabi, M. R., M. Moghri, H. R. Fard Masoumi, S. Amiri and N. Moosavi (2014). "Optimization of Reactive Blue 21 removal by Nanoscale Zero-Valent Iron using response surface methodology." Arabian Journal of Chemistry.
Su, C. M. and R. W. Puls (2001). "Arsenate and arsenite removal by zerovalent iron: Kinetics, redox transformation, and implications for in situ groundwater remediation." Environmental Science & Technology **35**(7).
Su, Y., A. S. Adeleye, Y. Huang, X. Sun, C. Dai, X. Zhou, Y. Zhang and A. A. Keller (2014). "Simultaneous removal of cadmium and nitrate in aqueous media by nanoscale zerovalent iron (nZVI) and Au doped nZVI particles." Water Research **63**: 102-111.
Sun, H., L. Wang, R. Zhang, J. Sui and G. Xu (2006). "Treatment of Groundwater Polluted by Arsenic Compounds by Zero Valent Iron." Journal of Hazardous Materials **B 129**: 297-303.
Tajuddin Sikder, M., S. Tanaka, T. Saito and M. Kurasaki (2014). "Application of zerovalent iron impregnated chitosan-caboxymethyl-β-cyclodextrin composite beads as arsenic sorbent." Journal of Environmental Chemical Engineering **2**(1): 370-376.
Tanboonchuy, V., N. Grisdanurak and C.-H. Liao (2012). "Background species effect on aqueous arsenic removal by nano zero-valent iron using fractional factorial design." Journal of Hazardous Materials **205–206**: 40-46.
Tanboonchuy, V., J.-C. Hsu, N. Grisdanurak and C.-H. Liao (2011). "Impact of selected solution factors on arsenate and arsenite removal by nanoiron particles." Environmental Science and Pollution Research **18**(6): 857-864.
Tanboonchuy, V., J. C. Hsu, N. Grisdanurak and C. H. Liao (2011). "Gas-bubbled nano zero-valent iron process for high concentration arsenate removal." Journal of Hazardous Materials **186**(2–3): 2123-2128.
Tang, L., J. Tang, G. Zeng, G. Yang, X. Xie, Y. Zhou, Y. Pang, Y. Fang, J. Wang and W. Xiong (2015). "Rapid reductive degradation of aqueous p-nitrophenol using nanoscale zero-valent iron particles immobilized on mesoporous silica with enhanced antioxidation effect." Applied Surface Science **333**: 220-228.
Thanos, I. C. G. (1986). "Investigation of corrosion of a rotating iron electrode in HNO3 by in-situ Raman spectroscopy." Journal of Electroanalytical Chemistry and Interfacial Electrochemistry **210**(2): 259-264.
Thirunavukkarasu, O., T. Viraraghavan and K. Subramanian (2003). "Arsenic removal from drinking water using granular ferric hydroxide." Water SA **29**: 161-170.
Triszcz, J. M., A. Porta and F. S. G. Einschlag (2009). "Effect of operating conditions on iron corrosion rates in zero-valent iron systems for arsenic removal." Chemical Engineering Journal **150**(2-3): 431-439.
Vasiliu, S., I. Bunia, S. Racovita and V. Neagu (2011). "Adsorption of cefotaxime sodium salt on polymer coated ion exchange resin microparticles: Kinetics, equilibrium and thermodynamic studies." Carbohydrate Polymers **85**(2): 376-387.

Vaughan Jr, R. L. and B. E. Reed (2005). "Modeling As(V) removal by a iron oxide impregnated activated carbon using the surface complexation approach." Water Research **39**(6): 1005-1014.
Vu, K. B., M. D. Kaminski and L. Nunez (2003). Review of arsenic removal technologies for contaminated groundwaters. Other Information: PBD: 2 May 2003**:** Medium: ED; Size: 43 pages.
Wang, Q. Z., X. G. Chen, N. Liu, S. X. Wang, C. S. Liu, X. H. Meng and C. G. Liu (2006). "Protonation constants of chitosan with different molecular weight and degree of deacetylation." Carbohydrate Polymers **65**(2): 194-201.
Weber, B., R. Betz, W. Bauer and S. Schlamp (2011). "Crystal Structure of Iron(II) Acetate." Zeitschrift für anorganische und allgemeine Chemie **637**(1): 102-107.
Wei, Y.-T., S.-c. Wu, S.-W. Yang, C.-H. Che, H.-L. Lien and D.-H. Huang (2012). "Biodegradable surfactant stabilized nanoscale zero-valent iron for in situ treatment of vinyl chloride and 1,2-dichloroethane." Journal of Hazardous Materials 373-380

Weng, X., S. Lin, Y. Zhong and Z. Chen (2013). "Chitosan stabilized bimetallic Fe/Ni nanoparticles used to remove mixed contaminants-amoxicillin and Cd (II) from aqueous solutions." Chemical Engineering Journal **229**: 27-34.
Westerhoff, P., D. Highfield, M. Badruzzaman and Y. Yoon (2005). "Rapid small-scale column tests for arsenate removal in iron oxide packed bed columns." Journal of Environmental Engineering-ASCE **131**(2).
Wittayakun, J. and N. Grisdanurak (2004). Catalysis: Fundamentals and Applications (In Thai), Thammasat University.
Yan, W., A. A. Herzing, C. J. Kiely and W.-x. Zhang (2010). "Nanoscale zero-valent iron (nZVI): Aspects of the core-shell structure and reactions with inorganic species in water." Journal of Contaminant Hydrology **In Press, Corrected Proof**.
Yang, G. C. C. and H.-L. Lee (2005). "Chemical reduction of nitrate by nanosized iron: kinetics and pathways." Water Research **39**(5): 884-894.
Yang, J., , , M.Z., X.W., P.J.J.A. and K.L. (2014). "Poly(vinylidene fluoride) membrane supported nano zero-valent iron for metronidazole removal: Influences of calcium and bicarbonate ions." Journal of the Taiwan Institute of Chemical Engineers.
Yang, J. E., J. S. Kim, Y. S. Ok and K. R. Yoo (2007). "Mechanistic evidence and efficiency of the Cr(VI) reduction in water by different sources of zerovalent irons." Water Science & Technology **55**(1-2): 197-202.
Yean, S., L. Cong, C. T. Yavuz, J. T. Mayo, W. W. Yu, A. T. Kan, V. L. Colvin and M. B. Tomson (2005). "Effect of magnetite particle size on adsorption and desorption of arsenite and arsenate." Journal of Materials Research **20**(12): 3255-3264.
Zeng, L. (2003). "A method for preparing silica-containing iron(III) oxide adsorbents for arsenic removal." Water Research **37**(18): 4351-4358.
Zhang, F. and H. Itoh (2005). "Iron oxide-loaded slag for arsenic removal from aqueous system." Chemosphere **60**(3): 319-325.
Zhang, S., H. Niu, Y. Cai, X. Zhao and Y. Shi (2010). "Arsenite and arsenate adsorption on coprecipitated bimetal oxide magnetic nanomaterials: MnFe2O4 and CoFe2O4." Chemical Engineering Journal **158**(3): 599-607.
Zhang, X., S. Lin, X.-Q. Lu and Z.-l. Chen (2010). "Removal of Pb(II) from water using synthesized kaolin supported nanoscale zero-valent iron." Chemical Engineering Journal **163**(3): 243-248.

Zhu, H., Y. Jia, X. Wu and H. Wang (2009). "Removal of arsenic from water by supported nano zero-valent iron on activated carbon." Journal of Hazardous Materials **172**(2-3): 1591-1596.

APPENDICES

APPENDIX A

Preliminary experimental raw data

Table A-1 Comparison of using different types of nanoparticles.

Time (min)	Normalized total arsenic concentration			
	chitosan	**NZVI**	**CNZVI-n**	**CNZVI-a**
0	1	1	1	1
2	0.983	0.378	0.356	0.191
5	0.971	0.260	0.284	0.059
10	0.969	0.168	0.162	0.047
15	0.962	0.077	0.107	0.041
25	0.941	0.054	0.057	0.038
40	0.949	0.051	0.027	0.024
60	0.939	0.028	0.022	0.019

Condition;

Material types = NZVI, CNZVI-n, CNZVI-a, Chitosan flake

Materials dosage = 0.067 g/L,

Initial As(V) concentration = 3000 µg/L

Initial pH solution = 7

Table A-2 Comparison of total dissolved iron in solution in preliminary experiment by using different types of nanoparticles.

Time (min)	**Total dissolved iron concentration (mg/L)**			
	chitosan	**NZVI**	**CNZVI-n**	**CNZVI-a**
0	0	0	0	0
2	4.076	1.344	1.016	4.076
5	5.550	3.534	1.493	5.550
10	6.518	4.963	0.665	6.518
15	4.453	3.491	0.336	4.453
25	0.337	0.502	0.275	0.337
40	0.172	0.305	0.271	0.172
60	0.049	0.080	0.182	0.049

Condition;

Material types = NZVI, CNZVI-n, CNZVI-a, Chitosan flake

Materials dosage = 0.067 g/L,

Initial As(V) concentration = 3000 µg/L

Initial pH solution = 7

APPENDIX B

Histogram of particle size by TEM analysis

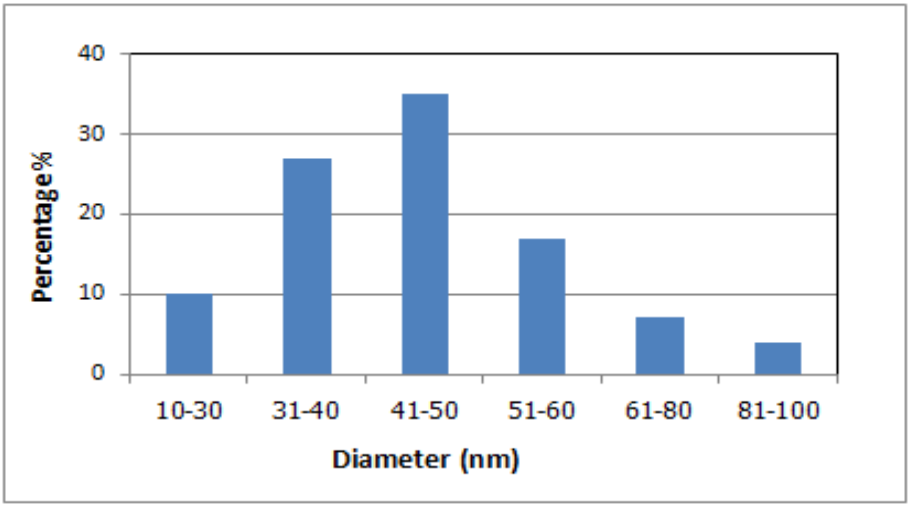

Figure B-1 Particle size distribution of NZVI.

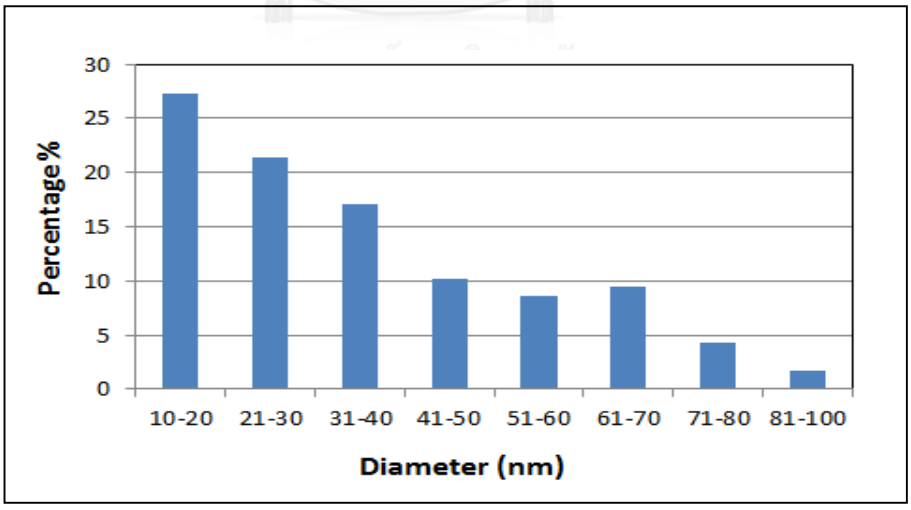

Figure B-2 Particle size distribution of 30%CNZVI.

APPENDIX C

Experimental raw data in Arsenic removal test

Table C-1 Remaining fraction of As(III) in arsenic removal test by using several percentages of chitosan loading on NZVI. (Effect of chitosan loading)

Time (min)	Normalized total arsenic concentration				
	NZVI	**2.5%CNZVI**	**7.5%CNZVI**	**15%CNZVI**	**30%CNZVI**
0	1	1	1	1	1
2	0.471	0.426	0.355	0.225	0.197
5	0.295	0.270	0.209	0.120	0.078
10	0.174	0.158	0.120	0.074	0.040
15	0.115	0.101	0.075	0.051	0.021
25	0.078	0.055	0.039	0.045	0.018
40	0.059	0.044	0.033	0.030	0.013
60	0.051	0.04	0.030	0.025	0.012

Condition;

Material types = NZVI and CNZVI at 2.5, 7.5, 15, and 30% chitosan loading

Materials dosage = 0.067 g/L,

Initial As(V) concentration = 3000 µg/L

Initial pH solution = 7

Table C-2 Comparison of total dissolved iron in solution in As(III) removal test by using several percentages of chitosan loading on NZVI.
(Effect of chitosan loading)

Time (min)	Total dissolved iron concentration (mg/L)				
	NZVI	2.5%CNZVI	7.5%CNZVI	15%CNZVI	30%CNZVI
0	0	0	0	0	0
2	5.761	2.895	3.287	2.367	0.961
5	7.978	4.662	4.926	0.2717	0.407
10	5.616	2.842	2.33	0.0506	0.060
15	0.849	0.58	0.569	0.062	0.038
25	0.440	0.052	0.050	0.045	0.0191
40	0.251	0	0.002	0.007	0
60	0	0	0.004	0	0

Condition;

Material types = NZVI and CNZVI at 2.5, 7.5, 15, and 30% chitosan loading

Materials dosage = 0.067 g/L,

Initial As(V) concentration = 3000 µg/L

Initial pH solution = 7

Table C-3 Remaining fraction of As(V) in arsenic removal test by using several percentages of chitosan loading on NZVI (Effect of chitosan loading)

Time (min)	Normalized total arsenic concentration				
	NZVI	**2.5%CNZVI**	**7.5%CNZVI**	**15%CNZVI**	**30%CNZVI**
0	1	1	1	1	1
2	0.312	0.283	0.214	0.121	0.083
5	0.189	0.154	0.115	0.053	0.050
10	0.096	0.074	0.046	0.0240	0.0217
15	0.068	0.0457	0.031	0.021	0.019
25	0.053	0.038	0.031	0.02	0.018
40	0.046	0.032	0.025	0.018	0.016
60	0.043	0.029	0.018	0.015	0.013

Condition;

Material types = NZVI and CNZVI at 2.5, 7.5, 15, and 30% chitosan loading

Materials dosage = 0.067 g/L,

Initial As(V) concentration = 3000 µg/L

Initial pH solution = 7

Table C-4 Comparison of total dissolved iron in solution in As(V) removal test by using several percentages of chitosan loading on NZVI (Effect of chitosan loading)

Time (min)	Total dissolved iron concentration (mg/L)				
	NZVI	2.5%CNZVI	7.5%CNZVI	15%CNZVI	30%CNZVI
0	0	0	0	0	0
2	4.076	1.716	2.125	1.016	0.087
5	5.550	4.339	2.731	1.493	0.088
10	6.518	5.564	2.838	0.665	0.080
15	4.453	3.077	2.3	0.275	0.069
25	0.337	0.315	0.8	0.336	0.034
40	0.072	0.05	0.3	0.271	0.018
60	0.048	0.03	0.25	0.182	0.007

Condition;

Material types = NZVI and CNZVI at 2.5, 7.5, 15, and 30% chitosan loading

Materials dosage = 0.067 g/L,

Initial As(V) concentration = 3000 µg/L

Initial pH solution = 7

Table C-5 Comparison of As(III) removals by NZVI and 15% CNZVI in DI water and field groundwater.

Time (min)	Normalized total arsenic concentration			
	NZVI-DI	NZVI-GW	15%CNZVI-DI	15%CNZVI-GW
0	1	1	1	1
2	0.472	0.602	0.225	0.397
5	0.295	0.438	0.120	0.199
10	0.174	0.272	0.074	0.075
15	0.115	0.173	0.051	0.044
25	0.078	0.125	0.045	0.033
40	0.059	0.096	0.030	0.023
60	0.051	0.072	0.025	0.018

Condition;

Material types = NZVI and 15% CNZVI

Materials dosage = 0.067 g/L,

Initial As(III) concentration approx. 3000 µg/L

Initial pH solution = 7

Table C-6 Comparison of As(V) removals by NZVI and 15% CNZVI in DI water and field groundwater.

Time (min)	Normalized total arsenic concentration			
	NZVI-DI	NZVI-GW	15% CNZVI-DI	15% CNZVI-GW
0	1	1	1	1
2	0.312	0.491	0.121	0.262
5	0.189	0.343	0.053	0.097
10	0.096	0.203	0.024	0.077
15	0.068	0.095	0.021	0.063
25	0.053	0.056	0.020	0.052
40	0.046	0.032	0.019	0.024
60	0.043	0.026	0.015	0.018

Condition;

Material types = NZVI and 15% CNZVI

Materials dosage = 0.067 g/L,

Initial As(V) concentration approx. 3000 µg/L

Initial pH solution = 7

APPENDIX D

Supplemental data on Eh-pH diagram of iron (Fe)

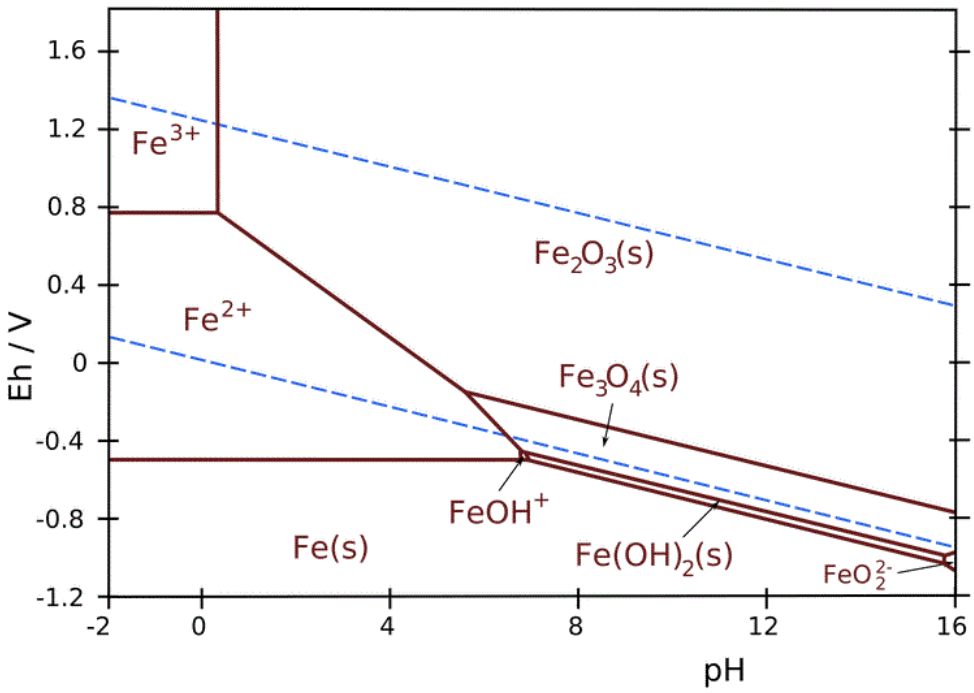

VITA

Name: Miss. Thanatorn Yoadsomsuay

Nationality: Thai

Education: 1995-1998 Master of Science (Environmental Technology) Faculty of Public Health, Mahidol University, Thailand.

1991-1994 Bachelor of Science (Biology) Faculty of Science, Chiangmai University, Thailand.

Employment: 1999-2001 Environmental Scientist, SECOT, Co.,Ltd. Bangkok

2001-Present Scientist, Department of Industrial Works, Ministry of Industry.

Conference:

1. Oral presentation at “2011 International Conference on Environmental Quality Concern, Control and Conservation”, May 20-21, 2011, Kaohsiung, Taiwan ROC.

2. Oral presentation at “2012 International Conferenceon Sustainable Environmental Technologies (ICSET)”, April 26-27, 2012, Bangkok, Thailand